AD-A078 799 UTAH STATE UNIV LOGAN SPACE MEASUREMENTS LAB F/G 4/1
ROCKETBORNE IONOSPHERIC STUDIES: 1976-1979.(U)
AUG 79 D A BURT , G D ALLRED F19628-76-C-0261
UNCLASSIFIED AFGL-TR-79-0179 NL

1 OF 2
AD-
A 078799



ADA078799

AFGL-TR-79-0179

LEVEL II

ROCKETBORNE IONOSPHERIC STUDIES: 1976-1979

David A. Burt
Glenn D. Allred

Space Measurements Laboratory
Utah State University
Logan, Utah 84322

DDC RECEIVED DEC 28 1979 E

6 August 1979

This research was sponsored by the Defense Nuclear Agency under subtask I25AAXHX632, Work Unit 72, untitled, "IR Ionospheric Program."

DDC FILE COPY

Approved for public release; distribution unlimited.

Final Report
Period Covered: 28 May 1976 through 30 September 1979

AIR FORCE GEOPHYSICS LABORATORY
AIR FORCE SYSTEMS COMMAND
UNITED STATES AIR FORCE
HANSCOM AFB, MASSACHUSETTS 01731

79-12 27 296

Qualified requestors may obtain additional copies from the Defense Documentation Center. All others should apply to the National Technical Information Service.

Unclassified
SECURITY CLASSIFICATION OF THIS PAGE (When Data Entered)

(19) REPORT DOCUMENTATION PAGE

READ INSTRUCTIONS BEFORE COMPLETING FORM

(18) REPORT NUMBER: AFGL-TR-79-0179

2. GOVT ACCESSION NO.

(9) 3. RECIPIENT'S CATALOG NUMBER

(6) 4. TITLE (and Subtitle): Rocketborne Ionospheric Studies: 1976-1979

5. TYPE OF REPORT & PERIOD COVERED: Final rept. 28 May 1976-30 Sep 1979

6. PERFORMING ORG. REPORT NUMBER

(10) 7. AUTHOR(s): D.A. Burt, G.D. Allred

(15) 8. CONTRACT OR GRANT NUMBER(s): F19628-76-C-0261

9. PERFORMING ORGANIZATION NAME AND ADDRESS: Space Measurements Laboratory, Utah State University, UMC 41, Logan, Utah 84322

10. PROGRAM ELEMENT, PROJECT, TASK AREA & WORK UNIT NUMBERS: 62101F, CDNA30AA

11. CONTROLLING OFFICE NAME AND ADDRESS: Air Force Geophysics Laboratory, Hanscon AFB, Massachusetts 01731, ~~Monitor/Thomas D. Conley/OPR~~

(11) 12. REPORT DATE: 6 August 1979

13. NUMBER OF PAGES: 148 (12) 143

14. MONITORING AGENCY NAME & ADDRESS (if different from Controlling Office): Elmer Keith ACO (ONR), University of California 239 Campbell Hall, Berkeley, California 94720

15. SECURITY CLASS. (of this report): Unclassified

15a. DECLASSIFICATION/DOWNGRADING SCHEDULE

16. DISTRIBUTION STATEMENT (of this Report)

(17) 30, X632

Approved for public release; distribution unlimited.

17. DISTRIBUTION STATEMENT (of the abstract entered in Block 20, if different from Report)

(16) CDNA, I25AAXH

18. SUPPLEMENTARY NOTES

This research was sponsored by the Defense Nuclear Agency under subtask I25AAXHX632, Work Unit 72, entitled, "IR Ionospheric Program".

19. KEY WORDS (Continue on reverse side if necessary and identify by block number)

Ionospheric research
Electron dosing
Infrared emissions measurement
Rocket instruments

20. ABSTRACT (Continue on reverse side if necessary and identify by block number)

Eight instrumented sounding rockets were flown during the period of this contract to investigate ionospheric parameters and to further the development of new instruments and measurements techniques for investigating such parameters. Particular emphasis has been placed upon the development of instrumentation for electron dosing via large electron accelerators aboard the payloads and assessment of the effects of such dosing as manifest by ultraviolet.

DD FORM 1 JAN 73 1473 EDITION OF 1 NOV 65 IS OBSOLETE

Unclassified
SECURITY CLASSIFICATION OF THIS PAGE (When Data Entered)

i

Near
411 514

JAB

20. (cont) visible, and particularly infrared emissions. Launches have been accomplished under a variety of ionospheric conditions ranging from the quiescent, undisturbed ionosphere through intense auroral conditions. This report describes the program of launches and instrumentation ~~employed~~ used to accomplish the measurements.

Accession For
NTIS GRA&I
DDC TAB
Unannounced
Justification
By
Distribution/
Availability Codes
Dist | Avail and/or special
A

LIST OF CONTRIBUTORS
-SCIENTISTS AND ENGINEERS-
UTAH STATE UNIVERSITY



K.D. Baker, Principal Investigator. . . . . .

D.J. Baker
B.Y. Bartschi
D.A. Burt
C.L. Craw
W.I. Fletcher
D.G. Frodsham
R.H. Haycock
L.C. Howlett
C.L. Wyatt
R.J. Huppi
L.L. Jensen
J.C. Kemp
D.E. Morse
E.F. Pound
A.J. Steed
G.A. Ware
P.R. Williamson

RELATED CONTRACTS AND PUBLICATIONS

F19628-74-C-0130
F19628-77-C-0203
F19628-73-C-0048
F19628-72-C-0255
F19628-70-C-0302

Baker, K.D., D.J. Baker, J.C. Ulwick, and A.T. Stair, Jr., "Measurements of 1.5-5.3-μm infrared enhancements associated with a bright auroral breakup," J. Geophys. Res., 82, 3518, September, 1977.

Smith, Michael A., 'Design and development of telemetry logging system," Sci. Rept. No. 2, AFGL-TR-78-0180, 114 pp., Contract F19628-76-C-0261, Space Science Laboratory, Utah State University, Logan, 1978.

Baker, K.D., D.J. Baker, L.C. Howlett, and L.L. Jensen, "Studies of the disturbed upper atmosphere utilizing rocketborne instrumentation," Final Report, AFGL-TR-77-0223, 68 pp., Contract F19628-74-C-0130, Space Science Laboratory, Utah State University, Logan, 1977.

TABLE OF CONTENTS

	Page
List of Contributors	iii
Related Contracts and Publications	iii
List of Figures	vii
List of Tables	xi
INTRODUCTION	1
ATMOSPHERIC DOSING	5
Talos Castor EX 651.92-1 EXCEDE	7
Aerobee 170 AO 4.602 PRECEDE II	10
Talos Castor EX 851.44-1 (EXCEDE II SPECTRAL)	13
DEVELOPMENTAL FLIGHTS - FIELD-WIDENED INTERFEROMETER-SPECTROMETER	19
Sergeant IC 730.09-1	19
Sergeant IC 830.09-1A	25
AURORAL WIDEBAND COMMUNICATIONS	27
Sergeant Hydac IC 819.08-1	27
AURORAL DYNAMICS AND ENERGETICS	33
Nike Hydacs IC 807.15-1, IC 807.15-2 and IR 807.57-1.	33
Supporting Measurements	41
INSTRUMENTATION	43
Atmospheric Electron Dosing	43
High Energy Electron Accelerators	43
Measurements of Electron Density	44
DC Probe.	44
Plasma Frequency Probe	45
C Probe	47
Instruments for Measurements of Optical Emissions.	47
Photometers.	47
Infrared Radiometers.	49
Infrared Spectrometers	50
Instruments for Measurement of Vehicle Potential	51
Skin Current Probe	51
Charge Probe	52
Measurements of Energy Deposition	52
Energy Deposition Scintillator	52
Measurements of Atmospheric Constituents.	53
Atomic Oxygen Detector	53
SUBCONTRACTS UNDER CONTRACT F19628-76-C-0261	55
REFERENCES	59

TABLE OF CONTENTS (CONT.)

	Page
APPENDIX A, TALOS CASTOR EX651.92-1	61
APPENDIX B, SERGEANT IC730.09-1.	69
APPENDIX C, AEROBEE 170 A04.602.	77
APPENDIX D, SERGEANT HYDAC IC819.08-1.	81
APPENDIX E, NIKE HYDAC IC807.15-1	99
APPENDIX F, NIKE HYDAC IR807.57-1	111
APPENDIX G, SERGEANT IC830.09-1A	123
APPENDIX H, DISTRIBUTION LIST	131

LIST OF FIGURES

Figure No.		Page
1	EX 651.92-1 Vehicle Configuration	8
2	EX 651.92-1 Payload Configuration	9
3	AO 4.602 Vehicle Configuration	11
4	AO 4.602 Payload Configuration	12
5	EX 851.44-1 Vehicle Configuration	17
6	EX 851.44-1 Payload Configuration	18
7	Sergeant IC 730.09-1 and Sergeant IC 830.09-1A Vehicle Configuration.	23
8	Sergeant IC 730.09-1 and Sergeant IC 830.09-1A Payload Configuration.	24
9	Sergeant Hydac IC 819.08-1 Vehicle Configuration	31
10	Sergeant Hydac IC 819.08-1 Payload Configuration	32
11	Nike Hydac IC 807.15-1 and IC 807.15-2 Vehicle Configuration.	36
12	Nike Hydac IC 807.15-1 and IC 807.15-2 Payload Configuration.	37
13	Nike Hydac IR 807.57-1 Vehicle Configuration	39
14	Nike Hydac IR 807.57-1 Payload Configuration	40
15	C Probe Block Diagram	48
A-1	EX 651.92-1 Trajectory	62
A-2	DC Probe (DCP 76A-1) Low Gain Calibration	63
A-3	DC Probe (DCP 76A-1) Medium Gaw Calibration	63
A-4	DC Probe (DCP 76A-1) High Gain Calibration	64
B-1	Sergeant IC 730.09-1 Trajectory	70
B-2	Photometer (PM2-15) Field-of-View	71
B-3	Photometer (PM2-15) Bandpass Filter	71
B-4	Photometer (PM2-15) Responsivity	72
B-5	Energy Deposition Scintillator (EDS 75-4) Calibration	73
C-1	Aerobee 170 AO 4.602 Trajectory	78
D-1	Sergeant Hydac IC 819.08-1 Main Payload Trajectory	82
D-2	Sergeant Hydac IC 819.08-1 Nosetip Payload Trajectory	83
D-3	Photometer (PM2-42) Field-of-View	84

LIST OF FIGURES (CONT.)

Figure No.		Page
D-4	Photometer (PM2-42) Bandpass Filter Transmission	84
D-5	Photometer (PM2-42) Responsivity	85
D-6	Photometer (PM2-51) Field-of-View	86
D-7	Photometer (PM2-51) Bandpass Filter Transmission	86
D-8	Photometer (PM2-51) Responsivity	87
D-9	Energy Deposition Scintillator (EDS 75-3 Main Payload) Calibration	88
D-10	C-Probe (CP76M-1) Calibration	89
D-11	DC Probe (DCP 76-1) Calibration	90
D-12	Plasma Frequency Probe (PFP 6M-1) Analog Calibration	91
D-13	Plasma Frequency Probe (PFP 76M-1) Digital PCM Format	91
D-14	Energy Deposition Scintillator (EDS 75-1, Nosetip) Calibration	92
D-15	Energy Deposition Scintillator (EDS 75-2 Nosetip) Calibration	93
E-1	Nike Hydac IC 807.15-1 Trajectory	100
E-2	Photometer (PM2-48) Field-of-View	101
E-3	Photometer (PM2-48) Bandpass Filter Transmission	101
E-4	Photometer (PM2-48) Responsivity	102
E-5	Photometer (PM2-56) Field-of-View	103
E-6	Photometer (PM2-56) Bandpass Filter Transmission	103
E-7	Photometer (PM2-56) Responsivity	104
E-8	Radiometer NR4-C-1 (4.3 μm Channel) Near-Field-of-View	105
E-9	Radiometer NR4-C-1 (4.3 μm Channel) Far-Field-of-View	105
E-10	Radiometer NR4-C-1 (4.3 μm) Linearity Data & Transfer Function	106
E-11	Rad ometer NR4-C-1 (2.7 μm Channel) Near-Field-of-View	107
E-12	Rad ometer NR4-C-1 (2.7 μm Channel) Far-Field-of-View	107
E-13	Radiometer NR4-C-1 (2.7 μm) Linearity Data & Transfer Function	108
F-1	Nike Hydac IR 807.57-1 Trajectory	112
F-2	Photometer (PM2-83) Field-of-View	113
F-3	Photometer (PM2-83) Bandpass Filter Transmission	113
F-4	Photometer (PM2-83) Variable Gain Responsivity	114

LIST OF FIGURES (CONT.)

Figure No.		Page
F-5	Photometer (PM2-83) × 10 Gain Responsivity	114
F-6	Photometer (PM2-95) Field-of-View	115
F-7	Photometer (PM2-95) Bandpass Filter Transmission	115
F-8	Photometer (PM2-95) Variable Gain Responsivity	116
F-9	Photometer (PM2-95) × 10 Gain Responsivity	116
F-10	DC Probe (DCP 77A-12) Calibration	118
F-11	Plasma Frequency Probe (PFP 77A-12) Digital PCM Format	118
F-12	Nike Hydac IR 807.57-1 Nosespike Electrode Configuration	119
F-13	Plasma Frequency Probe (PFP 77A-12) Analog Calibration	119
F-14	Energy Deposition Scintillator (EDS 75-5) Calibration	120
G-1	Sergeant IC 830.09-1A Trajectory	124
G-2	Photometer (PM2-15A) Field-of-View	125
G-3	Photometer (PM2-15) Bandpass Filter Transmission	125
G-4	Photometer (PM2-15A) Responsivity	126
G-5	Energy Deposition Scintillator (EDS 75-4A) Calibration	127

LIST OF TABLES

Table No.		Page
1	Chronological Summary of Rocket Flights and Measurements--Contract F19628-76-C-0261	2
2	Launch Summary-Electron Dosing Rockets	6
3	Talos Castor EX 651.92-1 Instrumentation	10
4	Aerobee 170 AO 4.602 Instrumentation.	13
5	Talos Castor EX 851.44-1 Instrumentation	15
6	Sergeant IC 730.09-1 Instrumentation.	21
7	Coordinated Ground Support Instrumentation Sergeant IC 730.09-1	22
8	Sergeant IC 730.09-1 Instrumentation.	26
9	Sergeant Hydac IC 819.08-1 Instrumentation.	29
10	Nike Hydac IC 807.15-1 and IC 807.15-2 Instrumentation.	35
11	Nike Hydac IC 807.57-1 Instrumentation	38
12	Ground Based Instrumentation and Measurements.	41
A-1	Talos Castor EX 651.92-1 Telemetry Technical Data	65
A-2	Talos Caster EX 651.92-1 2.5 × 64 Commutator	66
B-1	Photometer Parameters (PM2-15).	72
B-2	Energy Deposition Scintillator Parameters (EDS 75-4)	74
B-3	Sergeant IC 730.09-1 Telemetry Technical Data.	74
B-4	Sergeant IC 730.09-1 1 × 48 NRZ Irig Commutator Assignment	75
C-1	Aerobee 170 AO 4.602 Telemetry Technical Data.	79
C-2	Aerobee 170 AO 4.602 1 × 60 RZ Commutator Assignments	79
D-1	Photometer Parameters (PM2-42).	85
D-2	Photometer Parameters (PM2-51).	87
D-3	Energy Deposition Scintillator (EDS 75-3) Parameters	89
D-4	Energy Deposition Scintillator (EDS 75-1 & EDS 75-2 nosetip) Parameters	94
D-5	Sergeant Hydac Multi IC 819.08-1 Telemetry Technical Data	94
D-6	Sergeant Hydac Multi IC 819.08-1 Telemetry Technical Data	95
D-7	Sergeant Hydac Multi IC 819.08-1 Telemetry Technical Data	95
D-8	Sergeant Hydac IC 819.08-1 1 × 60 Commutator Assignments	96
E-1	Photometer (PM2-48) Parameters	102

LIST OF TABLES (CONT.)

Table No.		Page
E-2	Photometer (PM2-56) Parameters	104
E-3	Radiometer NR4-C-1 (4.3 μm) Transfer Functions . . .	106
E-4	Radiometer NR4-C-1 (2.7 μm) Transfer Functions . . .	108
E-5	Nike Hydac IC 807.15-1 Telemetry Technical Data . . .	109
E-6	Nike Hydac IC 807.15-1 1 × 16 Commutator Assignment .	109
F-1	Nike Hydac IR 807.57-1 Photometer Parameters (PM2-83 & PM2-95)	117
F-2	Energy Deposition Scintillator (EDS 75-5) Parameters .	121
F-3	Nike Hydac IR 807.57-1 Telemetry Technical Data . . .	121
F-4	Nike Hydac IR 807.57-1 1 × 32 Commutator Assignments .	122
G-1	Photometers (PM2-15A) Parameters	126
G-2	Energy Deposition Scintillator Parameters (EDS 75-4A) .	128
G-3	Sergeant IC 830.09-1A Telemetry Technical Data . . .	128
G-4	Sergeant IC 830.09-1A 1 × 48 NRZ Commutator Assignment	129

INTRODUCTION

During the period extending from 28 May 1976 through 30 Sept. 1979 Utah State University, under contract from the Air Force Geophysics Laboratory, has conducted a program of ionospheric research with two primary objectives, i.e., 1) data accumulation from both the naturally and artificially disturbed and quiescent ionosphere, and 2) techniques and instrumentation development. Particular emphasis has been placed upon measurements related to such parameters as energy deposition, optical emissions (ultraviolet, visible and infrared), electron and ion densities, and ion and neutral composition. Equally important during the contractual period has been the emphasis placed upon the development of new and improved techniques for performing ionospheric measurements. Research efforts under this contract have been closely correlated with work efforts and measurements conducted under the auspices of earlier contracts, with this effort directly following that accomplished on contract F19628-74-C-0130 [*Baker et al.*, 1977].

The program of research has been primarily conducted on an *in situ* basis, using instrumented, rocketborne payloads as the measurements platforms, but additionally, ground-based measurements programs have been conducted in conjunction with the rocketborne probes and on specific occasions (as later described) measurements have been conducted in conjunction with an orbiting satellite pass. Measurements have been accomplished during both quiescent and disturbed ionospheric conditions and also in areas artificially perturbed by electron dosing, all to assist in determining ionospheric reaction rates, composition, and responses to external stimuli.

The program of rocket flights and measurements accomplished over the 40 month contractual period is summarized chronologically in Table 1.

The following sections of this report describe the experimental philosophy, design and application of the eight payloads summarized in Table 1. Instruments which have been newly developed or refined are discussed or fully referenced if earlier documentation has been completed.

The reporting format adopted groups the vehicles according to experimental philosophy rather than chronologically. Experimental objectives are discussed for each group, applications and methods are described and subsequently individual instruments are grouped into categories for discussion. The appendices provide calibrations etc. for the instrumentation aboard each payload and are presented chronologically to match the format of Table 1.

TABLE 1

CHRONOLOGICAL SUMMARY OF ROCKET FLIGHTS

AND MEASUREMENTS--CONTRACT F19628-76-C-0261

Rocket No.	Program	Site	Date Time (GMT)	Purpose(s)
Talos Castor EX 651.92-1	EXCEDE	PFRR*	19 Nov. '76 0406	Flight test of high power electron gun. Measurements of electron density (ionization) and vehicle potential in association with atmospheric electron dosing.
Sergeant IC 730.09-1	RBFWI	PFRR	13 Nov. '77 0855	Initial flight (engineering rnd.) of Rocketborne Field-widened Interferometer with accompanying measurements of auroral activity (energy deposition and emission intensity) Field-widened Interferometer developed under contract no. F19628-77-C-0203.
Aerobee 170 A04.602	PRECEDE II	WSMR**	13 Dec. '77 0550	High power electron gun test. Initial flight test (engineering) of liquid nitrogen cooled interferometer developed under contract no. F19628-77-C-0203.

TABLE 1 (cont.)

Rocket No.	Program	Site	Date Time (GMT)	Purpose(s)
Sergeant-Hydac IC 819.08-1	AURORAL WIDEBAND	PFRR	28 Feb. '78 0811	Measurements of ionospheric and auroral parameters during intense auroral activity, including auroral energetics and electron density structure, E-fields, energy deposition, energy spectra and optical emissions. Flight made in conjunction with DNA wideband satellite pass, Chatenika radar observations and extensive ground based measurements.
Nike Hydac IC 807.15-1	AURORAL DYNAMICS	PFRR	26 Nov. '78 0916:31	Correlation of spatial and temporal SWIR emissions with visible emissions and hence, with energy inputs and atmospheric transport during defined auroral arc conditions.
Nike Hydac IR 807.57-1	AURORAL ENERGETICS	PFRR	26 Nov. '78 0929:00	Definition of auroral parameters of power density, electron density (high spatial resolution and accuracy), auroral emissions intensity at 5577Å and 3914Å, Atomic Oxygen density.
Talos Castor EX 851.44-1	EXCEDE II (spectral)	PFRR	29 Oct. '78 0502	Atmospheric excitation via electron dosing from four 10A, 3kV electron guns. Measurements of UV, visible and IR emission intensity and spectra utilizing onboard optical sensors. Measurements of electron density and vehicle potential due to gun operation.

TABLE 1 (cont.)

Rocket No.	Program	Site	Date Time (GMT)	Purpose(s)
Sergeant IC 830.09-1A	RBFWI	PFRR	13 Nov. '78 1244:32	High resolution measurements of spectra as a function of altitude during auroral conditions. Measurements of energy deposition and 3914Å emission intensity to characterize aurora. Cryogenically cooled, Field-widened Interferometer developed under contract F19628-77-C-0203.

* Poker Flat Research Range, Alaska
** White Sands Missile Range, New Mexico

ATMOSPHERIC DOSING

Based upon a concept originated in 1971 by Dr. A.T. Stair, Jr., and later jointly sponsored by AFGL/DNA, electron accelerators and measuring instruments have been incorporated into rocketborne platforms to create and optically monitor artificial auroras for the study of atmospheric infrared emissive processes. These studies are steps toward greater understanding and definition of the emissive processes operative in the naturally occurring, but highly complex auroral phenomena. In the naturally occurring aurora excitation parameters such as electron density and power, deposition volume, altitude and duration of inputs, are elusive, and the resulting effects, i.e., observable emissions, typically are the result of the integration of a wide range of varying input and output conditions. Excitation parameters and intermediate processes therefore, must be inferred rather than empirically determined. In the case of the artificial aurora created via dosing from electron accelerators however, the excitation parameters can to a large extent be controlled, localized and closely monitored, and output emissions coming from a restricted, prescribed volume of close proximity can be more directly assessed, thereby promoting investigations within an area of prime scientific interest, that is, the examination of the specific production and loss processes associated with atmospheric atomic and molecular species in their excited electronic and rotational-vibrational states; accomplished via optical monitoring of emissions as energetic primary electrons, their secondary and all subsequent generation electrons interact with the atmosphere.

Since the inception of the electron dosing concept six vehicles (three under the auspices of this contract) incorporating electron accelerators and monitoring instrumentation have been launched to accomplish the above mentioned research and additional launches are planned for future dates. These vehicles, their launch dates, sites and measurements are briefly summarized in Table 2 in order that the program may be viewed in context. Loosely categorized (and with some varying degree of overlapping) these vehicles can be placed within three groups, i.e.,

1. Engineering rounds for instrument and systems test,
2. Photometric and radiometric measurements of optical emissions in conjunction with atmospheric dosing,
3. Number 2 (above) combined with interferometric and spectrometric measurements of emission spectra.

TABLE 2

LAUNCH SUMMARY-ELECTRON DOSING ROCKETS

Vehicle	Launch Date	Launch Site	Measurements
PRECEDE* Nike Hydac EX 401.41-1	17 Oct 1974	WSMR	Particle flux, vehicle potential 2 Kw Electron Gun
EXCEDE II (test)* Castor C 75-1	13 April 1975	PFRR	Visible, UV & IR intensity, particle flux, vehicle potential, 30 Kw Electron Gun
EXCEDE (SWIR)* Sergeant EX 530.42-1	28 Feb 1976	PFRR	Visible, UV & IR intensity, positive ions, 3 Kw Electron Gun
EXCEDE Talos Castor EX 651.92-1	19 Nov 1976	PFRR	Electron density, vehicle potential, 20 Kw Electron Gun
PRECEDE II Aerobee 170 AO 4.602	12 Dec 1977	WSMR	IR spectra, 20 Kw Electron Gun
EXCEDE II (SPECTRAL) Talos Castor EX 851.44-1	29 Oct 1978	PFRR	Visible, UV & IR emission intensity and spectra, electron density, vehicle potential, 120 Kw Electron Gun (4 at 30 Kw)

*Developed under previous contracts.

Talos Castor EX 651.92-1

EXCEDE

On 19 November 1976, at 0406:40 (GMT) Talos Castor EX 651.92-1 (EXCEDE) was launched from the Poker Flat Research Range, Alaska. This shot was essentially an engineering round, initially with the prime purpose being a test of the recovery system designed for use on large, rocketborne, electron dosing and measurements payloads. It was determined however, that the flight would also provide a good opportunity to test the electron accelerators under rather stringent conditions. Consequently, provisions were made within the payload for two high power electron accelerators and instrumentation to monitor their effects. The final configuration of the payload is described in Figures 1 and 2; Table 3 further documents the instrumentation incorporated within the payload.

It was realized in advance that the high apogee of this flight (265 KM) would give too high of a vehicle velocity for good scientific data on the interaction of the electron beam with the atmosphere in the lower range (95 - 150 Km) but it was felt that the flight would provide a severe test for the electron guns. The guns were turned on at T + 78 seconds as planned. Because of the high dynamic pressure the electron guns had not outgassed to a proper working pressure. Consequently, an electrical discharge appeared as a short circuit to the accelerator. The electronic control circuitry functioned as designed for approximately 60 seconds, i.e., it continued to pulse into the short circuit and then automatically shut down. After 60 seconds, the severe pulse overload currents of greater than 50 amps at 4000 volts appeared to weld the power relay contacts of one gun together, probably resulting in destruction of the unit. The second electron gun continued pulsing for approximately 15 additional seconds. At that time the pressure decreased to a value that allowed the gun to work properly and produce the designed electron beam up to apogee and during descent to about 84 Km at which time it returned to a short circuit.

It was felt that the flight of this payload was successful, yeilding information about the design of the accelerators that would be useful on future flights.

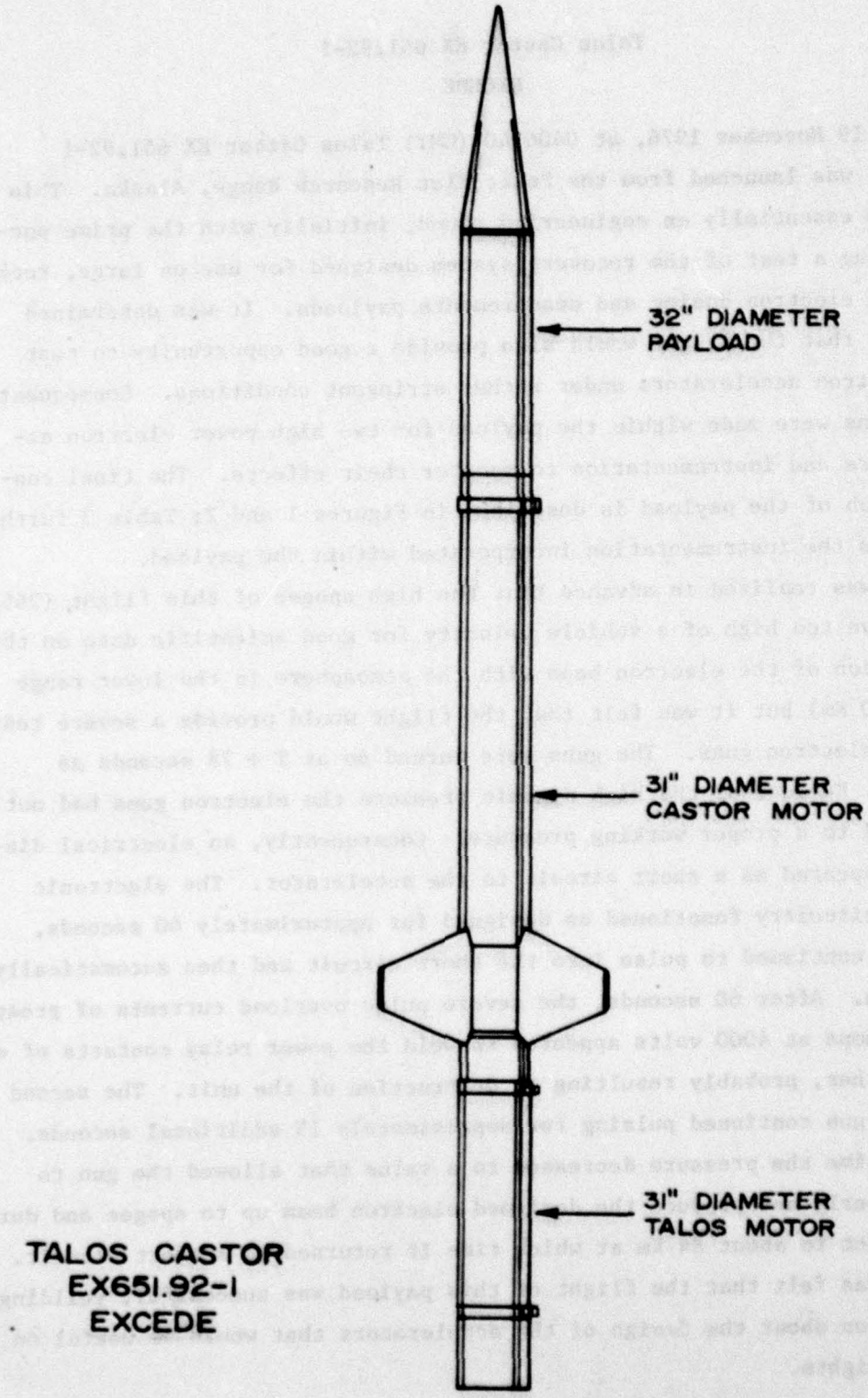


Figure 1. EX651.92-1 Vehicle Configuration.

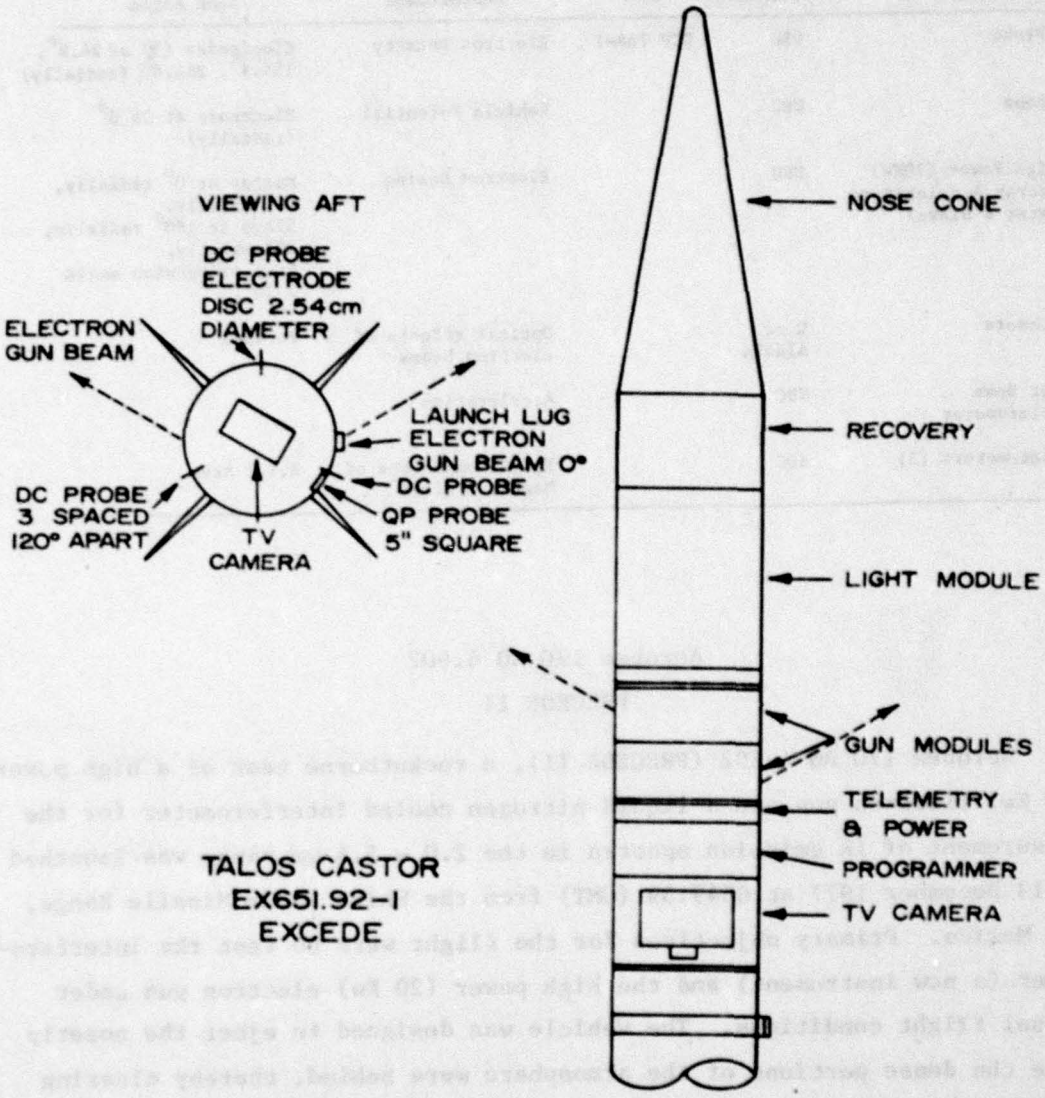


Figure 2. EX651.92-1 Payload Configuration.

TABLE 3

TALOS CASTOR EX 651.92-1 INSTRUMENTATION

Instrument	Experimenter	S/N	Measurement	Look Angle
DC Probe	USU	DCP 76A-1	Electron Density	Electrodes (3) at 24.6°, 155.9°, 264.4°, (radially)
Q Probe	USU		Vehicle Potential	Electrode at 35.8° (radially)
2 High Power (20KW) Electron Accelerators (Master & Slave)	USU		Electron Dosing	Master at 0° radially, 60° axially. Slave at 180° radially, 60° axially. Beam dispersion angle ≈ 30°.
TV Camera	U of Alaska		Optical effects of electron beams	Forward
Light Beam Accelerometer	SDC		Acceleration	
Magnetometers (3)	SDC		X,Y,Z Components of Magnetic Field	X,Y,Z Axes

Aerobee 170 A0 4.602

PRECEDE II

Aerobee 170 A0 4.602 (PRECEDE II), a rocketborne test of a high power (20 Kw) electron gun and a liquid nitrogen cooled interferometer for the measurement of IR emission spectra in the 2.0 - 5.6 μm range was launched on 13 December 1977 at 0549:59 (GMT) from the White Sands Missile Range, New Mexico. Primary objectives for the flight were to test the interferometer (a new instrument) and the high power (20 Kw) electron gun under actual flight conditions. The vehicle was designed to eject the nosetip once the dense portions of the atmosphere were behind, thereby clearing the field-of-view for the liquid nitrogen cooled interferometer. The payload of the vehicle including interferometer and TM sections was recoverable via parachute, but the electron guns were not recoverable, and were designed to remain with the Aerobee motor until impact. This concept and the overall payload and rocket configuration are illustrated in Figures 3 and 4. Table 4 further describes the instrumentation aboard the PRECEDE II payload.

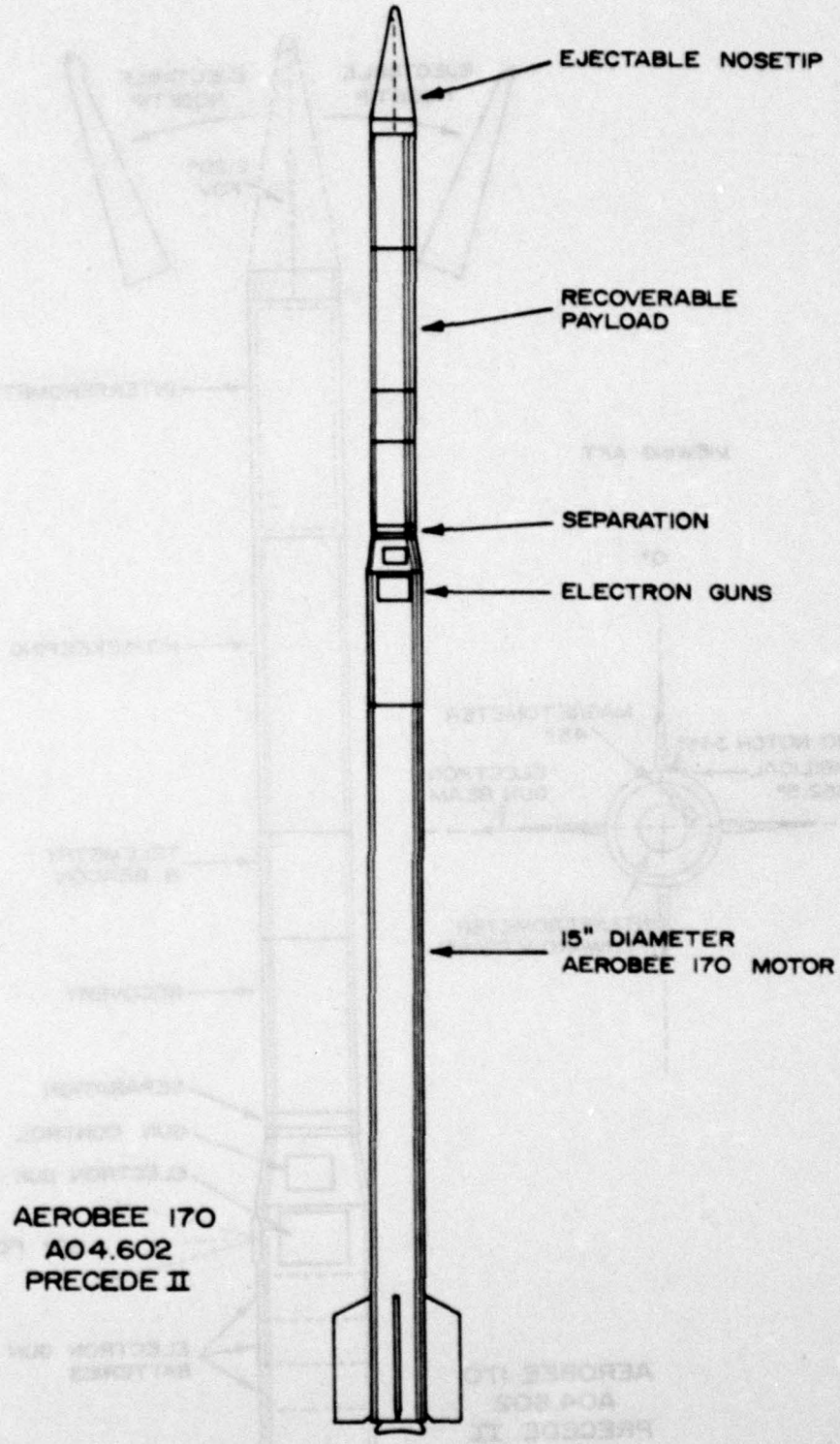


Figure 3. A04.602 Vehicle Configuration.

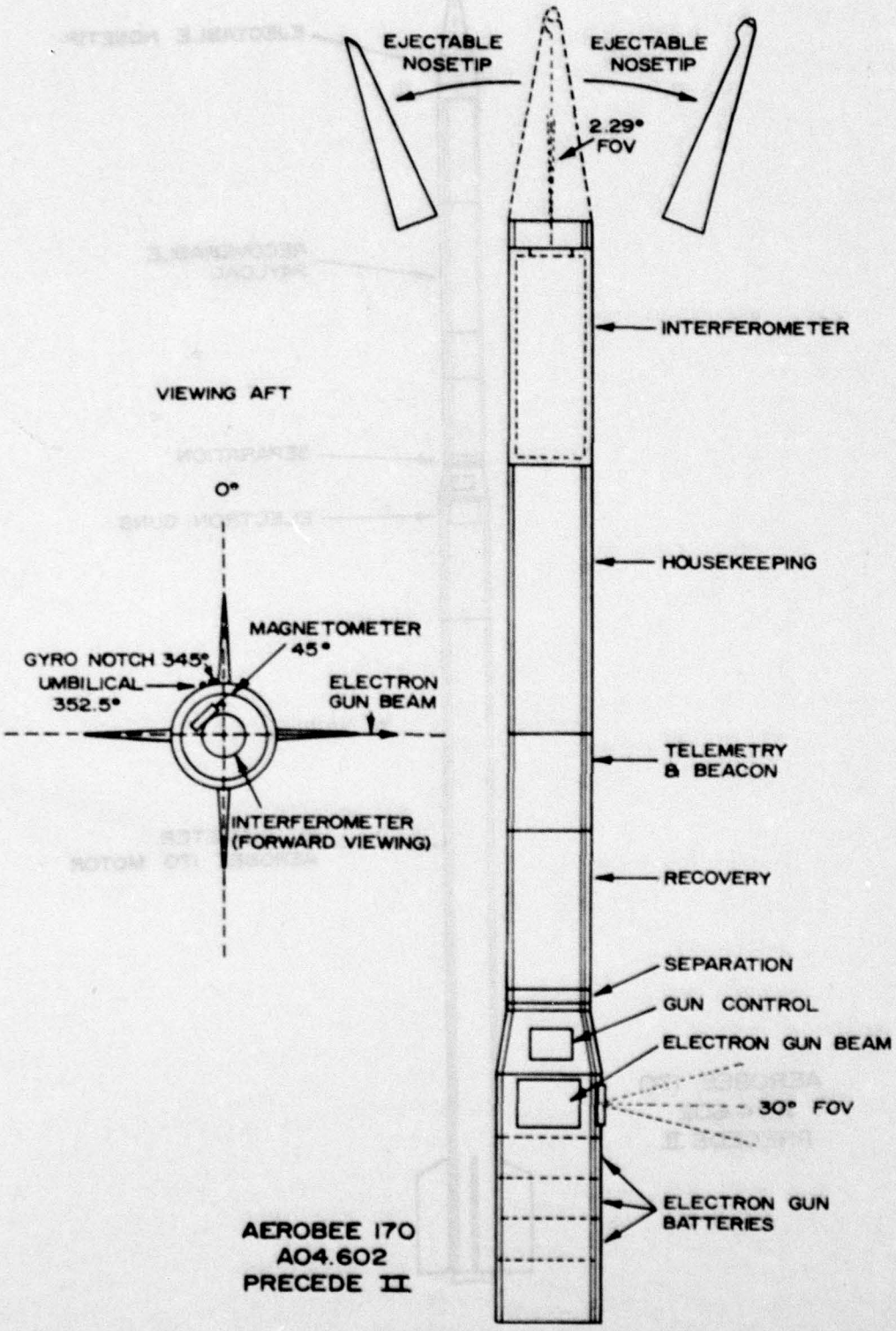


Figure 4. A04.602 Payload Configuration.

The rocket reached an apogee of just over 102 Km, slightly lower than expected, but the primary objectives of the flight were successfully met. The summarized results of the flight of AO 4.602 have been presented by *O'Neil* [1978].

TABLE 4

AEROBEE 170 AO 4.602 INSTRUMENTATION

Instrument	Experimenter	Measurement	Look Angle	Field of View
Liquid Nitrogen Cooled IR Spectrometer*	USU	SWIR Spectra 2.0 - 5.6 μm	Forward (Axially)	2.29°
Electron Accelerator	USU	Electron Beam	Radially at 90° with respect to Gyro Notch, Perpendicular to major axis	Beam $\sim 30^{\circ}$

* Developed under Contract F19628-77-C-0203

Talos Castor EX 851.44-1

(EXCEDE II SPECTRAL)

The payload of EXCEDE II (spectral) was designed for programmed electron dosing of the upper atmosphere by electron accelerators (electron guns) and optical photometric, radiometric, interferometric and spectrometric monitoring of the effects of such dosing in the ultraviolet, visible and infrared regions of the spectrum. Additional instruments provided for measurements of ionization and vehicle charging as a result of the operation of the electron guns [*O'Neil et al.*, 1976].

The payload was launched aboard a Talos Castor vehicle (EX 851.44-1) from the Poker Flat Research Range, Alaska at 0502:00 (UT) on 20 October 1978. The flight plan for EX 851.44-1 called for separation of the payload from the motor section after motor burnout, despin of the vehicle and an attitude control manuever to orient and stabilize the payload at 43° (with respect to horizontal) in order that the electron beam (canted 60° from the rocket's major axis) from the accelerators would be directed along the B-field (77° inclination at Poker Flat). Instrument doors were

to be removed to clear the field-of-view of the optical instruments and the electron beam path for the accelerators. Optical measurements of the effects of the 120 Kw beam were to be monitored for a duration of approximately 165 seconds (from approximately 95 Km (ascent) through an apogee of 120 Km down to 80 Km). After completion of the measurements portion of the flight the instruments section and accelerator sections were to be separated for recovery, each with its own recovery system. Although launch and flight of the vehicle were as planned, unfortunately the door behind which all optical measuring devices were situated, failed to deploy. Flight records indicate that the measurements instrumentation aboard the payload functioned normally, but due to the fact that the payload door did not deploy, no data were obtained.

Flight records and ground based observations indicate that of the four, 10 amp, 3000 volt electron accelerators only one functioned normally.

Post flight recovery was successfully accomplished for the measurements section of the EXCEDE II (spectral) payload with minimal damage incurred. Examination at the impact area (accelerators) was accomplished and portions of the accelerators were returned to the launch site for further post flight examination.

Abbreviated post flight summaries of the operation of the vehicle and support instrumentation and the measurements instruments aboard EXCEDE II (spectral) have been accumulated and presented by *O'Neil* [1978].

Due to the fact that no data were obtained from the flight of EX 851.44-1 it is deemed inappropriate to present calibration data for the instruments provided. This report does include however, a complete listing of the instruments included aboard the payload and later sections discuss philosophy and operation principles of this instrumentation. Table 5 and Figures 5 and 6 summarize instruments aboard the payload and portray their locations and general payload/rocket configuration.

Tentatively in October 1979, the EXCEDE (spectral) experiment will be repeated under the auspices of Contract No. F19628-79-C-0080 with refinements and modifications based upon the information accumulated from the October, 1978 flight. An instrumentation report detailing the new payload is planned for that experiment.

Launch and flight of the EXCEDE II (spectral) payload was monitored by extensive ground based instrumentation. These instruments also monitored

the flights of IC 807.15-1 and IC 807.57-1. A complete listing of this instrumentation is included in a following section as Table 12.

TABLE 5

TALOS CASTOR EX 851.44-1 INSTRUMENTATION

Instrument	Experimenter	S/N	Measurement	Look Angle	Field of View (Full Angle)
Photometer	USU	PM2-70	3910A	0° radially, perpendicular to major axis	4°
Photometer	USU	PM2-33	5579A	0° radially, perpendicular to major axis	4°
Photometer	USU	PM2-71	5270A	0° radially, perpendicular to major axis	4°
Photometer	USU	PM2-79	7860A	0° radially, perpendicular to major axis	4°
Photometer	USU	PM2-82	5579A	0° radially, perpendicular to major axis	4°
Photometer	USU	PM2-81	4416A	0° radially, perpendicular to major axis	4°
Photometer	USU	PM2-87	3914A	0° radially, perpendicular to major axis	4°
Photometer	USU	PM2-74	3914A	0° radially, perpendicular to major axis	2.2°
CVF Spectrometer	USU	HS-3B-1	13.05-22.43 μm, 4.04-6.74 μm	0° radially, perpendicular to major axis	4x4°
Dual-Channel Radiometer	USU	NR-5-4	2.7μm & 5.4μm	0° radially, perpendicular to major axis	4x4° 4x4°
CVF Spectrometer	USU	NS-6-4	2.07-3.54 μm, 3.37-5.28 μm	0° radially, perpendicular to major axis	4x4°
Interferometer	USU (SRL)	CM-1-1	2.0-5.6 μm	0° radially, perpendicular to major axis	2.3°
Plasma Frequency Probe	USU	PFP78-1	Electron density	Electrode at 226° radial	N/A
Skin Current Probe 1	USU	SCP77-1	Return Current	Sensor at 319° radial	N/A
Skin Current Probe 2	USU	SCP77-2	Return Current	Sensor at 180° radial	N/A
Q Probe	USU	QP77-2	Vehicle Potential	Sensor at 180° radial	N/A
TV Camera	U of AK		Ionization emission due to dosing by Electron Guns	0° radially, perpendicular to major axis	60°x80°
Cine Camera (B & W)	Photometrics		Ionization emission due to dosing by Electron Guns	0° radially, 105° with respect to major axis	90° x 60°
Cine Camera (Color)	Photometrics		Ionization emission due to dosing by Electron Guns	0° radially, 105° with respect to major axis	90° x 60°
Visible & UV Diodes				0° radially, perpendicular to major axis	90° x 60°
UV Spectrometer	Visidyne			0° radially, perpendicular to major axis	90°
Visible Spectrometer	Visidyne			0° radially, perpendicular to major axis	90°

TABLE 5 (cont.)

Instrument	Experimenter	S/N	Measurement	Look Angle	Field of View (Full Angle)
Electron Guns (4)	USU	A(master)	Dosing (programmed)	0° radially, 60° from major axis	∿ 30° Beam Angle
		B(slave)	Dosing (programmed)	0° radially, 60° from major axis	∿ 30° Beam Angle
		C(slave)	Dosing (programmed)	0° radially, 60° from major axis	∿ 30° Beam Angle
		D(slave)	Dosing (programmed)	0° radially, 60° from major axis	∿ 30° Beam Angle

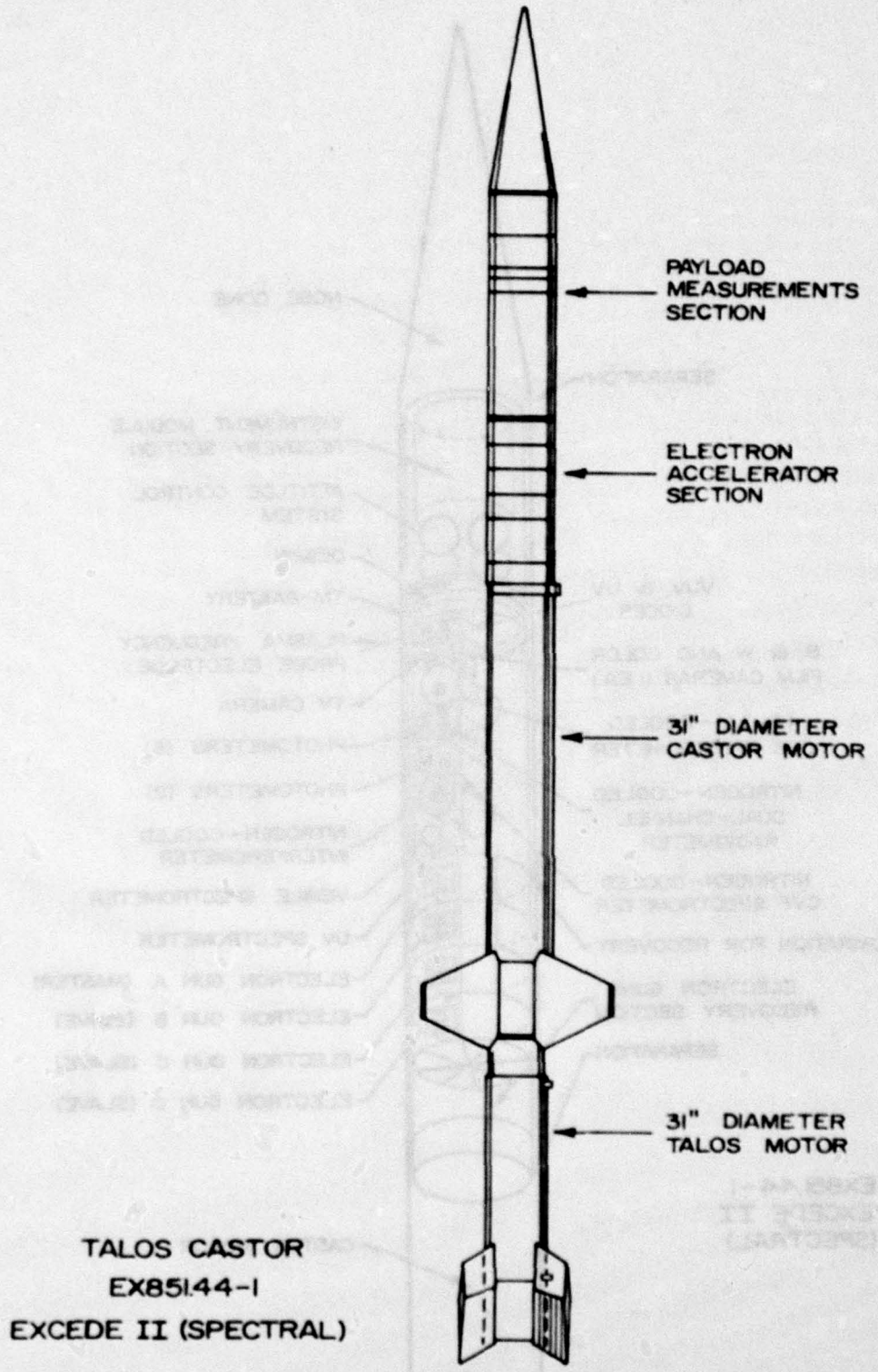


Figure 5. EX851.44-1 Vehicle Configuration.

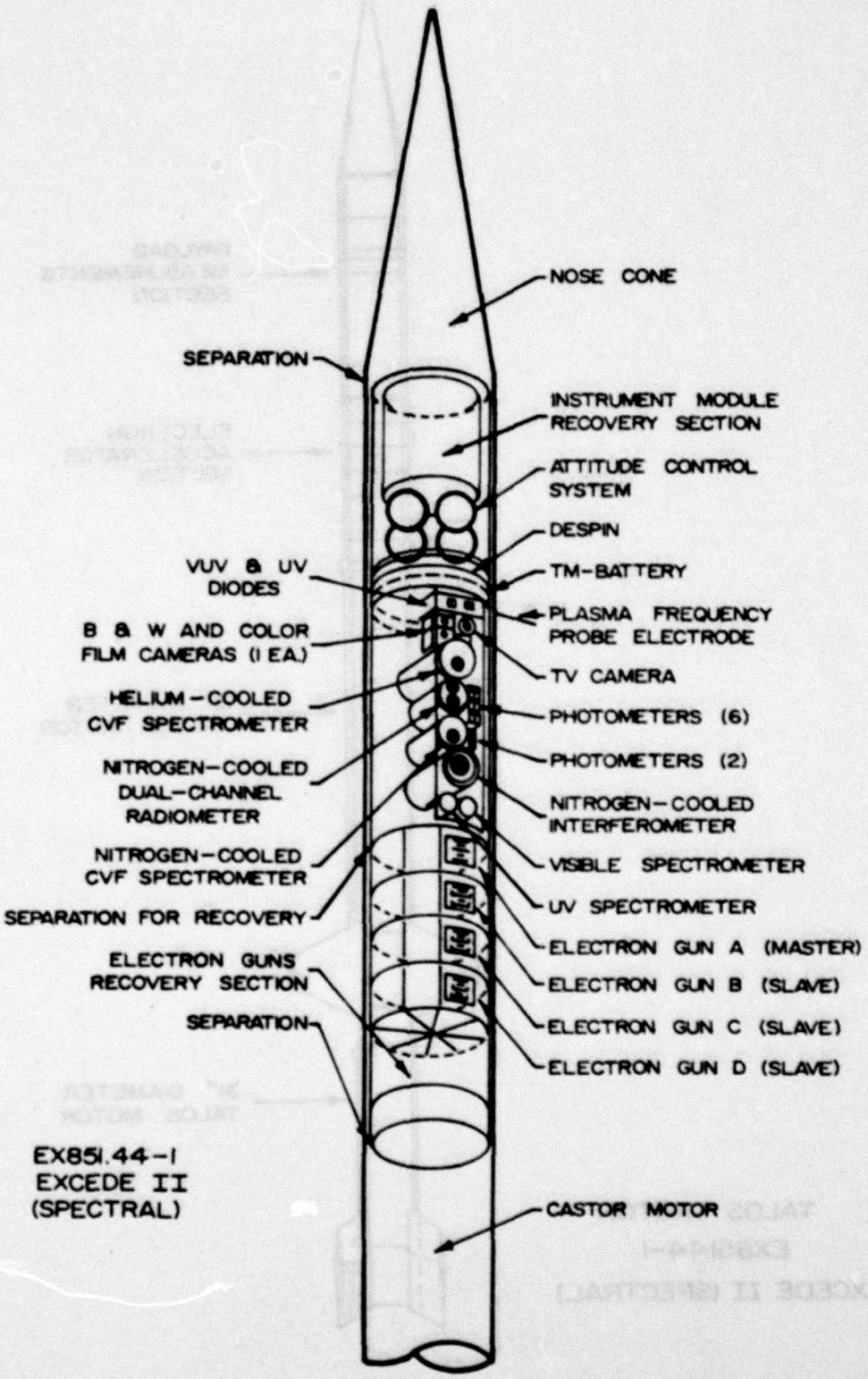


Figure 6. EX851.44-1 Payload Configuration.

DEVELOPMENTAL FLIGHTS - FIELD-WIDENED INTERFEROMETER-SPECTROMETER

Under the auspices of AFGL Contract Numbers F19628-67-C-0322 and F19628-73-C-0048 a successfully operating ground based instrument known as a Field-Widened Interferometer-Spectrometer has been developed at Utah State University for the Defense Nuclear Agency to support the ICECAP program.

This device is capable of measuring near infrared spectral emissions from the zenith night sky more than 100 times faster than conventional interferometers with equivalent collecting areas and detector sensitivities. The instrument is cryogenically cooled to liquid nitrogen and liquid helium temperatures in order to achieve the desired wavelength response, and field compensation and scanning are accomplished by the use of both fixed and mobil optical wedges and mirrors. The instrument is now being adapted to rocketborne flight so that infrared spectral emissions measurements may be made on an *in-situ* basis. The *in-situ* measurements will contribute greatly to overcoming the problems of emissions absorption and masking that are encountered when attempts to monitor these emissions are made from ground based locations, and will provide altitude profiles of emission intensity.

Although the adaptation for rocketborne flight of the field-widened interferometer is being accomplished under the auspices of other contracts (F19628-77-C-0203 and F19628-79-C-0080), complete payloads for support of the interferometer and launches of the two rockets that have contained field-widened interferometers to date (IC 730.09-1 and IC 830.09-1A) have been completed under the auspices of Contract Number F19628-76-C-0261. These payloads, instruments and flights are covered in the following pages.

Sergeant IC 730.09-1

Sergeant Rocket IC 730.09-1 was launched from the Poker Flat Research Range, Alaska at 0855:00, 13 November 1977 (GMT) into a 30-KR post-breakup auroral glow. The sensors on this developmental payload were a 1.5 to 8 μm cryogenically-cooled (liquid helium) field-widened interferometer-spectrometer, a 3914-A photometer, and an energy deposition scintillator. The

primary objectives of this flight were to flight test the newly developed 1.5 to 8.0 μm cryogenically cooled interferometer-spectrometer, and to recover the instrument for future flights. Consequently, the payload was instrumented for parachute recovery in addition to the measurements instrumentation. Launch criteria were established to conform to these objectives. In particular, the decision was made to launch into a post-auroral breakup in order to insure that the rocket would penetrate an aurorally disturbed atmosphere and that the auroral emissions would be bright enough to insure good signal strength. On-board supporting scientific instrumentation included a photometer for measurement of 3914 A emissions and an energy deposition scintillator (EDS) for measurement of energy deposition by electrons with energy greater than 5 KeV. These measurements were to assist in defining the energy input into the region scanned by the field-widened interferometer.

The cryogenically cooled, field-widened interferometer, which was the primary sensor flown aboard Sergeant IC 730.09-1, is an adaptation of the successfully operating ground based interferometer developed for the Defense Nuclear Agency to support the ICECAP program. A very significant modification, additional to the very difficult problem of adapting to a rocket, was the problem of extension of the spectral range from a cut off of 2.9 μm to 8.0 μm. The flight thus was in no way routine but an initial engineering test of an instrument that is advanced state-of-the-art. Since the interferometer was developed under the auspices of another contract, this report is restricted to supporting instruments, rocket configuration and flight. Figures 7 and 8 portray the configuration of the Sergeant IC 730.09-1 vehicle and its instruments. Table 6 details pertinent instruments and parameters.

The flight of IC 730.09-1 was supported by numerous ground based instruments to assist in characterizing the auroral conditions both prior to, during, and subsequent to the rocket flight. This supporting instrumentation is described in Table 7.

TABLE 6

SERGEANT IC 730.09-1 INSTRUMENTATION

Instrument	S/N	Measurement	Look Angle	Field of View (Full Angle)
Cryogenically cooled Field-widened Interferometer-Spectrometer	RBFWI 77-1	Infrared Spectra 2.0 - 7.5 μm	Forward axially	10.5°
Photometer	PM2-15	3914A Emissions (N_2^+)	Radially to mirror then forward axially (0°)	5°
Energy Deposition Scintillator	EDS 75-4	Electrons, E≥5Kev	60° axially 315° radially	19°

TABLE 7

COORDINATED GROUND SUPPORT INSTRUMENTATION

SERGEANT IC 730.09-1

Experimenter	Instrument	Parameters
USU	Field Widened Interferometer-Spectrometer	λ: 1.5 to 2.7 μm Resolution: 3 cm^{-1} Field of View: 12° full angle Scanning Rate: 15 sec.
USU	Field Widened Interferometer-Spectrometer	λ: 0.84 to 1.6 μm Resolution: 5 cm^{-1} Field of View: 12° full angle Scanning Rate: 2 min.
USU	Dual Channel Radiometer	λ: 1.7 and 1.27 μm Field of View: 5° full angle Temporal Resolution: 10 sec.
USU	Digital Photometers	λ: 5577A and 3914A Field of View: 5° full angle Temporal Resolution: 1 sec.
USU	Rocking Filter Photometer with Filter Wheel	λ: 4278A, 4861A, 5577A, 6300A, 8446A Field of View: 2° full angle Temporal Resolution: 1 rock/sec.
USU	Meridian Scanning Photometers	λ: 3914A, 5577A, 6300A Field of View: 2° full angle Temporal Resolution: 30 sec.
USU	Meridian Scanning Photometer (for Scientific Launch Control)	λ: 3914A, 5577A Field of View: 2° full angle Temporal Resolution: 30 sec.
USU	Data Handling and Processing System	PDP8 with disc and dual tape drives - Near real time transform
U of Alaska	Four Meridian Scanning Photometers	λ: 4278A, 4861A, 5577A, 6300A Field of View: 2° Temporal Resolution: 2 sec.
U of Alaska	One-meter Grating Spectrometer	
U of Alaska	One-half-meter Grating Spectrometer	
U of Alaska	Tilting Filter Photometers	λ: 7774A and 8447A
U of Alaska	Three-Axis Magnetometers	

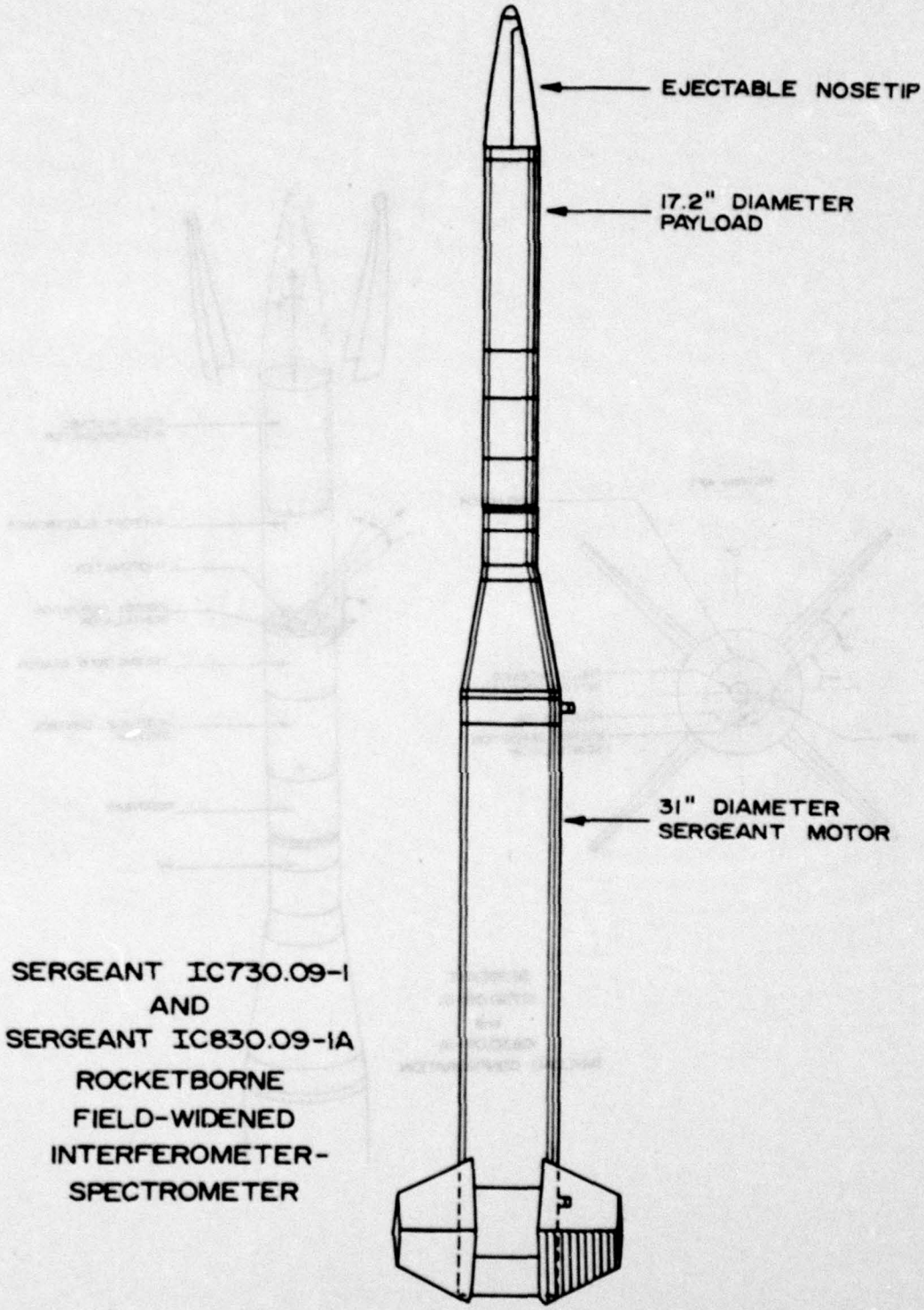


Figure 7. Sergeant IC730.09-1 and Sergeant IC830.09-1A Vehicle Configuration.

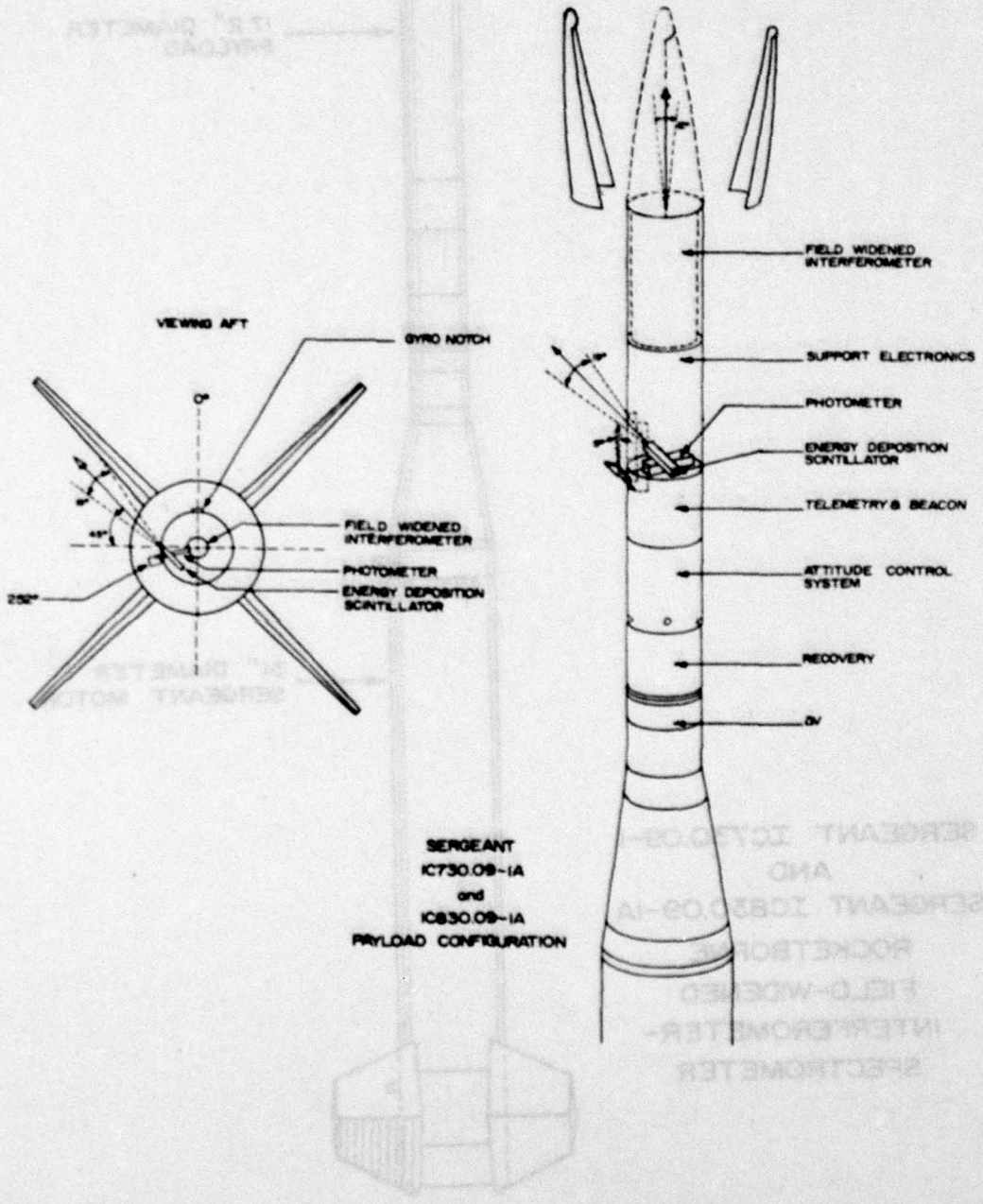


Figure 8. Sergeant IC730.09-1 and Sergeant IC830.09-1A Payload Configuration.

Sergeant IC 830.09-1A

On 13 November 1978 at 1244:32 (GMT) Sergeant IC 830.09-1A was launched from the University of Alaska's Poker Flat Research Range. The purpose of the flight was to obtain high resolution shortwave infrared spectra as a function of altitude in an aurorally disturbed atmosphere, and additionally to provide measurements of energy deposition and 3914Å emission intensity to assist in characterizing the auroral event. The prime sensor aboard the rocketborne payload was the cryogenically cooled, field-widened interferometer-spectrometer for measurements of infrared emissions to provide spectra in the 2.0 - 7.5 μm region.

The vehicle was launched through an overcast sky into enhanced electron density conditions (auroral) as indicated by Chatanika incoherent scatter radar measurements. Onboard monitors indicated that the payload penetrated intense auroral conditions. Post flight recovery of the payload was accomplished on 14 November 1978.

No auroral data were obtained from the prime sensor aboard the payload due to an apparent failure of the instruments' pop cover seal and subsequent warming to levels which resulted in instrument saturation. Diagnostic measurements from monitors within the prime sensor, however, indicate that a major objective of sustaining the alignment of the instrument after rocket engine burnout was achieved.

Supporting measurements of 3914A emission intensity and energy deposition were good and indicate that the payload penetrated intense auroral conditions.

An analysis of the flight of IC 830.09-1A has been completed and submitted to DNA [*AFGL and USU*, 1978].

The payload of IC 830.09-1A had previously flown as IC 730.09-1, hence configurations were identical. The reader is referred to Figures 7 and 8 of this report for a graphic summary of configuration details. Table 8 lists the instrumentation aboard the payload of IC 830.09-1A.

TABLE 8

SERGEANT IC 830.09-1A INSTRUMENTATION

Instrument	S/N	Measurement	Look Angle	Field of View (Full Angle)
Cryogenically cooled Field-widened Interferometer-Spectrometer	RBFWI 78-1	Infrared Spectra 2.0 - 7.5 μm	Forward axially	10.5°
Photometer	PM2-15A	3914A Emissions (N_2^+)	Radially to mirror then forward axially (0°)	5
Energy Deposition Scintillator	EDS 75-4A	Electrons, E≥5KeV	60° axially 315° radially	19°

AURORAL WIDEBAND COMMUNICATIONS

Sergeant Hydac IC 819.08-1

In conjunction with certain circumstances and conditions, as yet only partially defined and understood, radio waves transmitted through the upper atmosphere are subject to interference caused by atmospheric phenomena. The interference takes the form of amplitude and phase changes in the propagating waves - the result being scintillations of the signal. Such scintillations are detrimental to the quality of transmissions, especially where satellites are involved, and can affect frequencies as high as S-band.

To investigate these scintillations, Sergeant Hydac IC 819.08-1 (multi) was launched from the Poker Flat Research Range, Alaska at 0810:50 UT on 28 February 1978. This payload was an integral part of a coordinated program which also employed the DNA/SRI wideband satellite and the Chatanika radar. Launch of the IC 819.08-1 payload was accomplished in conjunction with intense auroral activity, a simultaneous overpass of the wideband satellite, measurements by Chatanika radar and extensive ground based optical (and other) measurements.

The payload of the vehicle was multi-instrumented to measure electron density distributions with spatial resolution down to about a meter, while simultaneously measuring the energy input mechanisms of complete energetic electron spectra and pitch angle distribution, and complete AC and DC electric fields.

Configuration of the multi payload was such that a nosetip section, instrumented for the measurement of electron pitch angles, was ejected from the main payload during rocket flight. The ejected nosetip was equipped with its own independent telmetry system, scintillators, and three-axis magnetometers to accomplish its purpose. Table 9 is a summary of instrumentation included in the main payload and ejected nosetip payload of Sergeant Hydac IC 819.08-1 along with the parameters of field-of-view and look angles of the instruments. Figures 9 and 10 graphically portray the vehicle configuration and the main and nosetip payloads.

Preliminary results from the multi-measurements payload along with those from the Chatanika radar and the Wideband Satellite pass have been reported to the Defense Nuclear Agency in *Coordinated Investigations of High Latitude Scintillations by Wideband Satellite, Chatanika Radar and Sergeant-Hydac Multi Rocket Conducted 08:10:05 UT on 28 February 1978.* This report was jointly submitted by Air Force Geophysics Laboratory, Stanford Research Institute and Utah State University. The *SUMMARY* of that report is included here for reference:

> "This report contains a quick look overview of the results of the DNA sponsored coordinated experiment [directed] towards an understanding of radio wave scintillations from an upper atmospheric region disturbed by high energy electron excitation. The rocket flight of the multi-instrumented Sergeant Hydac rocket, the simultaneous overpass of the DNA/SRI wideband satellite, measurements by the Chatanika radar, measurements by ground based optical and other sensors, and, very importantly, the desired auroral conditions, resulted in the most complete and successfull investigation of this kind ever attempted. Although complete data reduction will take several months, nevertheless it should be noted that this report contains (in addition to quick look samples of key results) a significant amount of complete altitude profiles from the rocketborne sensors. This was possible only due to a significant field effort, the development of many detectors/sensors with this in mind and the acquisition of portable field data reduction equipment from DNA specifically for this purpose.
>
> "The rocket (SH 819.08-1) was launched at 0810:50 UT, 28 February 1978 reaching an apogee altitude of 450 Km, penetrating and overflying a region that had just experienced an intense auroral breakup - which was the desired critera for launch established by the DNA Project Manager and participating agencies. A distinct plus, however, was the fact that the rocket after apogee overflew an extremely bright arc (over 150 KR at 5577A emission) that remained in position throughout the rocket flight. The satellite pass, although at a relatively low elevation, traversed the general regions probed by the rocket during the period of the intense auroral activity.
>
> "All instruments aboard the rocket functioned beautifully throughout the flight providing a wealth of data on the energetics and electron density structure associated with the auroral disturbance. Electron densities in the E-region recorded values as high as 8×10^5 electron per cm^3. The electric field sensors detected a rapidly varying field with values as high as 140 millivolts per meter, which may be the largest values ever recorded. This occurred at rocket passage through the magnetic field lines connected to the bright arc. Simultaneous measurement by the onboard scintillator indicated total energy deposition of the auroral electrons with energies greater than 3.0 KeV was over 250 ergs per cm^3 per sec, which is extremely

intense. The onboard electrostatic analyzer indicated a flat energy spectra which means the precipitating particle flux was mainly composed of high energy electrons. The preliminary analysis of the electric field data from Chatanika Radar indicates the presence of an enhanced eastward component of the electric field in the vicinity of the northernmost arc. This arc was first noted by radar during rocket flight about 250 Km to the north with electron densities greater than 4×10^5 electrons per cm^3. The wideband scintillation data indicates a high degree of irregularity development during the overpass. During the most disturbed period, the intensity scintillation saturated at VHF ($S_4 \simeq 1$) and the phase variance (σ_0) exceeded 10 radians.

"Detailed analysis of the wideband data in conjunction with the all-sky TV data should provide a measure of the irregularity spectrum and irregularity drifts of the same structures probed by the multipayload."

TABLE 9

SERGEANT HYDAC IC 819.08-1 MULTIPAYLOAD

INSTRUMENTATION

MAIN PAYLOAD

Instrument	S/N	Measurement	Look Angle	Field of View (Full Angle)
Photometer	PM2-42	3914A(N_2^+)	Forward (axially)	5°
Photometer	PM2-51	6300A(O)	Forward (axially)	5°
Energy Deposition Scintillator	EDS-75-3	Total electron energy deposition (>3KeV)	45° Forward with respect to major axis, 25° radially with respect to launch lug	19°
Electrostatic Analyzer 1	211	Primary Electrons 1-30 KeV	45° Forward with respect to major axis, 25° radially with respect to launch lug	
Electrostatic Analyzer 2	202	Primary Electrons 1-30 KeV	45° Forward with respect to major axis, 205° radially with respect to launch lug	
C-Probe	C76M-1	Electron density, Δ Electron density (1M)	110° radially with respect to launch lug	N/A
DC-Probe	DCP76-1	Electron density, Δ Electron density (1M)	210° radially with respect to launch lug	N/A
Plasma Frequency Probe	PFP76M-1	Electron density	Sensor at 290° radially with respect to launch lug	N/A
HARP		Secondary and Soft Primary Electrons (1 - 1000eV) Electron Temperature	Forward (axially)	
3-Axis E-Field Probes		$\bar{E}_{DC}$ (>1mv/M) $\bar{E}_{DC}$ (>0.1uv/$Hz^{\frac{1}{2}}$)	Antennas at 1. 135° 2. 315° 3. 45° 4. 225° all radially with respect to launch lug	N/A
Magnetometers (2)		Magnetic Field (2 axes)	Aligned with ESA 1, & 2	N/A

TABLE 9 (cont.)

NOSETIP PAYLOAD

Instrument	S/N	Measurement	Look Angle	Field of View (Full Angle)
Magnetometers (3)		Magnetic Field (3 axes)	X,Y,Z	N/A
Energy Deposition Scintillator	EDS75-1	Electron Pitch Angles (E>3KeV)	180° Radially 30° Axially	19°
Energy Deposition Scintillator	EDS75-2	Electron Pitch Angles (E>3KeV)	0° Radially 30° Axially	19°

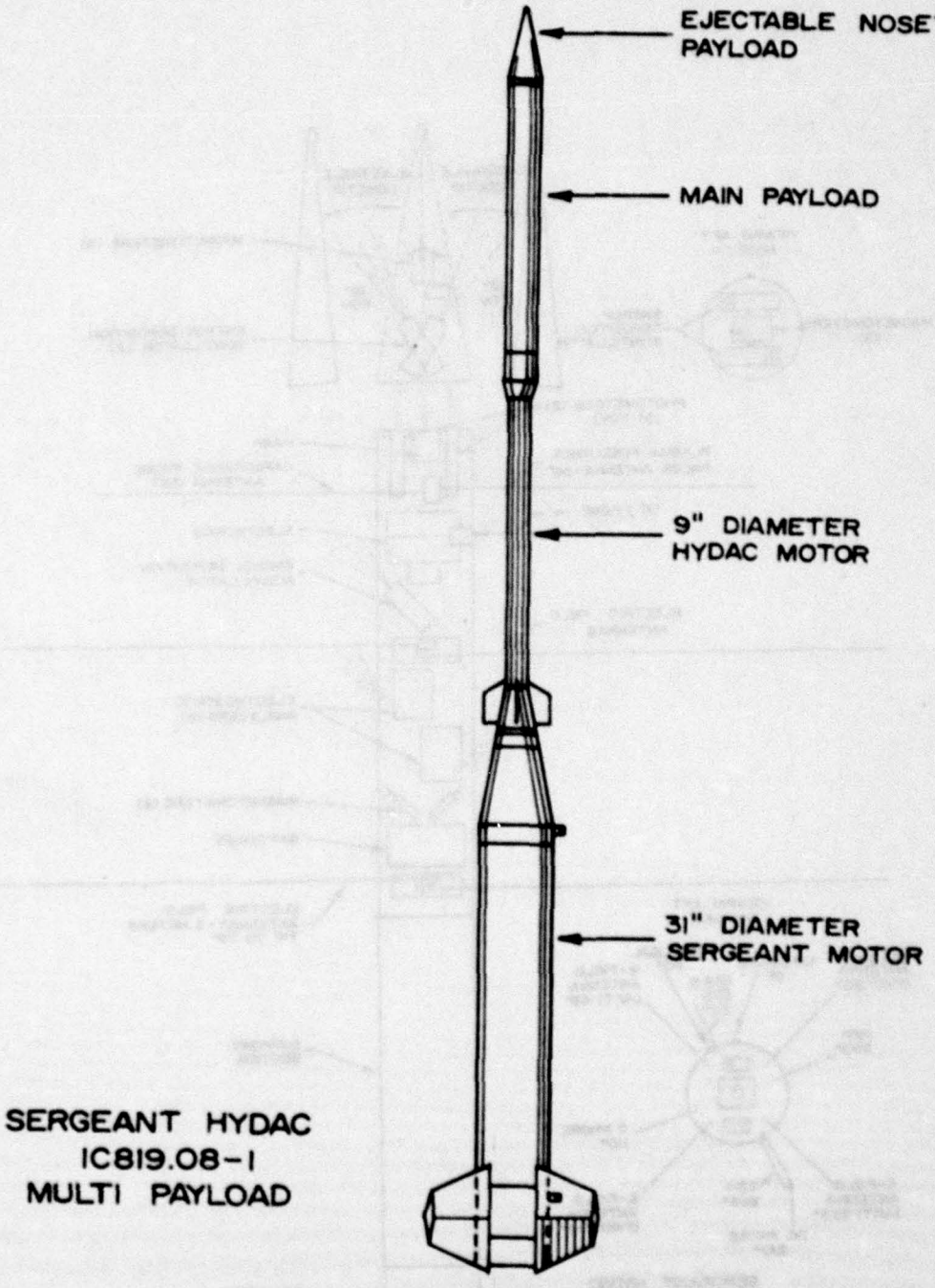


Figure 9. Sergeant Hydac IC819.08-1 Vehicle Configuration.

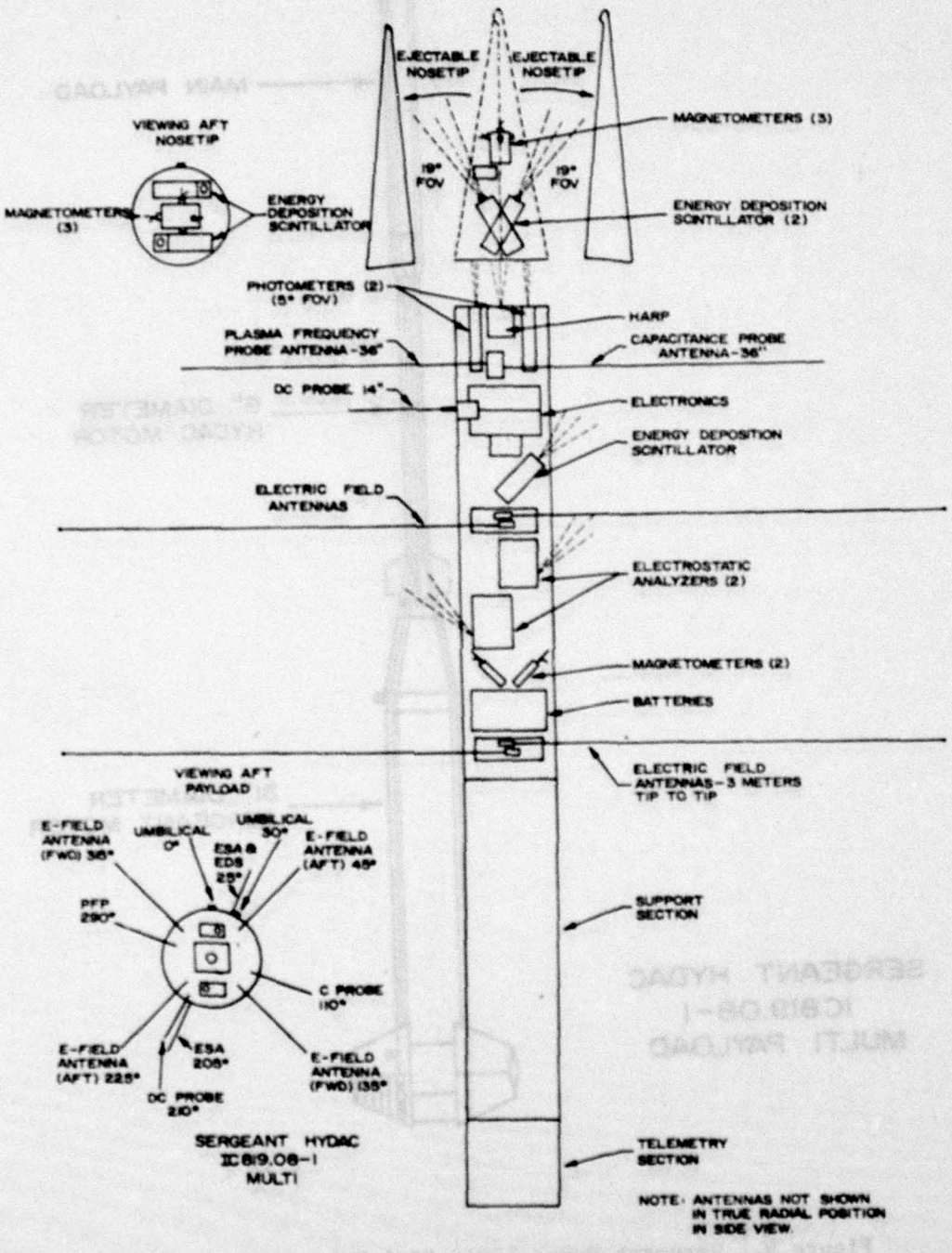


Figure 10. Sergeant Hydac IC819.08-1 Payload Configuration.

AURORAL DYNAMICS AND ENERGETICS

Nike Hydacs IC 807.15-1, IC 807.15-2 and IR 807.57-1

The Auroral Dynamics/Energetics program was conducted at the Poker Flat Research Range (PFRR), Alaska during October 1978. This program was a coordinated effort in which a defined auroral arc was examined in an attempt to provide measurements that would aid in correlating the spatial and temporal shortwave infrared emissions with visible emissions and hence, with energy inputs and atmospheric transport. The mission plan and objectives included rocketborne spatial and temporal sampling of infrared emissions from CO_2 and NO at 4.3 μm and 2.7 μm respectively, and sampling of ultraviolet emissions from the N_2^+ first negative system in order to determine the extent, magnitude and altitudes of origin of these emissions. Rocket trajectories were planned so that the instrumented payloads would traverse areas that were; (1) Not yet occupied by the auroral arc, (2) Occupied by the arc, and (3) Previously occupied by the arc. The long residence time of the 4.3 μm emissions (approximately 10 minutes) dictated the necessity for other simultaneous measurements relating to the parameters of excitation, radiation, diffusion, temperature and wind transport.

Execution of the full experimental program called for the sequential launchings of three rockets when auroral conditions were appropriate, i.e., two Nike Hydac boosted measurements payloads (IC 807.15-1 and IC 807.15-2) and a third Nike Javelin boosted chemical payload (IC 806.35-1) for a TMA release. The measurements payloads were instrumented by Utah State University with new, liquid nitrogen cooled radiometers which have improved NESR, field-of-view, dynamic range and baffling. The radiometers were configured to monitor the Shortwave Infrared (SWIR) emissions and their distributions. The TMA release from the third vehicle was to be monitored via the University of Alaska low light level TV system (ground based) to assess and record auroral structure and possibly also provide information about atmospheric winds. Upper atmospheric wind information was also to

be obtained by the SRI Chatanika radar and the Lockheed spatial - photometer array. Temperature (important in determining diffusion rates) was to be monitored by the USU field-widened interferometer (ARGUS system), ion temperature in the higher altitude regime would be available from Chatanika radar. On board photometers (IC 807.15-1 and IC 807.15-2) at 4278A and 4259A would provide a measure of the rotational temperature (related to ambient) of the N_2^+ first negative system.

On October 26, 1978 at 0916:31 GMT, Nike Hydac IC 807.15-1 was launched from Pad 5L at the University of Alaska Poker Flat Research Range into a bright (~50 kR), relatively stable auroral arc. The arc had developed throughout the evening, then before launch progressed northward and became bright and relatively stable in a suitable position for accomplishment of the auroral dynamics mission. The vehicle achieved an apogee of approximately 121 Km and impacted (LOS) at T + 339 (360 OKla) seconds.

At 0918:45 GMT (2 min. 14 sec. after the launch of IC 807.15-1) an attempt was made to launch IC 807.15-2 from Pad 5R. This launch however, was aborted due to a misfire of the vehicle. The misfire was later found to be the result of a detached igniter connection caused by debris accompanying the shock wave from the first launch.

At 0920:00 GMT (also on October 26) the TMA Nike Javelin IC 806.35-1 was launched. A misfire of the second-stage Javelin motor prevented attainment of sufficient altitude and the TMA release did not occur.

The bright auroral form remained unusually stable in the same general area for a sufficient length of time to provide the opportunity to launch a fourth rocket (Nike Hydac IC 807.57-1, auroral energetics payload) to more thoroughly define the auroral energy deposition and provide supporting data. This payload was launched at 0929:00 GMT. The rocket functioned normally, achieved an apogee of approximately 160 Km and impacted (LOS) at T + 386 seconds.

Suitable occasion for the launch of IC 807.15-2 did not occur within the launch window and this payload was removed from the program, possibly to be utilized at some future date.

Although the payload of IC 807.15-1 was instrumented for parachute recovery and the recovery system appears to have functioned properly,

heavy forestation in the recovery area and snows subsequent to launch have to date prevented the recovery of the payload.

Instrumentation of the identical payloads IC 807.15-1 and IC 807.15-2 is detailed in Table 10 along with particulars detailing instrument look angles, fields-of-view, etc. Figures 11 and 12 pictorially detail the payloads.

Table 11 and Figures 13 and 14 provide similar information for the IR 807.57-1 payload.

Individual instruments aboard the IC 807.15-1 and IR 807.57-2 payloads are discussed in a later section of this report.

TABLE 10

NIKE HYDAC IC 807.15-1 and IC 807.15-2

INSTRUMENTATION

Vehicle	Instrument/ Serial No.	Measurement	Look Angle	Field of View
IC 807.15-1	Dual-Channel Radiometer	2.7 μm	Forward	4° Full angle
	(NR4-C-1)	4.3 μm	Forward	4° Full angle
	Photometer (PM2-48)	4278 A	Forward	5° Full angle
	Photometer (PM2-56)	4259 A	Forward	5° Full angle
	Magnetometer	Spin Rate	Perpendicular to major axis	N/A
IC 807.15-2	Dual-Channel Radiometer	2.7 μm	Forward	4° Full angle
	(NR4-C-2)	4.3 μm	Forward	4° Full angle
	Photometer (PM2-36)	4278 A	Forward	5° Full angle
	Photometer (PM2-16)	4259 A	Forward	5° Full angle
	Magnetometer	Spin Rate	Perpendicular to major axis	N/A

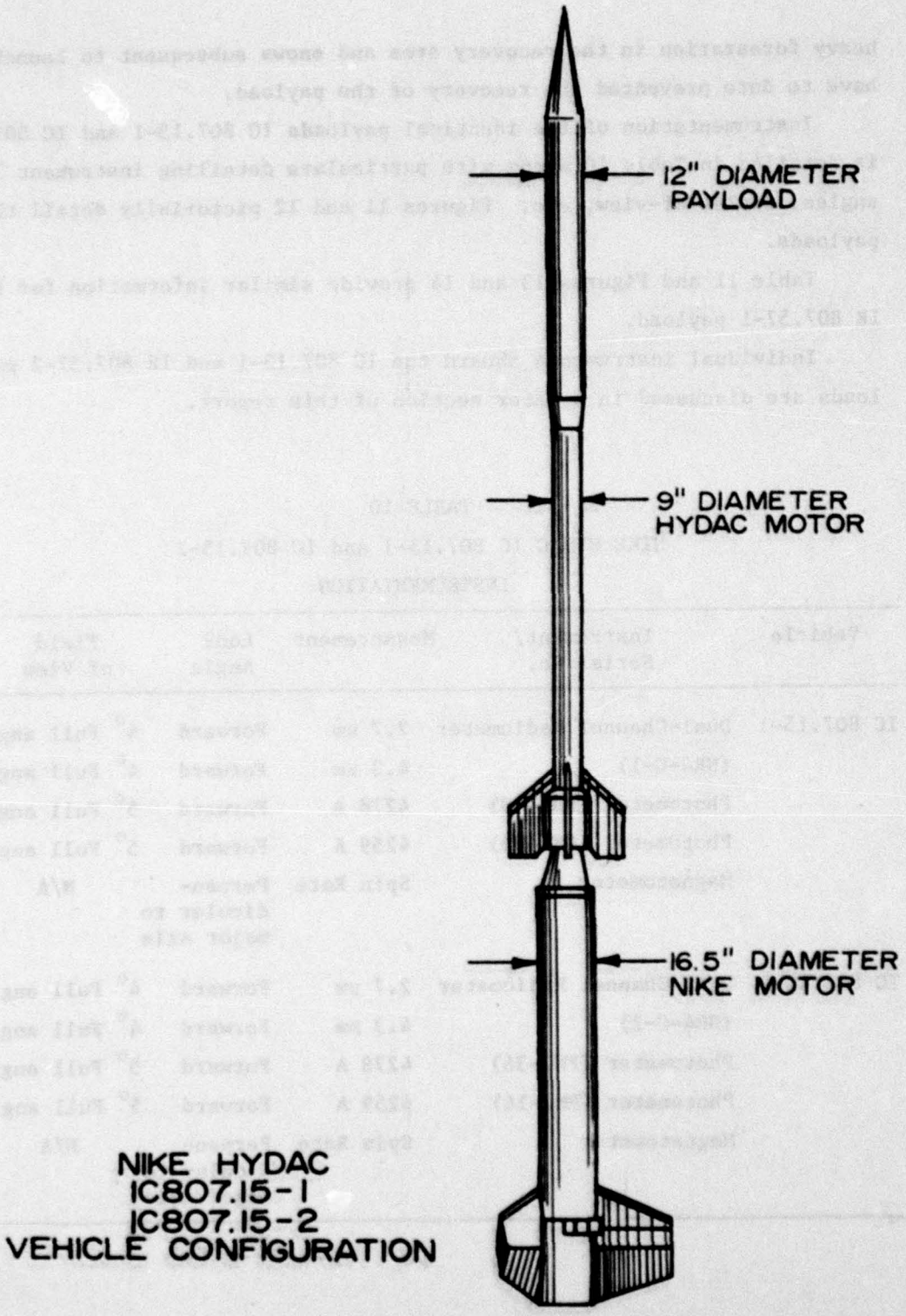


Figure 11. Nike Hydac IC807.15-1 and IC807.15-2 Vehicle Configuration.

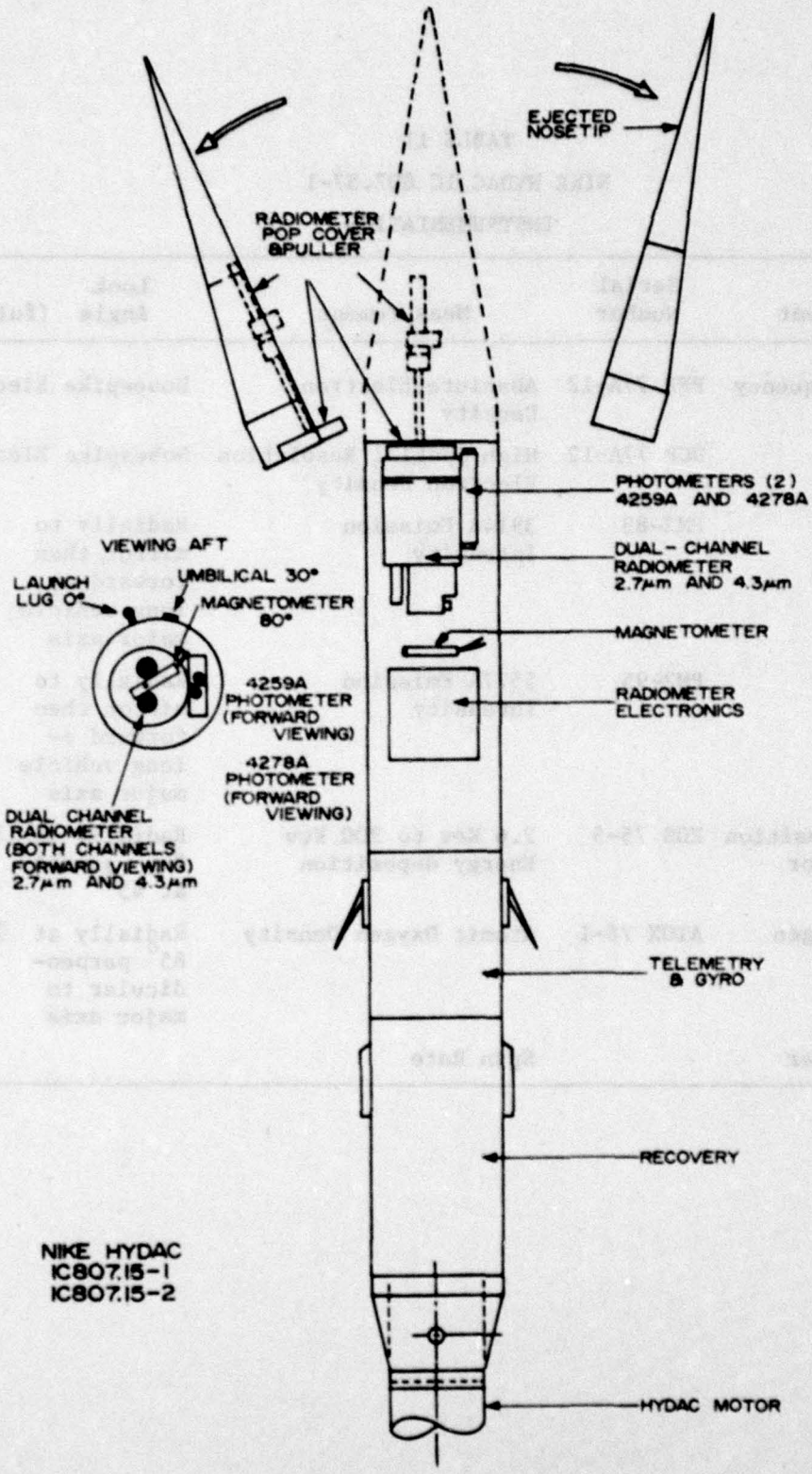


Figure 12. Nike Hydac IC807.15-1 and IC807.15-2 Payload Configuration.

TABLE 11

NIKE HYDAC IC 807.57-1

INSTRUMENTATION

Instrument	Serial Number	Measurement	Look Angle	FOV (full angle)
Plasma Frequency Probe	PFP 77A-12	Absolute Electron Density	Nosespike Electrode	
DC Probe	DCr 77A-12	High Spatial Resolution Electron Density	Nosespike Electrode	
Photometer	PM2-83	3914A Emission Intensity	Radially to mirror, then forward along vehicle major axis	5°
Photometer	PM2-95	5577A Emission Intensity	Radially to mirror, then forward along vehicle major axis	5°
Energy Deposition Scintillator	EDS 75-5	2.6 Kev to 200 Kev Energy deposition	Radially at 265° axially at 45°	19°
Atomic Oxygen Detector	ATOX 78-1	Atomic Oxygen Density	Radially at 85° perpendicular to major axis	14°
Magnetometer		Spin Rate		

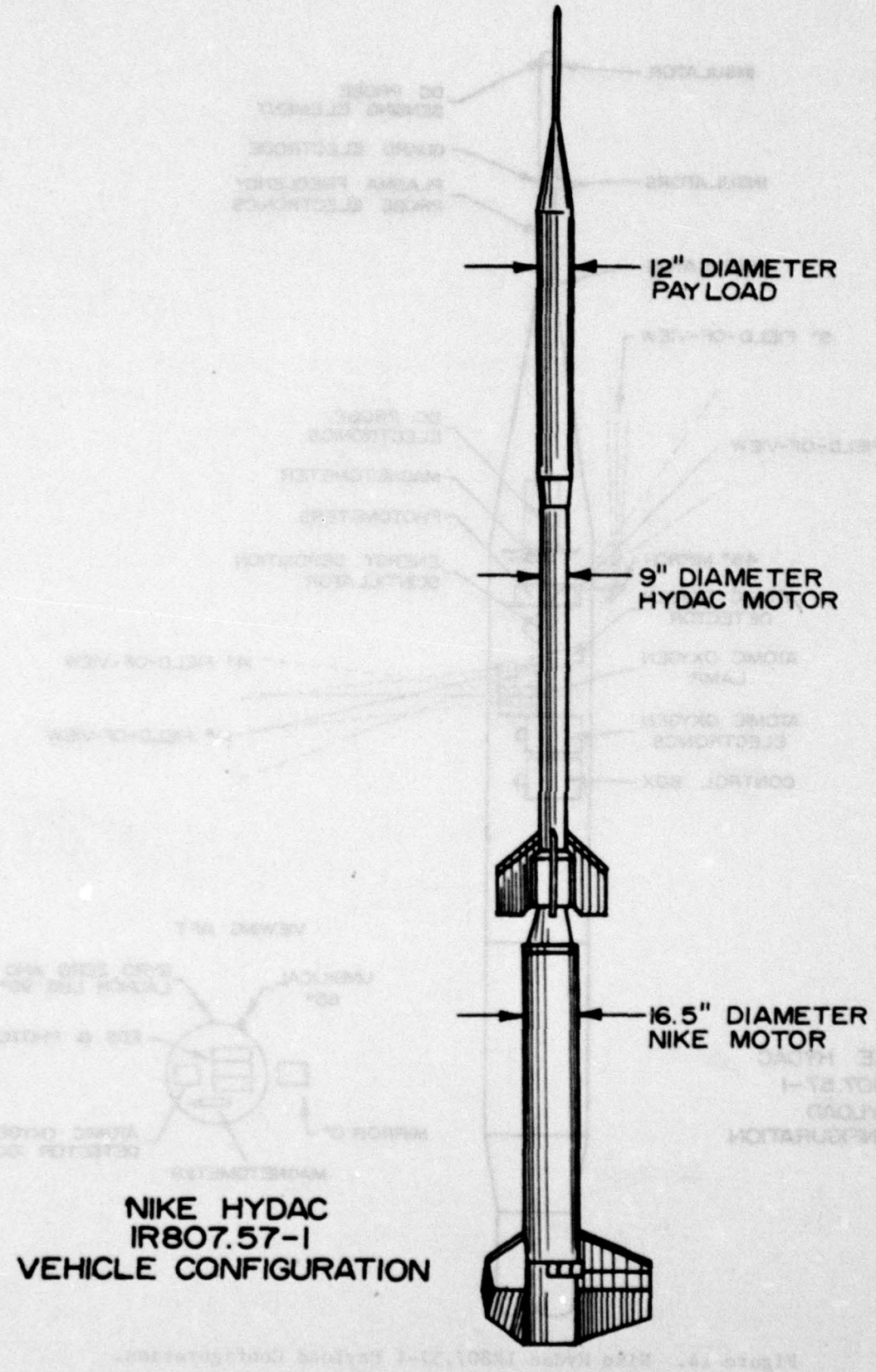


Figure 13. Nike Hydac IR807.57-1 Vehicle Configuration.

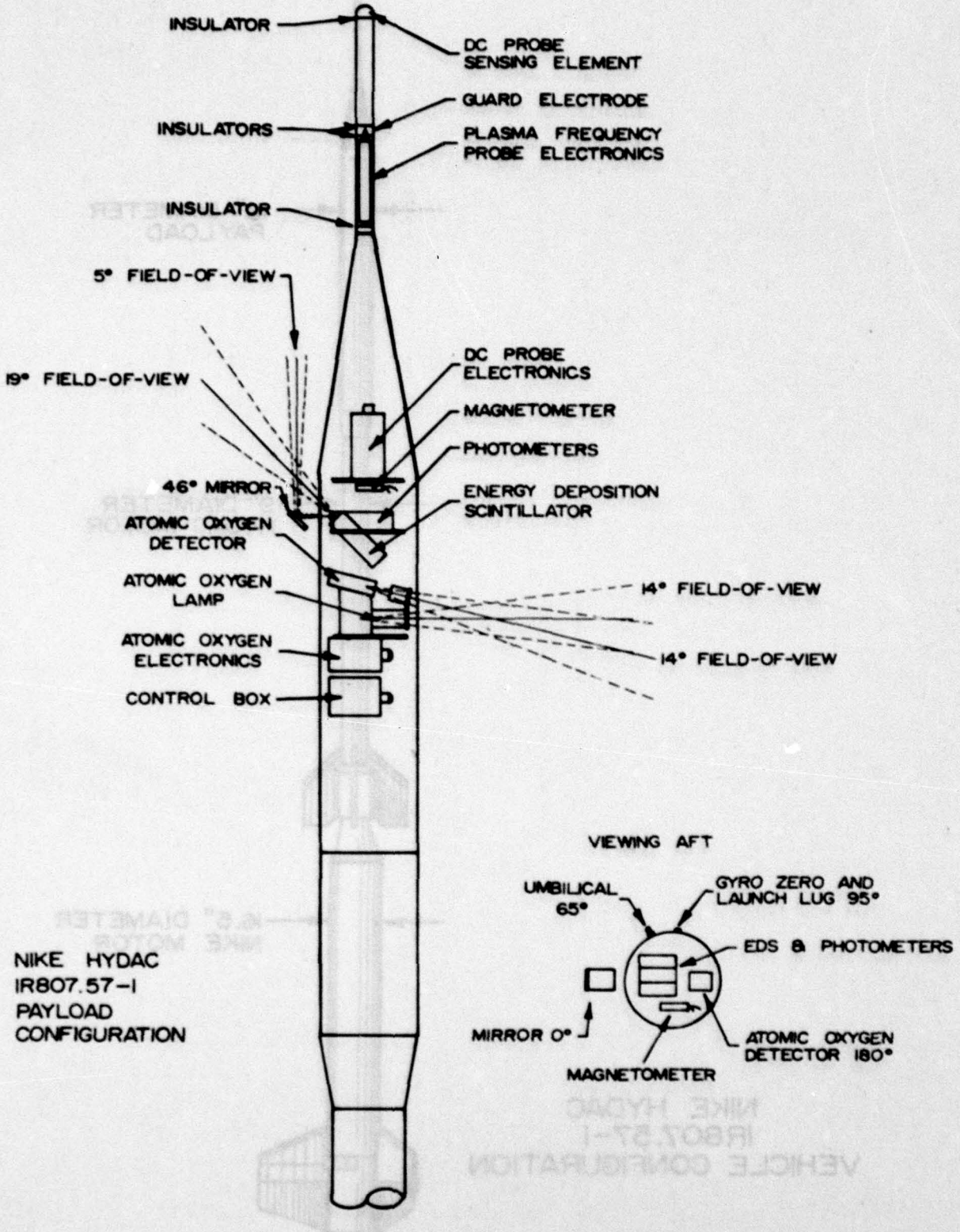


Figure 14. Nike Hydac IR807.57-1 Payload Configuration.

Supporting Measurements

The launch of the auroral dynamics and energetics payloads were supported by the ground based instrumentation described in Table 12, all of which were operational and recording at launch and during the flight of these vehicles. This instrumentation also monitored the flight of EX 851.44-1 (EXCEDE II Spectral) described earlier in this report.

TABLE 12

GROUND BASED INSTRUMENTATION AND MEASUREMENTS

Instrumentation	Site	Measurement	Experimenter
Field-Widened Interferometer	Poker Flat Optics (ARGUS)	OH Temperature 1.5-2.7 μm Spectra	USU
Rocking Filter Photometer	Poker Flat Optics (ARGUS)	Auroral/Airglow Intensity at rocket entry point 5577A 4278A 4861A 6300A 8446A	USU
2-Color Photometer (Narrow Field)	Poker Flat Optics (ARGUS)	3914A 5577A	USU
Dual Channel Radiometer	Poker Flat Optics (ARGUS)	1.7 μm 1.27 μm	USU
Meridian Scanning Photometers	Poker Flat Optics (ARGUS)	Auroral Spatial Structure 3914A 5577A 6300A	USU
Meridian Scanning Photometers (digital)	Poker Flat Optics	5577A 4278A 4861A 6300A	U of Alaska
Incoherent Scatter Radar	Chatanika	Winds Electron density Energy deposition Ion temperature Electric Fields	SRI

TABLE 12 (cont.)

Instrumentation	Site	Measurement	Experimenter
Narrow Field TV Camera ($12^{\circ} \times 16^{\circ}$)	Poker Flat Optics	TMA tracking	U of Alaska
Camera	Poker Flat Optics	TMA Tracking	TIC
Spatial Photometer Array	Chatanika	Auroral Motion 5577A 4278A	LMS Co.
All-sky TV Camera	Poker Flat Optics	Auroral Forms	U of Alaska
16 mm All-sky Camera	Poker Flat Optics	Patrol Mode 2 frames/min.	U of Alaska
35 mm All-sky Camera	Poker Flat Optics	Pre-post Launch 1 Frame/min. Launch-Impact 20 Frames/min. sequentially 4,4,2,1 sec	U of Alaska
16 mm All-sky Camera	Ft. Yukon	180° fov	U of Alaska
35 mm All-sky Camera	Ft. Yukon	160° fov	U of Alaska
Riometer (30 MHz)	Poker Flat & Ft. Yukon	General Geophysical Conditions Relative ionospheric opacity	U of Alaska
Magnetometers	Poker Flat & Ft. Yukon	Magnetic Field H,Z,D, Components	U of Alaska

INSTRUMENTATION

In the rocket payloads described in the earlier portions of this report, a broad array of instrumentation has been used to investigate and measure ionospheric parameters. Of this instrumentation many have been developed under previous contracts and were flown here without modification. Some have been refined and updated for application during this contract and others are newly developed instruments, flown initially under this contract. This multiplicity of instruments may be grouped into categories for discussion. These categories are as follows:

(1) Instruments for atmospheric electron dosing
(2) Instruments for measurement for electron density
(3) Instruments for measurements of optical emissions (infrared, visible, and ultraviolet)
(4) Instruments for measurement of vehicle potential
(5) Instruments for measurement of energy deposition
(6) Instruments for measurement of atmospheric constituents.

Detailed discussion of the instruments in their entirety is beyond the scope of this report, however, a general discussion of techniques and instrumentation philosophy for instruments within each of the above categories is presented on the following pages. Where a thorough scientific report detailing the operation of the instruments has been accomplished, such reports are referenced. The instruments are discussed from a basic philosophy point of view even though specific details of operation for each instrument may vary from payload to payload. The appendices which follow the instrument discussions give complete calibrations for each instrument developed and applied during this contract by Utah State Univsity.

Atmospheric Electron Dosing

High Energy Electron Accelerators

Electron dosing of the atmosphere through the use of electron guns has been an area of involvement throughout the period of this contract. Electron guns ranging upwards in power to 30 kw have been flown aboard a

total of three atmospheric research payloads during this period.

Current status of the development of electron accelerators for atmospheric dosing employs directly heated large cross section Tungsten filaments as the emitters to avoid filament poisoning at high pressures, and burnout even when operated at atmospheric pressures for several seconds. These features eliminate the need for a critical altitude determination for filament turn-on and exposure. The filaments are also directly heated, allowing the electron guns to be launched with the filaments turned off, then turned on at altitude with a very fast response time. This eliminates the need for a high vaccuum container for the gun during the launch and also maintains the filament in an unbreakable condition during rocket motor burn. The electron gun is focused to approximately 30 degrees full-angle to provide rapid beam dispersion to the gyro radius and provides for a rapidly formed and well defined deposition volume. Maximum efficiency of the high power electron accelerators is achieved by employing segmented, sealed and insulated battery packs comprised of rechargable nicad batteries.

For such high power electron accelerators the probability of arcing at low altitudes is very real and provisions are included to limit and turn off gun current when such circumstances occur. This is accomplished by providing a cutout which opens on excessive current. The accelerators are built in modular sections to enable build up and testing at low power with the addition of segments to reach the full power of the system. Although individual accelerators developed during this contract period have been limited to 30 kw output power, combination of individual units has been accomplished to provide a total output power of 120 kw in one application.

Measurements of Electron Density

DC Probe

The DC Probe for measurements of electron density has found repeated application on the payloads flown under the auspices of this contract. Although configurations have differed from payload to payload, fundamental operational principles of the DC Probe remain the same.

The DC probe operates on the principle that electron flow to a small positively charged electrode immersed in the ionospheric plasma is directly related to electron density of the plasma. As their sensing electrodes in contact with the ionospheric plasma the DC probes have used various configurations ranging from nose spikes to small discs placed around the circumference of the payload. The configurations of the electrodes used with each probe are detailed in the appendix.

The operation of the DC probe is exceptionally simple. The current collected by the probe electrode, which is normally biased positive with respect to the rest of the payload, is fed to the electronics system for conditioning for telemetry. With a finite sensing electrode current, the probe provides an output which is proportional to the electron flow. Typically the probes are provided with multiple outputs having gains ranging from x 1 to x 1000 with the outputs being fed directly to the telemetry section.

The probes are capable of measuring fine scale spatial variations of electron density. This high spatial resolution capability is determined by the dimensions of the probe electrode, the payload velocity and the electrical bandwidth of the telemetry system and may provide resolution to on the order of one meter.

The DC probe current measurements cannot be related independantly to electron density with high absolute accuracy, but will give reliable relative values. This often does not present a serious drawback since the relative changes are the important values and over a limited altitude range the electron density will be proportional to the probe current. By cross comparison to other measurements such as an RF probe or ionosonde, the DC probe can be calibrated in absolute numbers. In several applications the instrument used to provide this absolute calibration is the plasma frequency probe. Application of the DC probe has been discussed by [*Baker et al.*, 1978].

Plasma Frequency Probe

An RF excited, electrically short antenna placed into the earth's ionosphere exhibits impedance characteristics, which if monitored, can be utilized to determine the electron density in a region local to the

antenna. [*Despain*, 1966, *Bishop*, 1970]. Analysis of the measurements in terms of electron densities is particularly simple for the upper regions of the ionosphere where collision effects are negligible. The antenna appears as a capacitive reactance if the exciting RF is above a resonant frequency near the plasma frequency of the medium. This resonant frequency is often called the parallel resonant frequency of the antenna, since the impedance characteristics of the antenna behave analogously to a parallel resonant circuit. For the case of no external magnetic fields the parallel resonant point would correspond exactly to the plasma frequency of the medium. The presence of the earth's magnetic field, however, causes the parallel resonant frequency in the E- and F-regions to be shifted to a higher frequency known as the upper hybrid resonance, which is related to the plasma frequency and the electron gyro frequency. Therefore, by measuring the upper hybrid resonant frequency the electron density is easily determined. Once this determination has been accomplished and correlated with altitude, an absolute electron density profile is obtained.

The basic plasma frequency probe operates by applying a sweeping RF signal to an antenna and monitoring the antenna current and voltage relationship. During each frequency sweep, the sweep is stopped at the parallel resonant point and the frequency is measured by a digital counter. The counter information is stored in registers, and is telemetered out during the following sweep, thus giving a delay of from 20 to 64 milliseconds from the time it is obtained to the time it is telemetered.

A new phase locked loop variation of the plasma frequency probe has recently been used for high spatial resolution measurements with good results. In this version a phase-locked loop is used to track the frequency that produces zero phase angle between the RF current and voltage being fed to the sensing electrode. This version provides a digital output with excellant accuracy and a simultaneous analog output. The range of electron densities covered is from about 5×10^4 to 1.7×10^6 electrons per cm^3. Complete discussions of the plasma frequency probe and its application for ionospheric research have been given by [*Pound and Baker*, 1971, *Baker et al.*, 1972, *Baker et al.*, 1978].

C Probe

The C probe is a relatively new instrument used to give a measurement of the local electron density of a plasma in which the instrument's antenna is immersed. Since the antenna capacitance is a function of the frequency applied to the antenna and the electron density of the plasma, the electron density may be readily determined by measuring parameters related to the antenna capacitance. The C probe accomplishes this function by differentially comparing a voltage representing antenna capacitance with a voltage representing a known reference capacitance. Output voltages from this differential comparison are filtered, amplified and detected by linear detectors to provide x 1 and x 10 gain channels. An auto ranging circuit automatically switches between the x 1 and x 10 gain channels as appropriately determined by the magnitude of the output signal. Additional outputs indicating Δ capacitance or Δ capacitance x 10 are provided and an output from the auto ranging circuit indicates whether the output is at the x 1 or the x 10 level. Signals to telemetry are comprised of DC voltages representing either C x 1, ΔC x 1, and range; or C x 10, ΔC x 10, and range. Because the C probe has not been described in previously published literature, Figure 15, a block diagram of the instrument, is included for reference.

Instruments for Measurements of Optical Emissions

Optical emissions ranging in wavelength from ultraviolet through infrared have been extensively monitored by the payloads discussed in the earlier sections of this report. Instruments have been provided for measurement within two general categories i.e., measurement of emission intensity and measurement of spectra.

Photometers

Photometers provide a measurement of emission intensity at predetermined wavelengths. The basic photometer includes a miniture photomultiplier tube with its associated high voltage power supply and double gain amplifier. At small signal levels the output gain of the instrument is 10 times the gain at large signals, thus, extending the range of the instrument. Each photometer includes a removable optical section containing

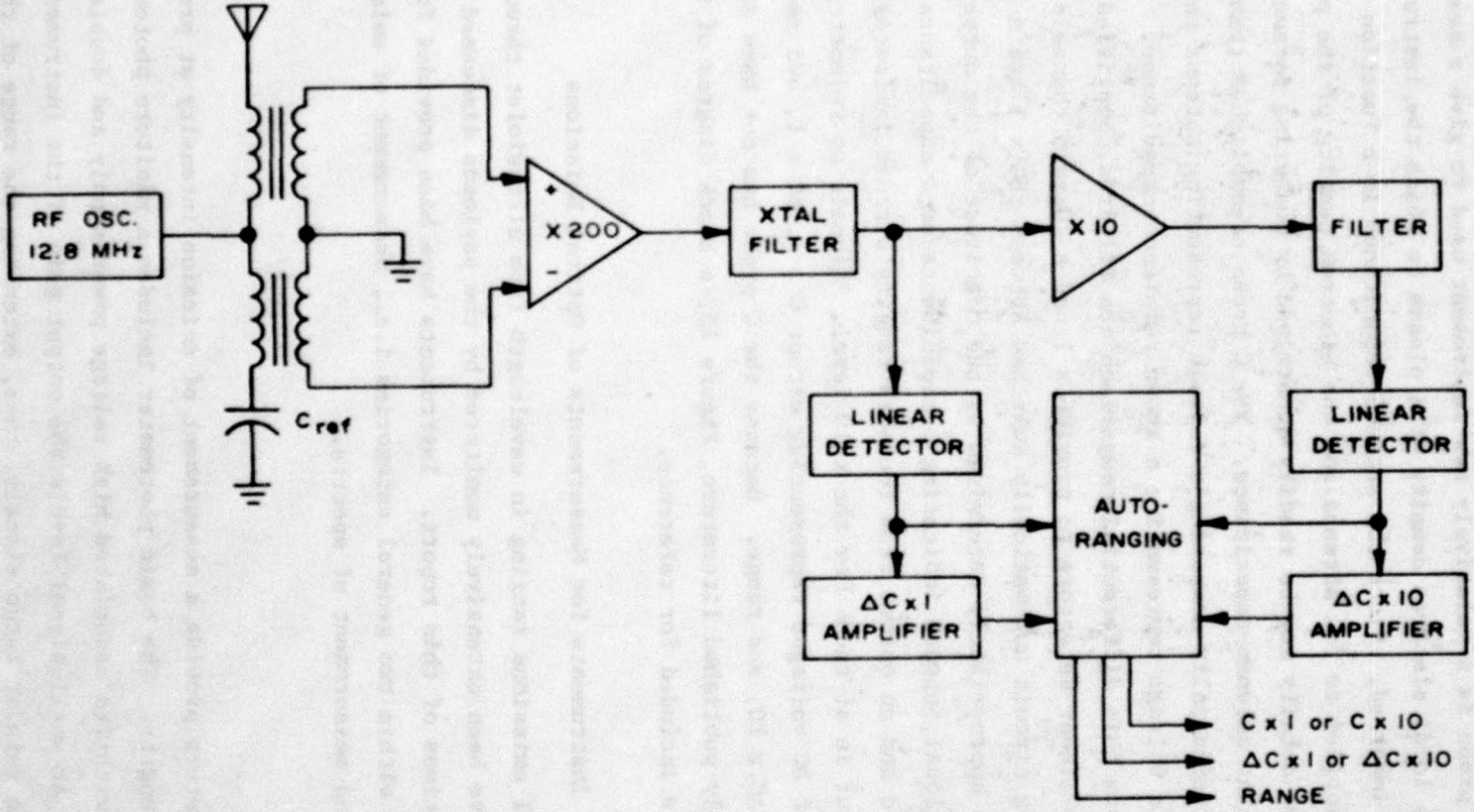


Figure 15. C Probe Block Diagram.

baffles, lens and a wavelength selection interference filter. This filter is preselected depending upon the wavelength to be monitored. Each photometer also contains a light emitting diode which is turned on periodically to provide a qualitative check on the operation of the instrument. Further details of design and operation for these ultraviolet and visible wavelength emission intensity measuring devices is straightforward and has been discussed by [*Burt*, 1975].

Infrared Radiometers

These instruments for the measurement of infrared emission intensity are typically two-channel cryogenically-cooled devices. Each has two independant measurement channels mounted in a single dewar and using a common motor driven chopper. The instruments are integral units with a liquid cryogen vessel in the center, a cooled optical compartment on the fore end, and an electronics compartment of the aft end. The baffles, lenses, selectable filters, detectors source followers, preamplifiers, and a motor driven chopper blade are located in the cold optics compartment. A cold cover is placed over this end of the optics compartment to maintain vacuum integrity and is removed at the appropriate altitude for measurements, exposing the optics to the atmospheric emissions. The aft electronics compartment contains the chopper motor reference generator and signal conditioning electronics.

The basic radiometer system is characterized by low background conditions achieved by cooling the entire optical compartment to near liquid nitrogen or liquid helium temperatures. Incoming radiation is filtered to provide measurements of the desired wavelength. Coated lenses focus the incident radiation of the detector. Prior to being detected, however, the radiation passes through a rotating chopper which yields an alternating signal, then by using tuned amplifiers a high signal to noise ratio is obtained in the system. Each channel is equipped with a variable-gain amplifier with two linear ranges. For small signal levels the gain is approximately 10 times the gain at large signal levels, thus extending the range of the instrument while providing good instrument sensitivity. Internal light-emitting diodes periodically activate the detectors and provide an inflight measure of relative system responsivity. Temperature

monitors are provided to yield detector and optics temperatures. The development, operation, and application of the infrared radiometers have been discussed in detail by [*Wyatt*, 1974, *Burt*, 1975, *Baker et al.*, 1977].

Infrared Spectrometers

Circular varible filter (CVF) spectrometers for spectral measurements of shortwave (liquid nitrogen cooled), and long wave (liquid helium cooled), infrared emissions have been developed at Utah State University and used on the rocket payloads discussed. Fundamentally these instruments are very simular in electronic design and principle of operation, with differences due to the special considerations necessary for handling the two liquid cryogens and differences in wavelengths scanned. The nitrogen cooled CVF spectrometer measures atmospheric emissions in the range of 1.8 through 5.91 μm. Atmospheric species of particular interest which emit in this range are hydroxl (OH), between 1.8 and 2.1 μm; NO^+, centered at 2.15 μm; CO_2 at 4.3 μm; and NO at 5.3 μm. The longer wavelength infrared emissions are monitored by the liquid helium cooled CVF spectrometer, designed to obtain measurements of the spectral radiance of atmospheric emissions in the spectral range 6.75 through 23.2 μm.

The instruments achieve a spectral scan by rotating a circular variable filter over the field stop so that the instrument scans the prescribed wavelengths during each revolution of the filter (a rate of 2 scans per second). The optical section of the spectrometers image the incoming radiation upon the detector and output from the detector is fed to two prime signal channels that differ in gain by a factor of 10 to provide a dynamic range of about 1000. Two spectral position references are provided for each type spectrometer. One consists of a pulse that occurs at the beginning of the scan on the low gain channel, the other is a continuous train of square wave pulses providing 20 transition reference points throughout the scan. The latter position reference requires an additional wideband telemetry channel. Several temperature monitor channels are provided to yield detector and optics temperatures and internal light-emitting diodes periodically activate the detector and provide and inflight measure of relative system responsivity. Each instrument incorporates a cover for the optical section. This cover is removed during flight exposing the

cold optical system in the front end. As with the radiometers, the warmer electronic and motor section are located in the aft end of the instrument.

The inflight output from the spectrometers is a spectroscopic measurement of the vertical distribution of active atomic and molecular gas species under varying conditions. The design, development, and application of the circular variable filter spectrometers have been described in detail by [*Wyatt*, 1971, *Wyatt*, 1974, *Wyatt and Baker*, 1974, *Burt*, 1975, *and Frodsham*, 1978].

Instruments for Measurement of Vehicle Potential

Many of the rocketborne instruments that are designed to measure ionospheric parameters, employ voltage biased or swept electrodes or apertures to collect particles from the plasma. In use, these collecting devices are often biased with respect to the vehicle, or in any case are referenced to the vehicle. In order to properly assess the significance of their accumulated measurements however, their bias with respect to the plasma must be known. During flight the rocket itself will acquire a potential with respect to the ionospheric plasma and this potential is governed by instrumentation, configuration, and local plasma conditions. The operation of electron accelerators aboard the payload greatly contributes to fluctuations of, and variations in vehicle to plasma potential. Obviously, when these conditions occur, the bias of the electrodes change with respect to the plasma and unless these changes are accounted or adjusted for, the accumulated measurements prove to be relatively worthless. Indeed, if vehicle to plasma potential values acquire magnitude high enough it is entirely possible that no measurements at all will be achieved. During the period of this contract two instruments were used to monitor vehicle to plasma potential.

Skin Current Probe

The Skin Current Probes were designed as rocketborne instruments to measure electrons flowing from the ionospheric plasma back to the skin of the vehicle. The electrode utilized for the skin current probe is a circular section of the rocket skin which is electrically insulated from the remainder of the payload. The circuitry involved maintains the electrode

potential within a few millivolts of the skin potential by utilizing a log diode feedback circuit. An oven and temperature control circuit is employed to keep the feedback circuit temperature constant thereby eliminating any drift problems. Signals originated by current flow from the plasma to the electrode of the skin current probe is differentially amplified giving an output proportional to sensing electrode current. The signal is made compatable with the telemetry system by use of an inverter to provide a positive output for telemetry. A stimulation circuit included in the instrument provides a means of verifying instrument operation both prior to and during flight. A 3.5 volt pulse on the instruments output is originated by applying a calibration pulse at the probe input. This calibration recurs each 20 seconds with a 17 millisecond duration.

Charge Probe

The Charge Probe is designed to measure the potential of the vehicle skin with respect to the ambient plasma. These measurements are accomplished using an isolated electrode separated from the ionosphere by a teflon dielectric. The probe achieves its measurements by monitoring the charge displacement between the skin of the vehicle and the surface of the dielectric exposed to the ionosphere. Two outputs are provided from the instrument , a peak detector output and a charge output. The peak detector measures fast charging spikes, which may occur with the operation of electron accelerators aboard the payload, but will also measure long term charging to full voltage. The charge output is a direct, slow output. This output is set for a more sensitive scale than the peak detector. The charge output is normally the prime measurement particularly during longer durations after equilibrium in vehicle potential sets in.

Measurements of Energy Deposition

Energy Deposition Scintillator

This instrument provides measurements of the total power carried by energetic electrons and protons. The instrument basically consists of a scintillation phosphor viewed by a photomultiplier tube. The photomultiplier output is amplified by four cascaded saturating amplifiers and the

instrument's output is the summation of the output of these amplifiers to provide data compression which can be described over four ranges by linear mathematical functions. The output of the instrument is a measurement of the rate of energy input due to particles having energies above a predetermined threshold. This threshold is determined by a thin aluminized window placed in front of the scintillation phosphor. Additionally, the aluminized window serves to prevent ambient light from directly entering the phototube. The maximum energy which can be measured by the instrument is contingent upon the type and thickness of the scintillation phosphor. Typically these scintillation phosphors are pilot-B plastic scintillation crystals.

The instrument contains two monitor circuits for check of its operation. A calibration lamp illuminates the phototube once approximately each 30 seconds for a period of about 0.1 second. This provides an instrument output pulse twice each minute and serves to provide a functional check. A high voltage monitor is also provided to check on operation in the high voltage power supply.

Measurements of Atmospheric Constituents

Atomic Oxygen Detector

The Atomic Oxygen measurement is based upon the resonant scattering of the 1302, 1304 and 1306 Å resonance triplet from an onboard source by the atmosphere to an onboard detector. The resonant lamp used in the instrument is of new design. In operation this lamp draws O_2 in a helium carrier gas from a tank into a discharge chamber where it is excited to emission by a 180 MHz modulated RF oscillator. The modulation, which is at 250 Hz, allows background illumination entering the detector to be subtracted from the data.

The lamp emissions are collimated into a beam which is normal to the rocket axis and which is viewed through an interference filter by a VUV solar-blind photomultiplier. The photomultiplier is in a photon counting mode, with counts accumulated and placed in one register during the half cycle that the lamp is on, and in a second register during the half cycle that the lamp is off. These register output are merged into a PCM format.

The oxygen resonance lamp emissions are viewed by a nitric oxide filled ionozation chamber with a CaF_2 window to provide a monitor of intensity of the oxygen resonance emissions. The NO ionozation potential eliminates response from longer wavelengths and the CaF_2 short wavelength cutoff of approximately 1240 Å eliminates any response from Lyman-α or Nitrogen emissions. The basic philosophy of the atomic oxygen detector has been discussed in a separate report by *Howlett and Baker*, [1977].

A description of calibration methods and procedures and corresponding calibration information is beyond the scope of this report and is not included in the appendices. It is anticipated that a special scientific report dealing with these procedures and details will be forthcoming in the near future.

SUBCONTRACTS

UNDER CONTRACT F19628-76-C-0261

Subcontractor: Concord Sciences Corporation

Work Statement

A quick study whose purpose was the derivation of criteria for advanced sensor qualities which would enhance the capability of detecting small bodies or radiating sources in the presence of diffuse, but structured backgrounds, such as those which may occur in aurora.

Period: 1 April 1977 - 30 Nov. 1977

Abstract of Final Report [*Sutton*, 1977].

As part of a series of analyses to determine the best candidate sensor for the detection of aircraft from satellites, a concept for the detection of aircraft plume radiation based on a gas absorption correlation cell has been assessed in this note. The sensor system, proposed by the GE Space Sciences Laboratory is based on the detection of plume radiation from the $C^{13}O_2$ isotope radiating in the 2240 to 2280 cm^{-1} spectral region. The combination of better atmospheric transmittance and correlation detection by an absorption cell containing pure $C^{13}O_2$ was proposed as a technique which would improve detected signal strengths.

An analysis of some of the performance features for such a sensor shows that the $C^{13}O_2$ plume signals transmitted to space will be weaker than at first anticipated and reasonable signal-to-noise ratios cannot be achieved for desired field-of-view element sizes. Such systems would certainly be background photon noise limited for satellites at geosynchronous altitudes and marginal for lower altitude systems.

The gas absorption cell has attractive features for other military applications due to its good signal efficiency when discriminating molecular band radiation from greybody radiation. Its modest size, simple and rugged nature could lead to a number of applications including its addition to other optical systems as a filter for the detection of radiation from specific molecular bands.

Subcontractor: Optical Sciences Co.

Work Statement

1. Define a set of cryogenic infrared sensor concepts of current potential relevance, and generate a preliminary assessment of the potential and limitations of each concept.
2. Perform a detailed analysis of the expected performance of each sensor concept, starting with the highest ranked sensor concept first.
3. Prepare a final report defining the sensor concepts considered, presenting the relevant performance analysis, and comparing the potential of the various sensor concepts.

Period: 1 April 1977 - 30 Sept. 1977

Final Report by *Fried* [1977].

Subcontractor: HSS, Inc.

Work Statement

Furnish all labor, equipment, facilities, services and materials except as noted to deploy, operate and maintain the Super Cygnus Echelle Spectrograph during the operational phase of Project PRECEDE II, and to process the film records. Also make modifications to an AFGL Dual Channel Telephotometer for use during this project.

Period: 10 May 1977 - 15 January 1978

Final Report by *HSS, Inc.*, [1978].

Subcontractor: Synoptics Associates

Work Statement

1. Provide technical services in the area of medium and long wave background modeling for earth spatial clutter and earth atmospheric temporal fluctuations (Murcray phenomena) by extrapolation from measurements.

2. Conduct support analyses relative to effects of spatial and temporal background fluctuations on obscuration target detection and infrared plume detection.

Period: 1 November 1977 - 31 December 1977

Final Report by *Synoptics Assoc. Co.*, [1978].

REFERENCES

Air Force Geophysics Laboratory and Utah State University, *Quick Look Report on Rocket IC 830.09-1A Field Widened Interferometer Auroral Flight*, Submitted to Maj. James Mayo, program manager, Defense Nuclear Agency, RAAE, Washington D.C., 1978.

Baker, K.D., Earl F. Pound, Richard H. Bishop and Glenn D. Allred, Electron density measurements in and near barium clouds (Secede II Program), 49 pp., *Final Report*, Subcontract under Prime contract No. F30602-70-C-0174, Space Measurements Laboratory, Utah State University, Logan, 1972.

Baker, K.D., Doran J. Baker, L. Carl Howlett, and Larry L. Jensen, Studies of the disturbed upper atmosphere utilizing rocketborne instrumentation, *Final Report, AFGL-TR-77-0223*, 68 pp., Contract F19628-74-C-0130, Space Science Laboratory, Utah State University, Logan, 1977.

Baker, K.D., L.C. Howlett, N. Grossbard, J.C. Ulwick, G.D. Allred, M.C. Kelley, D. Delorey, Electron density structure in barium clouds - measurements and interpretation, *Final Report, DNA 4561F*, Contract DNA 001-76-C-0278, Space Science Lab., Utah State University, Logan, 1978.

Bishop, R.H., *Antenna Impedance in the Lower Ionosphere*, 152 pp., Space Science Lab., Utah State University, Logan, 1970.

Burt, David A., Black Brant 18.219-1 Instrumentation for ICECAP 74A, *Scientific Report No. 3, AFGL-TR-76-0058*, 152 pp., Contract F19628-73-C-0048, Space Science Laboratory, Utah State University, Logan, 1975.

Despain, A.M., Antenna impedance in the ionosphere, *UARL Sci. Rep. No. 3, AFCRL 66-412*, Upper Air Research Laboratory, University of Utah, Salt Lake City, 1966.

Fried, David L., Final report on Utah State University Subcontract No. SC-77-027, *Report No. DR-094*, The Optical Sciences Co., Placentia, Calif., 1977.

Frodsham, D.G., Cryogenically cooled radiometers and spectrometers for infrared measurements, *Final Report, AFGL-TR-79-0059*, 51 pp., Contract F19628-75-C-0014, Electro-Dynamics Laboratories, Utah State University, Logan, 1979.

Howlett, L.C., and K.D. Baker, Development of a rocketborne resonance lamp system for the measurement of atomic oxygen, *Scientific Report No. 5, AFGL-TR-77-0227*, 88 pp., Contract No. F19628-74-C-0130, Space Science Laboratory, Utah State University, Logan, 1977.

HSS, Inc., Quick-look report on image-intensified spectrograph measurements, *Final Report, Contract No. SC-77-039*, HSS Inc., Bedford, Mass., 1978.

O'Neil, Robert R., Edward T.P. Lee, A.T. Stair, Jr., and James C. Ulwick, EXCEDE II, *AFGL-TR-76-0308*, Optical Physics Division, Air Force Geophysics Laboratory, Bedford, 1976.

O'Neil, Robert R. (ed.), Precede II: Summarized results of an artificial auroral experiment, *AFGL-TR-78-0063*, Optical Physics Division, Air Force Geophysics Laboratory, Bedford, 1978.

O'Neil, Robert R., Summarized results EXCEDE: SPECTRAL, *AFGL-TM-16*, Air Force Geophysics Laboratory, Bedford, 1978.

Pound, Earl F., and K.D. Baker, *A Superheterodyne Plasma Frequency Probe for Ionospheric Research*, Space Science Lab., Utah State University, Logan, 1971.

Sutton, Emmett A., An assessment of the gas correlation absorption cell for aircraft detection, *CSC RN-7*, Final Report, Subcontract No. SC-77-026, Concord Sciences Corporation, Concord, Mass., 1977.

Synoptics Associates Co., Comparative detection of targets from background, *Rept. No. SA-78-005, Final Report, Subcontract SC-78-0006*, Synoptics Associates Co., Long Beach, Calif., 1978.

Wyatt, Clair L., Infrared helium-cooled circular-variable filter spectrometer, Model HS-1, *Final Report, AFGL-71-0340*, Contract No. F19628-67-C-0322, Electro-Dynamics Laboratories, Utah State University, Logan, 1971.

Wyatt, Clair L., and Doran J. Baker, Rocketborne far-infrared circular-variable filter spectrometer development, *Final Report, AFCRL-TR-74-0360*, 26 pp., Contract No. F19628-70-C-0289, Electro-Dynamics Laboratories, Utah State University, Logan, 1974.

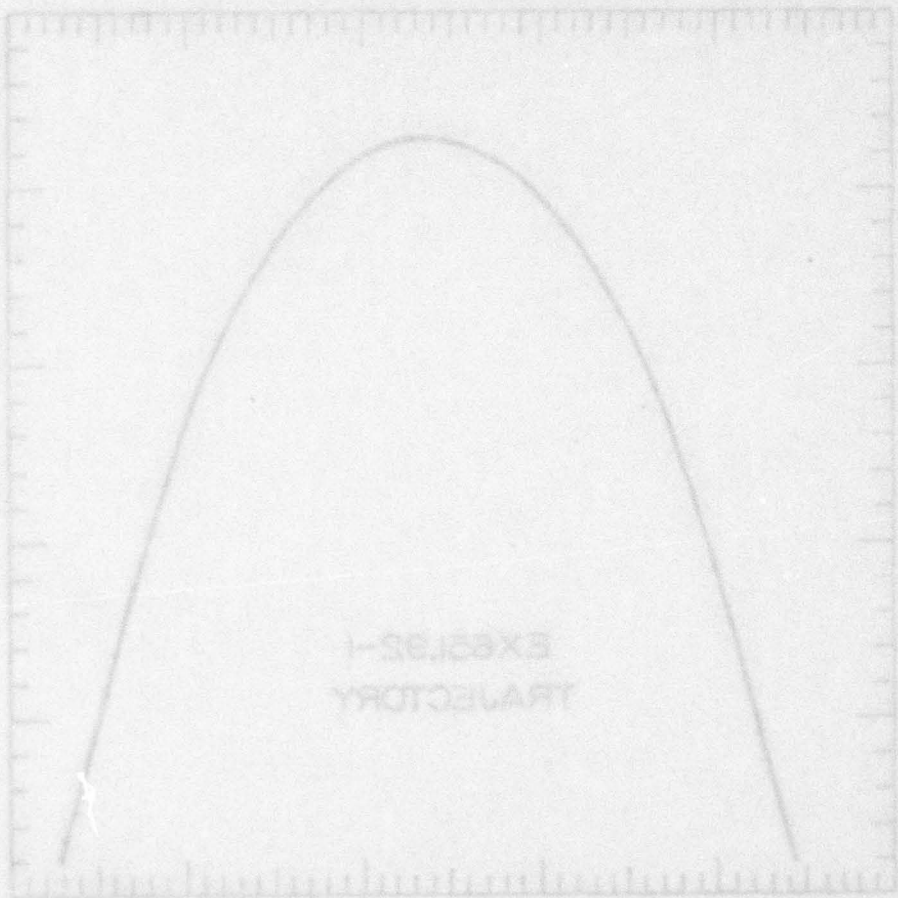
Wyatt, Clair L., Rocketborne near-infrared radiometer system, Model NR-1, *Final Report, AFCRL-TR-74-0059*, 44 pp., Contract F19628-70-C-0280, Electro-Dynamics Laboratories, Utah State University, Logan, 1974.

Wyatt, Clair L., Infrared spectrometer: liquid-helium cooled rocketborne circular-variable filter, *Applied Optics, Vol. 14, No. 12, pp. 3,086-3,091*, 1975.

APPENDIX A

TALOS CASTOR EX 651.92-1

INSTRUMENTS AND PARAMETERS



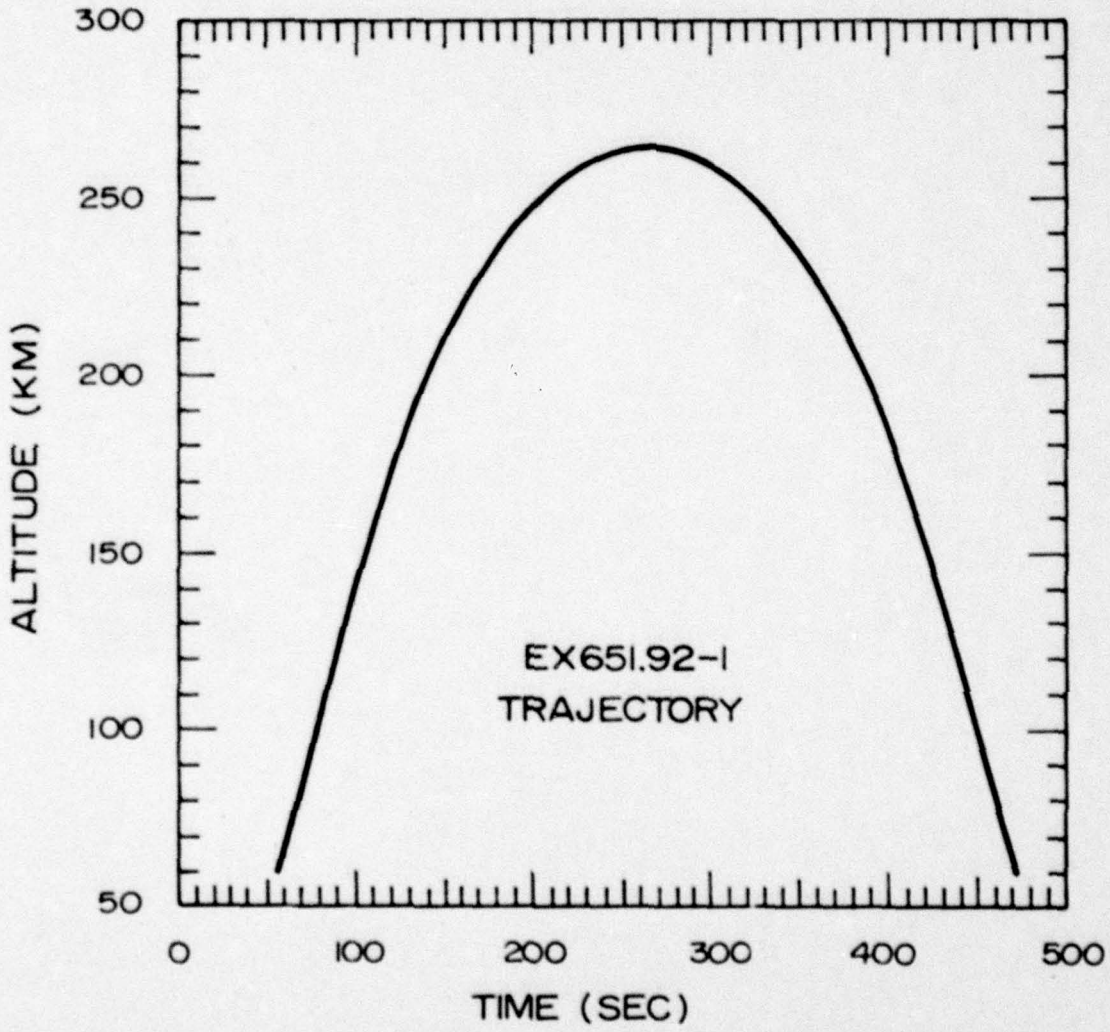


Figure A-1. EX 651.92-1 Trajectory.

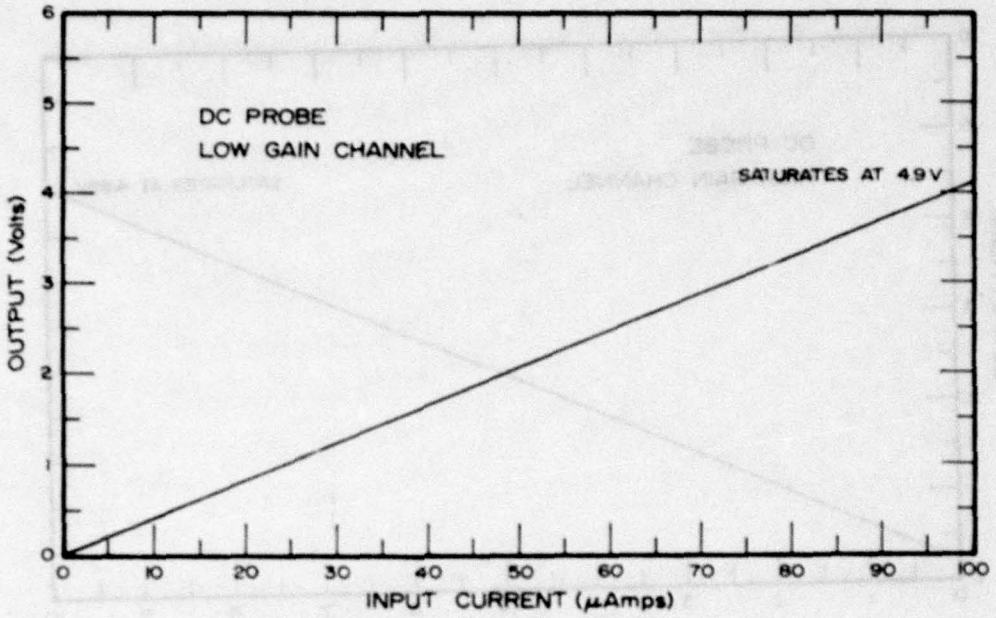


Figure A-2. DC Probe (DCP 76A-1) Low Gain Calibration.

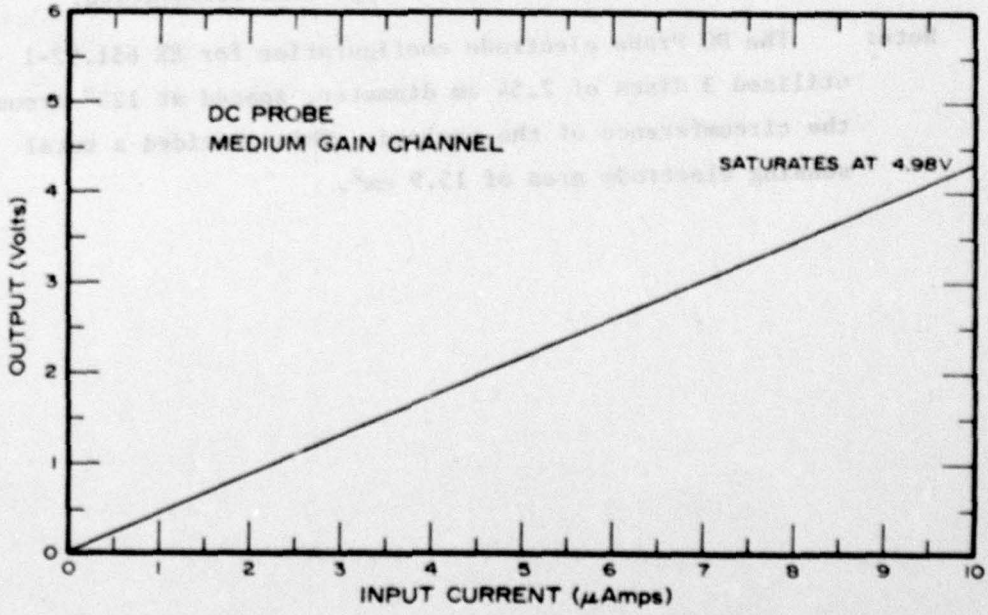


Figure A-3. DC Probe (DCP 76A-1) Medium Gain Calibration.

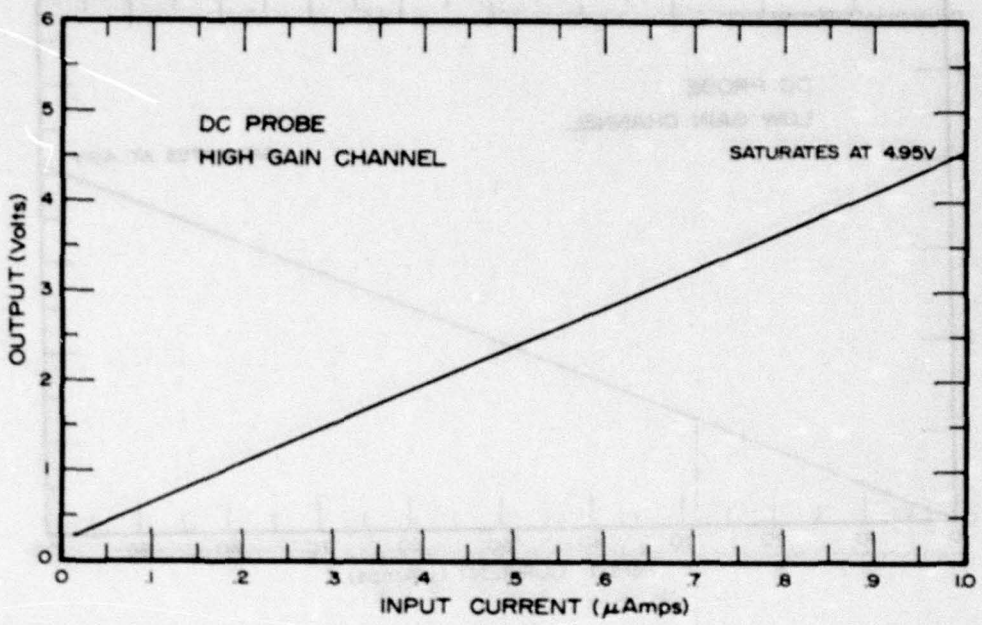


Figure A-4. DC Probe (DCP 76A-1) High Gain Calibration.

Note: The DC Probe electrode configuration for EX 651.92-1 utilized 3 discs of 2.54 cm diameter, spaced at 120° around the circumference of the payload. This provided a total sensing electrode area of 15.9 cm^2.

TABLE A-1

TALOS CASTOR EX 651.92-1 TELEMETRY TECHNICAL DATA

LINK I 2215.5 MHz

Transmitter: Conic Model CTM-UHF 305	Subcarrier: Conic Model C50 220-1
Deviation: 250 KHz	
Antenna: PSL Type 55.901	Input Signal: 0 - +5V

IRIG Channel	Channel Description
21	Gyro Roll
20	Gyro Pitch
19	Gyro Yaw
18	Commutator, 2.5 x 64
17	Gun Current (Master)
16	Gun Current (Slave)
15	Vehicle Potential Monitor
14	Ranging
13	DC Probe, Low Gain
12	DC Probe, Medium Gain
11	DC Probe, High Gain
10	Accelerometer $\pm$ 40 G's
9	Roll Magnetometer
8	Pitch Magnetometer
7	Yaw Magnetometer
6	Gun Voltage (Master)
5	Gun Voltage (Slave)
4	Q Probe time constant
3	Q Probe signal
2	Gyro Roll Rate

Link II 2279.5 MHz
TV Camera

Link III 2244.3 MHz
Casette Recording

TABLE A-2

TALOS CASTOR EX 651.92-1 2.5 x 64 COMMUTATOR

ASSIGNMENTS, LINK I IRIG 18

Channel	Data
1	0 volts Calibration
2	5 volts Calibration
3	Heat Shield off Monitor
4	Main and Drogue Chute Break Wire Monitor
5	Nose Cone Separation Monitor
6	Payload Separation Monitor
7	Door Monitor (Master Gun)
8	Door Monitor (Slave Gun)
9	Roll Rate Controller +5V Monitor
10	Roll Rate Controller Pressure Monitor
11	Vehicle Potential High Voltage Monitor
12	TV Camera Poser Monitor
13	Casette Battery Pack Monitor
14	Aft Instrument Section Battery Pack Monitor
15	Gyro Battery Pack Monitor
16	Temp. Monitor (Aft Section)
17	Temp. Monitor (S-Band Antenna)
18	Temp. Monitor (Gyro Section)
19	Temp. Monitor (Heat Shield)
20	Temp. Monitor (Recovery Section)
21	Temp. Monitor (Nose Cone #1)
22	Temp. Monitor (Nose Cone #2)
23	Heat Shield off Monitor
24	Main and Drogue Chute Break Wire Monitor
25	Nose Cone Separation Monitor
26	Payload Separation Monitor
27	Door Monitor (Master)
28	Door Monitor (Slave)
29	Roll Rate Controller +5V Monitor
30	Roll Rate Controller Pressure Monitor
31	Vehicle Potential High Voltage Monitor
32	TV Camera Power Monitor
33	Casette Battery Pack Monitor
34	Aft Instrument Section Battery Pack Monitor
35	Gyro Battery Pack Monitor
36	Temp. Monitor (Aft Section)
37	Temp. Monitor (S-Band Antenna)
38	Temp. Monitor (Gyro Section)
39	Temp. Monitor (Heat Shield)
40	Temp. Monitor (Recovery Section
41	Temp. Monitor (Nose Cone #1)
42	Temp. Monitor (Nose Cone #2)
43	Heat Shield off Monitor
44	Main and Drogue Chute Break Wire Monitor
45	Nose Cone Separation Monitor
46	Payload Separation Monitor

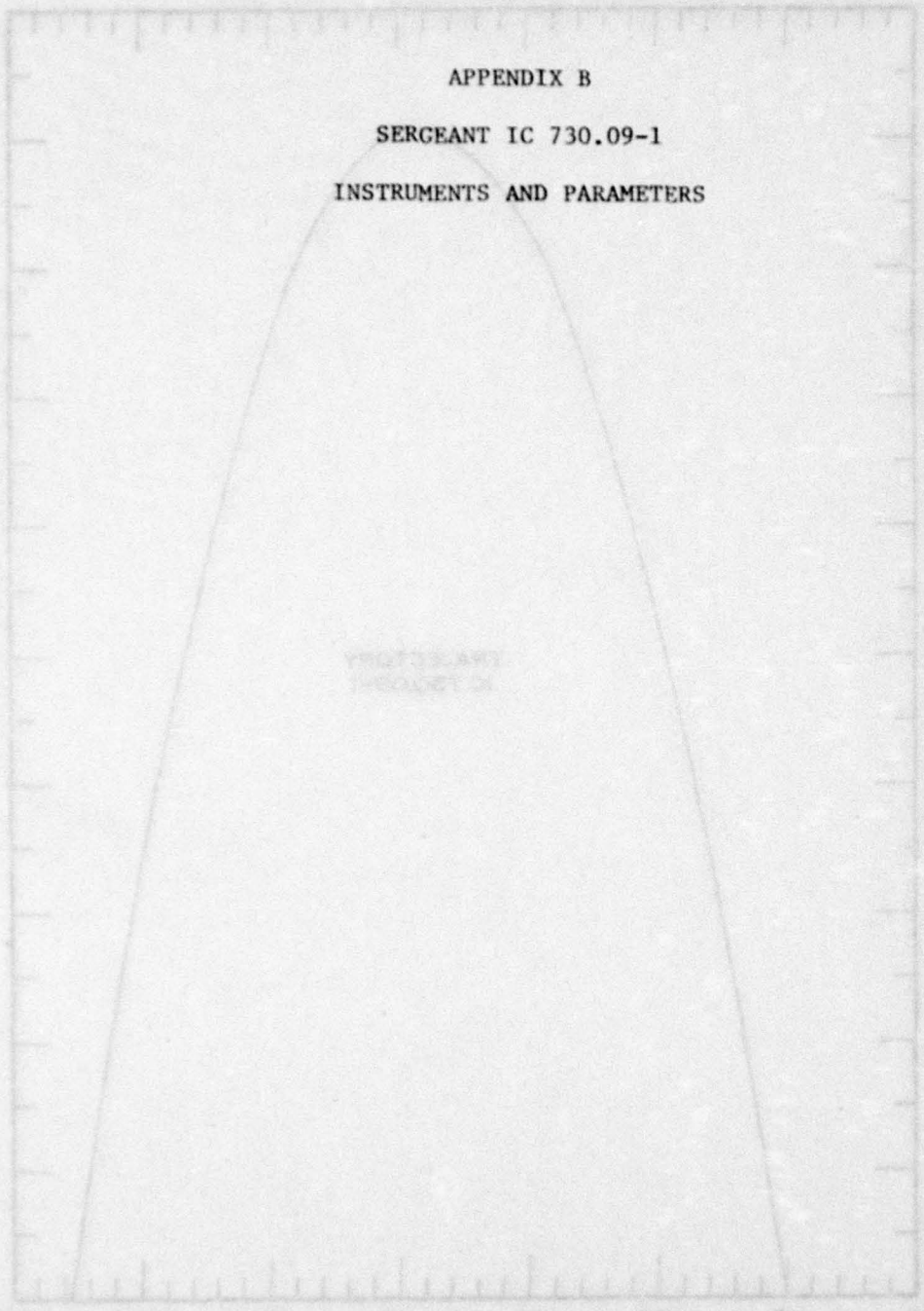
TABLE A-2 (cont.)

Channel	Data
47	Door Monitor (Master)
48	Door Monitor (Slave)
49	Roll Rate Controller +5V Monitor
50	Roll Rate Controller Pressure Monitor
51	Vehicle Potential High Voltage Monitor
52	TV Camera Power Monitor
53	Casette Battery Pack Monitor
54	Aft Instrument Section Battery Pack Monitor
55	Gyro Battery Pack Monitor
56	Temp. Monitor (Aft Section)
57	Temp. Monitor (S-Band Antenna)
58	Temp. Monitor (Gyro Section)
59	Temp. Monitor (Heat Shield)
60	Temp. Monitor (Recovery Section)
61	Temp. Monitor (Nose Cone #1)
62	Temp. Monitor (Nose Cone #2)
63	Sync
64	Sync

APPENDIX B

SERGEANT IC 730.09-1

INSTRUMENTS AND PARAMETERS



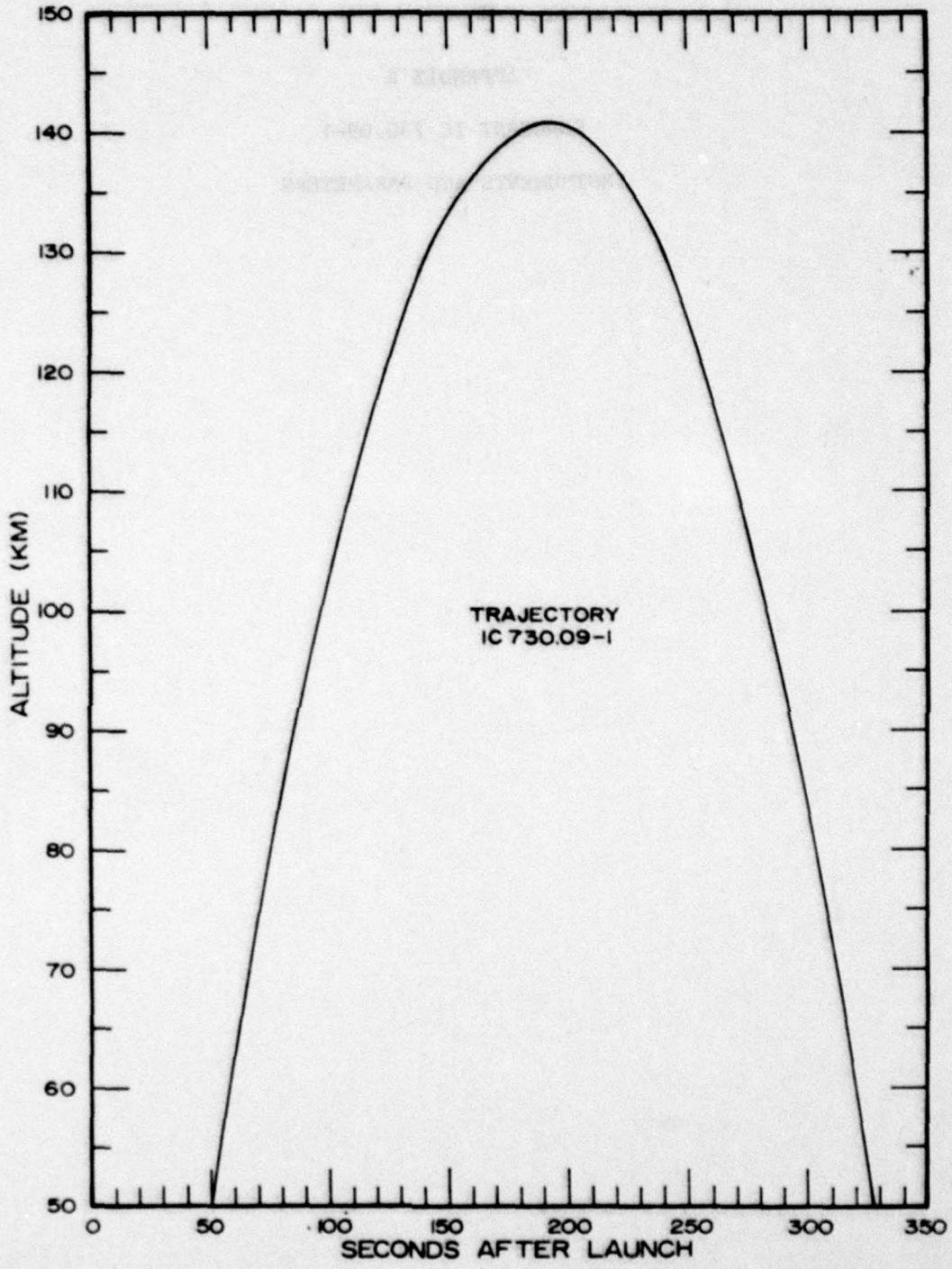


Figure B-1. Sergeant IC730.09-1 Trajectory.

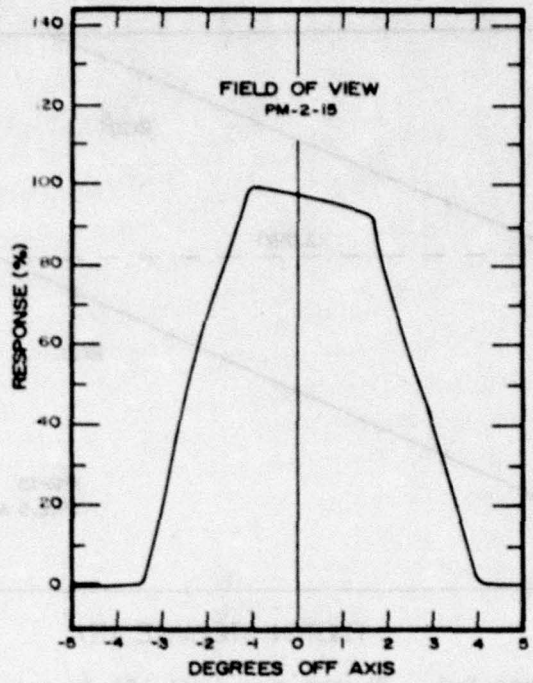


Figure B-2. Photometer (PM2-15) Field-of-View.

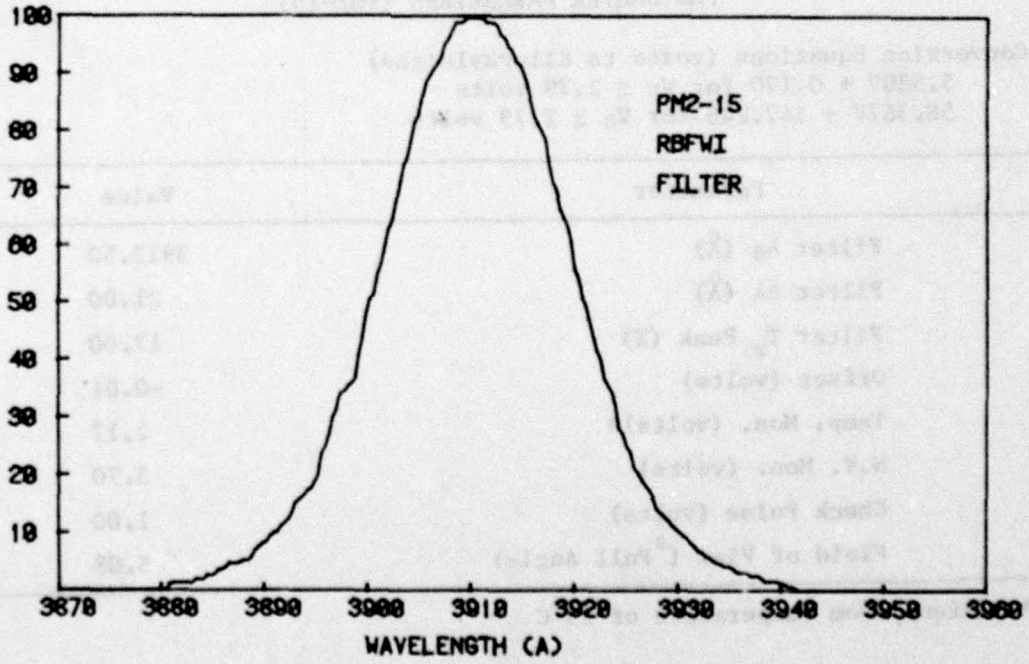


Figure B-3. Photometer (PM2-15) Bandpass Filter.

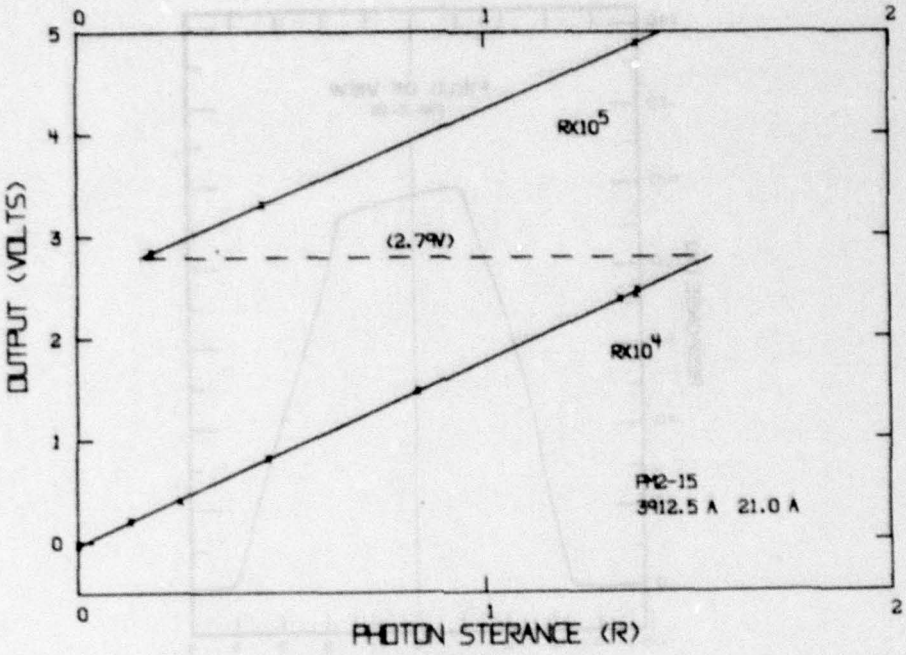


Figure B-4. Photometer (PM2-15) Responsivity.

TABLE B-1

PHOTOMETER PARAMETERS (PM2-15)

Conversion Equations (volts to Kilorayleighs)
5.530V + 0.170 for $V_0 \leq 2.79$ volts
58.367V + 147.245 for $V_0 \geq 2.79$ volts

Parameter	Value
Filter λ_0 (Å)	3912.50
Filter $\Delta\lambda$ (Å)	21.00
Filter T_r Peak (%)	17.00
Offset (volts)	-0.01
Temp. Mon. (volts)*	2.17
H.V. Mon. (volts)	3.70
Check Pulse (volts)	1.00
Field of View ($^\circ$Full Angle)	5.08

* Ambient room temperature of 23°C

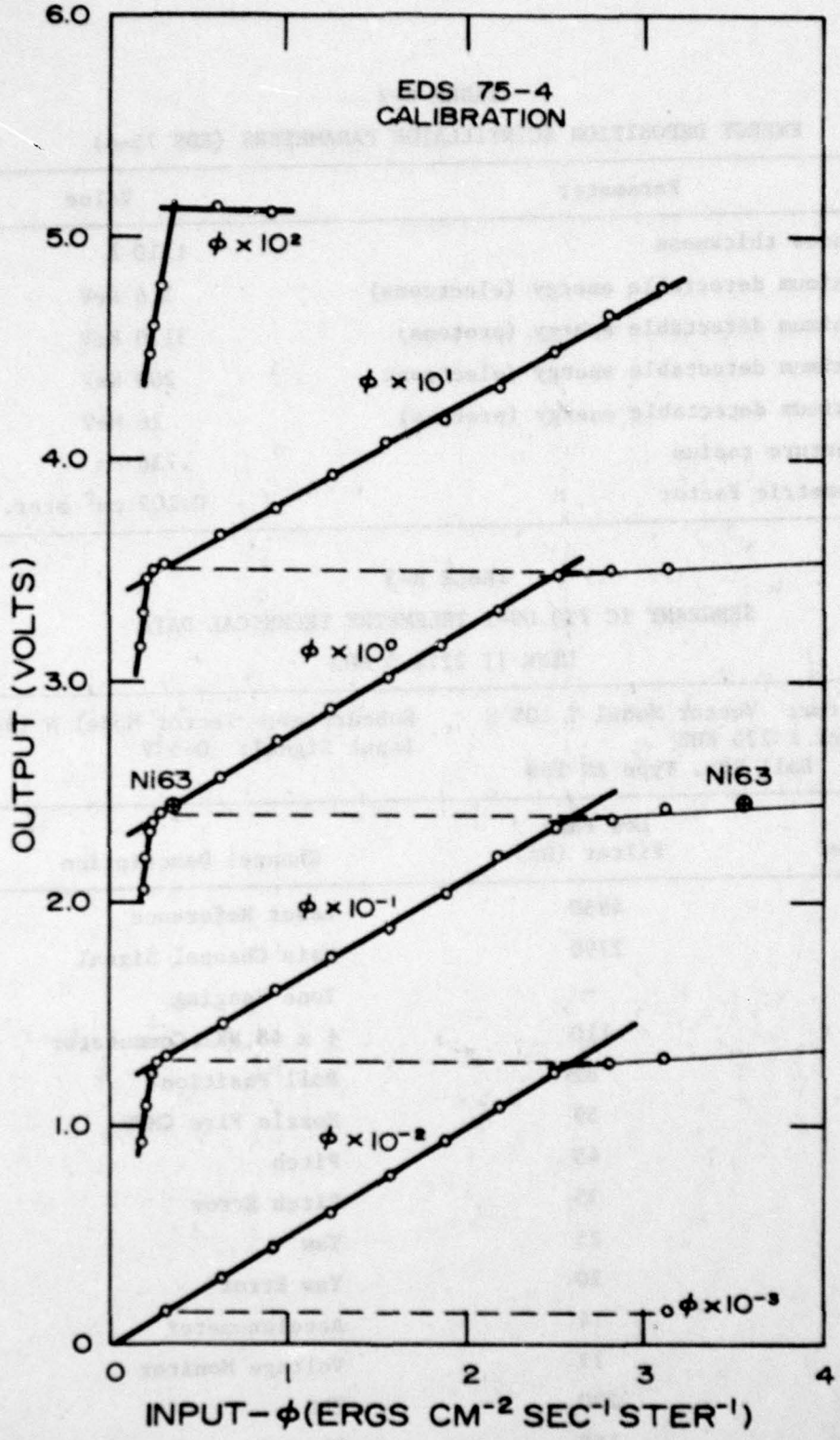


Figure B-5. Energy deposition scintillator (EDS 75-4) calibration.

TABLE B-2

ENERGY DEPOSITION SCINTILLATOR PARAMETERS (EDS 75-4)

Parameter	Value
Window thickness	1510 Å
Minimum detectable energy (electrons)	3.6 KeV
Minimum detectable energy (protons)	31.0 KeV
Maximum detectable energy (electrons	200 KeV
Maximum detectable energy (protons)	26 MeV
Aperture radius	.736 cm
Geometric Factor	0.109 cm^2 ster.

TABLE B-3

SERGEANT IC 730.09-1 TELEMETRY TECHNICAL DATA

LINK II 2279.5 MHz

Transmitter: Vector Model T 105 S
Deviation: ± 225 KHZ
Antenna: Ball Bro. Type AN 16B

Subcarrier: Vector Model N 194 A
Input Signal: 0-5 V

IRIG Channel	Low Pass Filter (Hz)	Channel Description
H	4950	Laser Reference
F	2790	Main Channel Signal
14	-	Tone Ranging
11	110	1 x 48 NRZ Commutator
10	81	Roll Position
9	59	Nozzle Fire CMND
8	45	Pitch
7	35	Pitch Error
6	25	Yaw
5	20	Yaw Error
4	14	Accelerometer
3	11	Voltage Monitor
13	220	EDS
12	160	Photometer

Link I is used for the PCM signal
and the format is NRZ with 420K bit rate.

TABLE B-4

SERGEANT IC 730.09-1 1 x 48 NRZ IRIG COMMUTATOR ASSIGNMENT

LINK II IRIG CHANNEL 11

Data Channels: 0.0 - +5.0 volts
Frame SYNC Pulse: +5.0 volts Switch Action: Make Before Break

Channel	Data
1	Main Pre Amp Temp
2	Main Detector Temp
3	CUTM Up Right
4	Slide Casting Temp
5	Beam Splitter Temp
6	Window Temp
7	Ref. Pre Amp Temp
8	Ref. Detector Temp
9	EDS H.V.
10	Photometer EDS Door Mon
11	Pressure Tank
12	Cal Diode & Pop Cover Mon
13	OV Ref.
14	Main +15V
15	Main -15V
16	Ref. +15V
17	Ref. -15V
18	+28V
19	Drive +15V
20	Drive -15V
21	PCM +18V
22	PCM -18V
23	Primary PYRO
24	Secondary PYRO
25	OV Ref.
26	Main Pre Amp Temp
27	Main Detector Temp
28	CUTM Up Right
29	Slide Casting Temp
30	Beam Splitter Temp
31	Window Temp
32	Ref. Pre Amp Temp
33	Ref. Detector Temp
34	OV Ref.
35	Nose Tip Mon
36	Lid Eject
37	IV Ref.
38	OV Ref.
39	OV Ref.
40	ACS Press (ACS)
41	AV Press (ACS)
42	Photometer H.V.
43	Photometer Temp

TABLE B-4 (cont.)

Channel	Data
44	0V Ref.
45	+5V Ref.
46	+5V Ref.
47	+5V Ref.
48	0V Ref.

APPENDIX C

AEROBEE 170 AO 4.602

INSTRUMENTS AND PARAMETERS

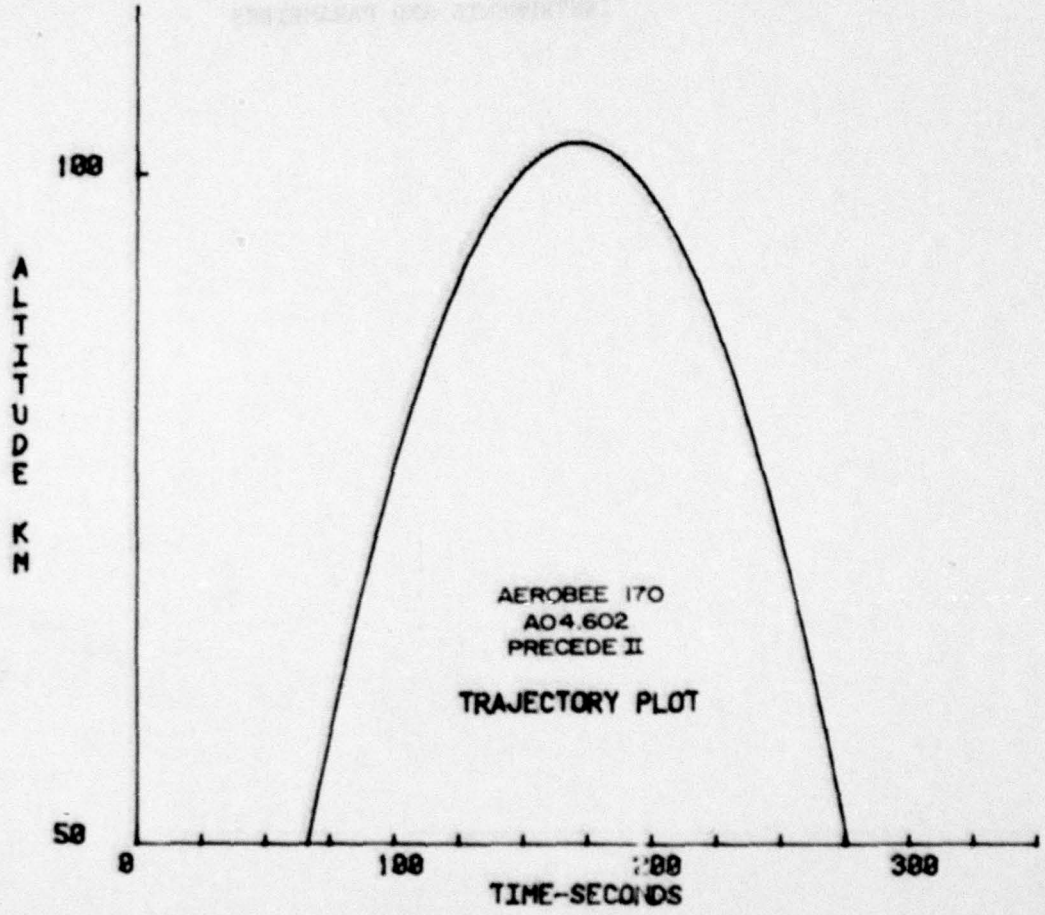


Figure C-1. Aerobee 170 A0 4.602 Trajectory.

TABLE C-1

AEROBEE 170 AO 4.602 TELEMETRY TECHNICAL DATA

LINK I 2279.5 MHz

IRIG Channel	Channel Description
H	Interferometer Mono Reference (-2.5 to +2.5 Volts in)
F	Interferometer Detector Analyzer
16	Mitas Gyro
13	Commutator, 1 x 60 RZ
12	Accelerometer
8	Magnetometer
7	Gyro Analog Roll
6	Electron Gun Monitor Voltage
5	Electron Gun Monitor Current
TM Link II PCM 2251.' MHz	

TABLE C-2

AEROBEE 170 AO 4.602 1 x 60 RZ COMMUTATOR ASSIGNMENTS

LINK I IRIG CHANNEL 13

Channel	Data
1	0 volts
2	Tip Monitor
3	Cap Monitor
4	Cal #1 off
5	Cal #2 off
6	Mirror Relay on
7	Baroswitch 1
8	Baroswitch 2
9	+5V Reg.
10	Ground
11	Position Monitor
12	DC Comp. High Range
13	DC Comp. Low Range
14	Exper. Battery Mon.
15	Instr. Battery Mon.
16	Mirror Relay on
17	Cal #1 Enable on
18	Cal #2 Enable on
19	Tip Monitor

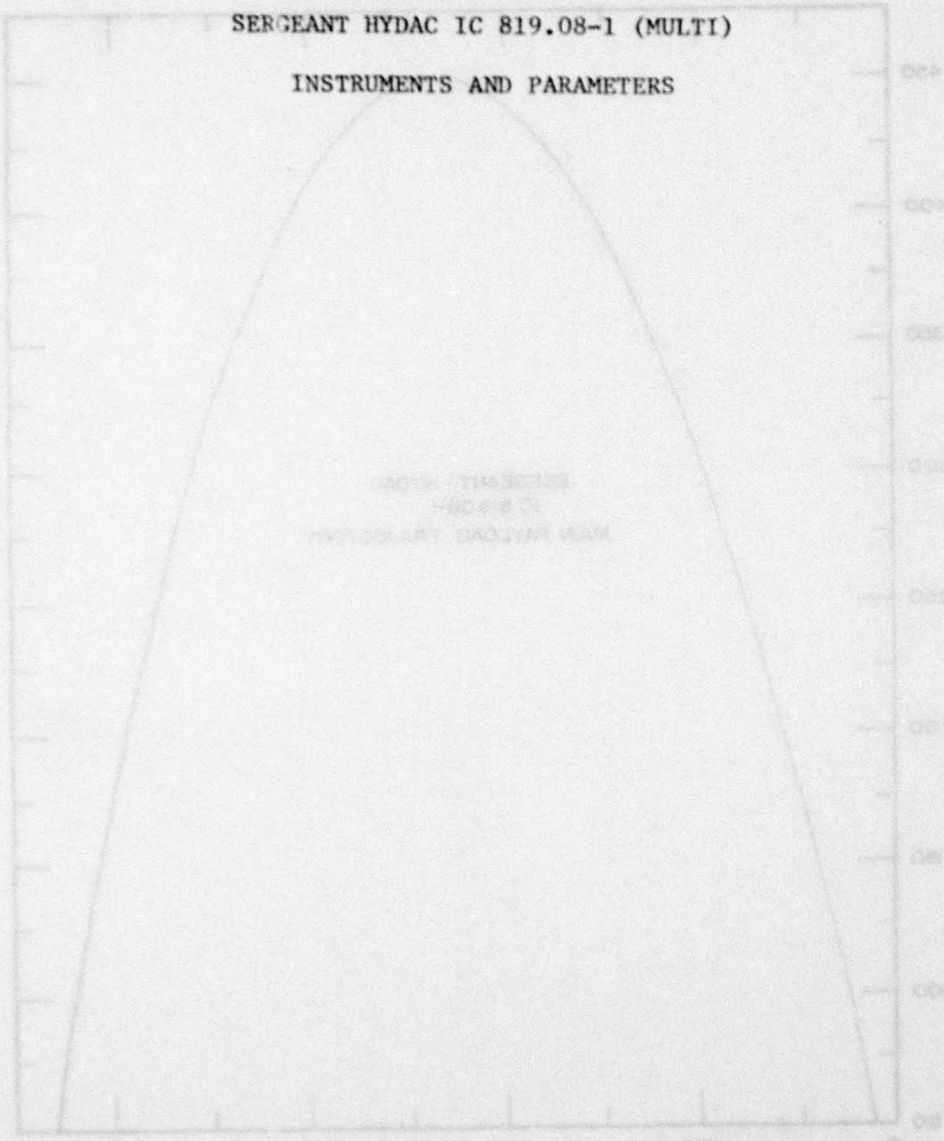
TABLE C-2 (cont.)

Channel	Data
20	0 Volts
21	Position Monitor
22	DC Comp. High Range
23	DC Comp. Low Range
24	Cap Mon.
25	Cal #1 off
26	Cal #2 off
27	Mirror Relay on
28	Baroswitch 1
29	Baroswitch 2
30	OV
31	Position Monitor
32	DC Comp. High Range
33	DC Comp. Low Range
34	Preamp Temp Mon
35	Frame Temp Mon
36	Dewar Elect. Temp Mon
37	Ext. Elect. Temp Mon
38	Batt. Temp Mon
39	Cal #1 Temp Mon
40	OV
41	Position Monitor
42	DC Comp. High Range
43	DC Comp. Low Range
44	Cal #2 Monitor
45	Mirror Unlock Mon
46	PZT Point Mon
47	Sig. Power +18V
48	Sig. Power -18V
49	Ref. Power +18V
50	OV
51	Position Mon
52	DC Comp. High Range
53	DC Comp. Low Range
54	Ref. Power -18V
55	PCM Power +18V
56	PCM Power -18V
57	Mirror Drive Power +24V
58	Mirror Drive Power -24V
59	Frame Sync (+5V)
60	Frame Sync (+5V)

APPENDIX D

SERGEANT HYDAC IC 819.08-1 (MULTI)

INSTRUMENTS AND PARAMETERS



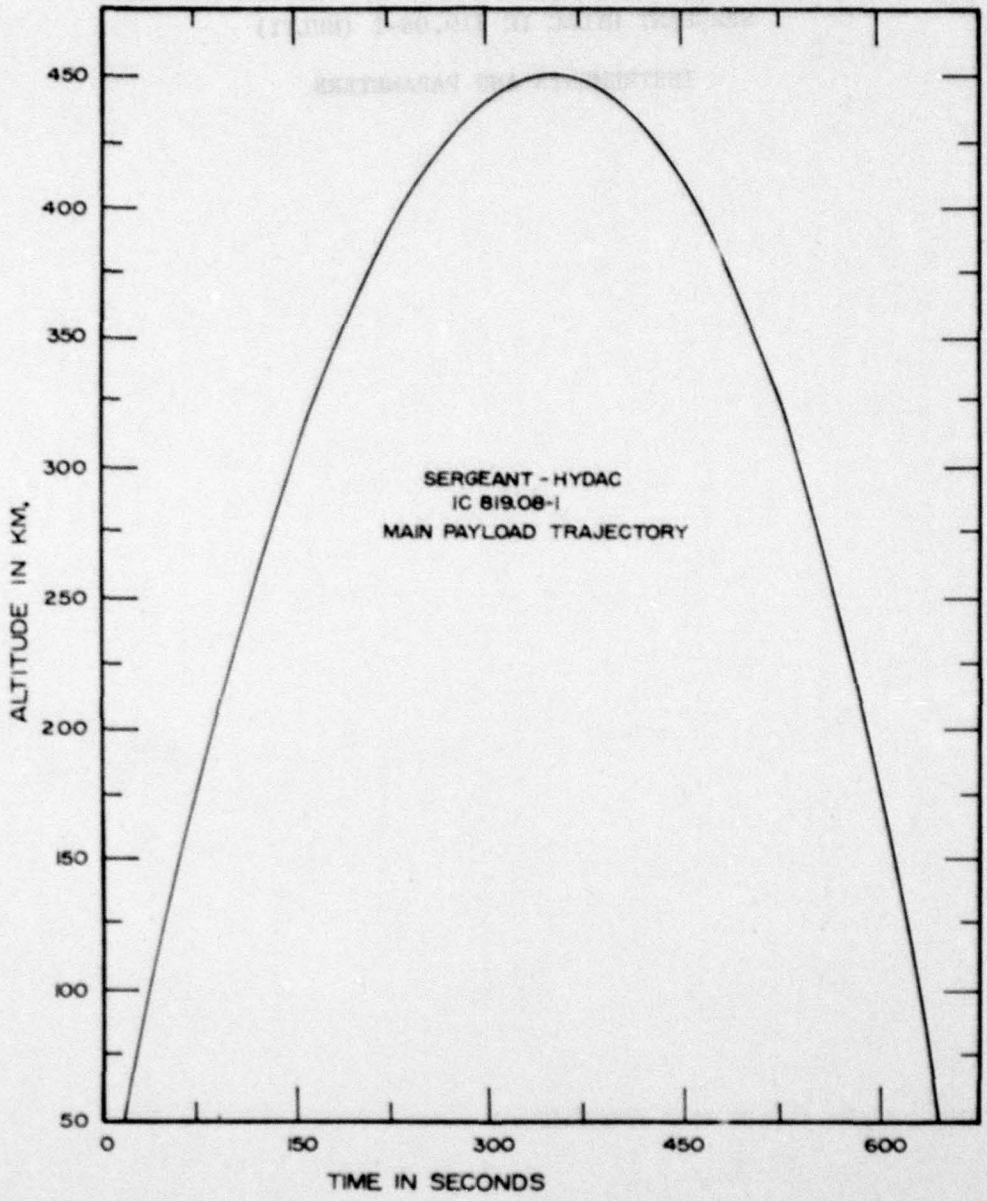


Figure D-1. Sergeant Hydac IC 819.08-1
Main Payload Trajectory.

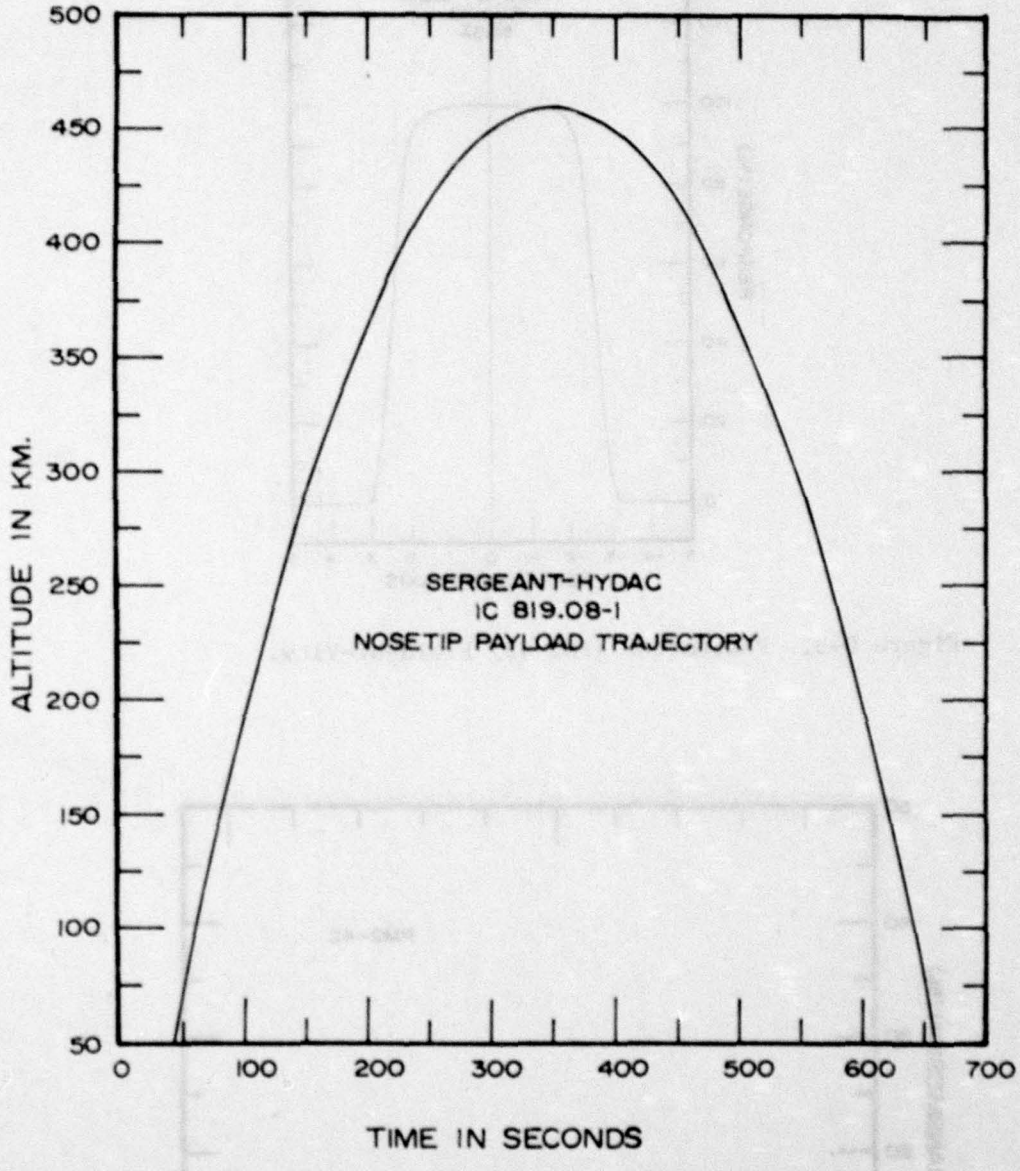


Figure D-2. Sergeant Hydac IC 819.08-1 Nosetip payload trajectory.

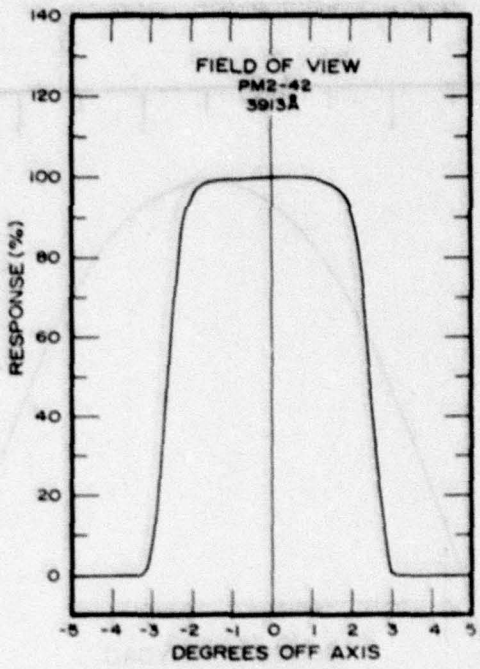


Figure D-3. Photometer (PM2-42) Field-of-View.

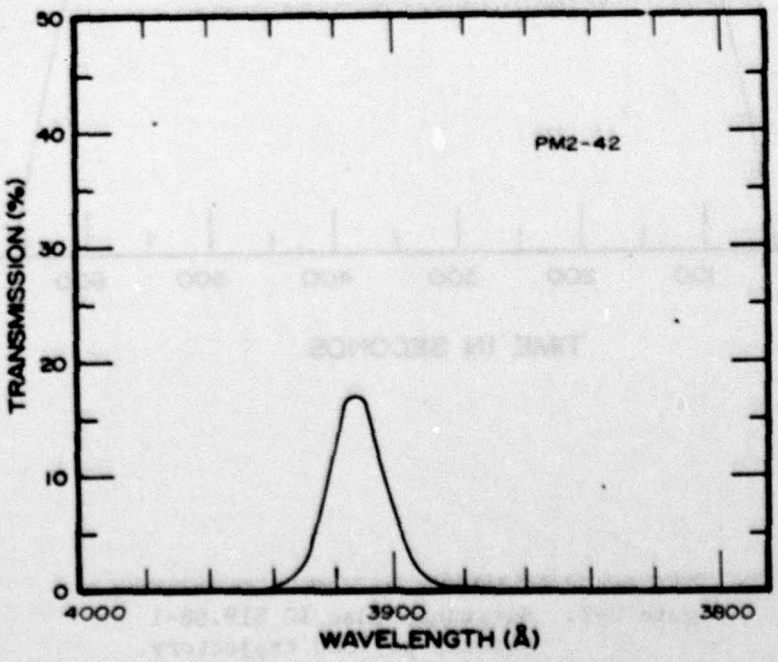


Figure D-4. Photometer (PM2-42) Bandpass Filter Transmission.

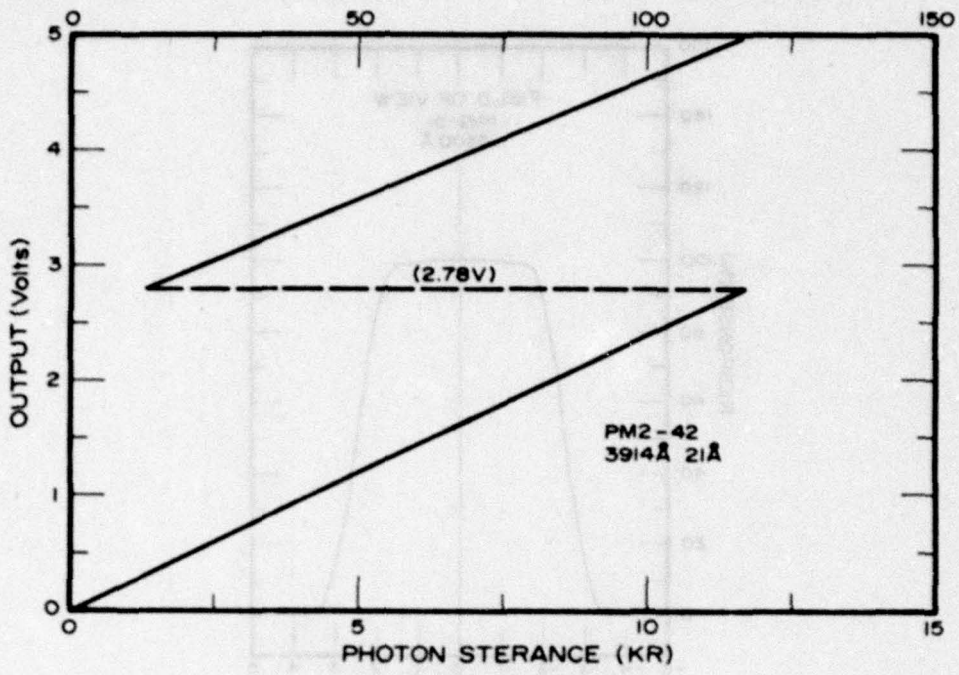


Figure D-5. Photometer (PM2-42) Responsivity.

TABLE D-1

PHOTOMETER PARAMETERS (PM2-42)

Conversion Equations (volts to Kilorayleighs)
4.177V - 0.089 for $V_0 \leq 2.748$ volts
46.813V - 117.252 for $V_0 \geq 2.748$ volts

Parameter	Value
Filter λ_0 (Å)	3913.0
Filter $\Delta\lambda$ (Å)	20.0
Filter T_r Peak (%)	17.0
Offset (volts)	+0.01
H.V. Mon. (volts)	2.25
Temp. Mon. (volts)*	1.68
Check Pulse (volts)	0.50
Field of View ($^{\circ}$Full Angle)	5.0

* Ambient room temperature of 24°C

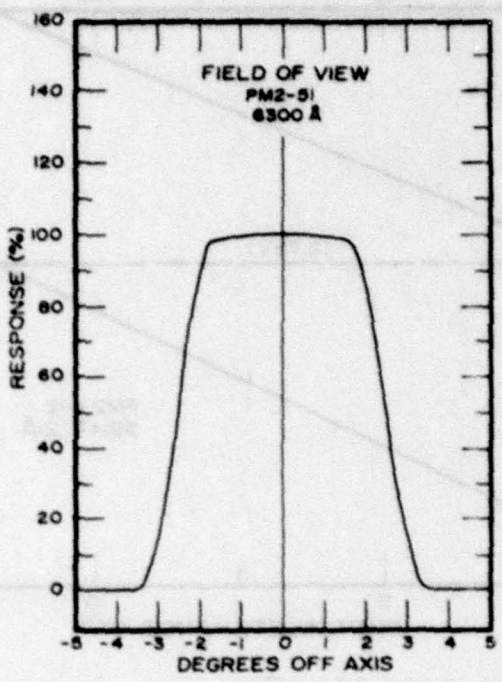


Figure D-6. Photometer (PM2-51) Field-of-View.

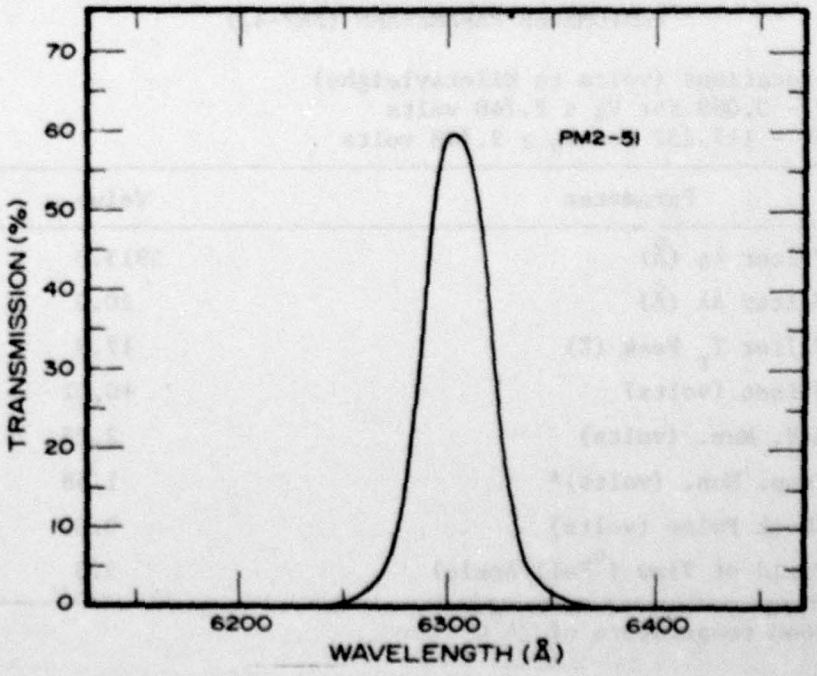
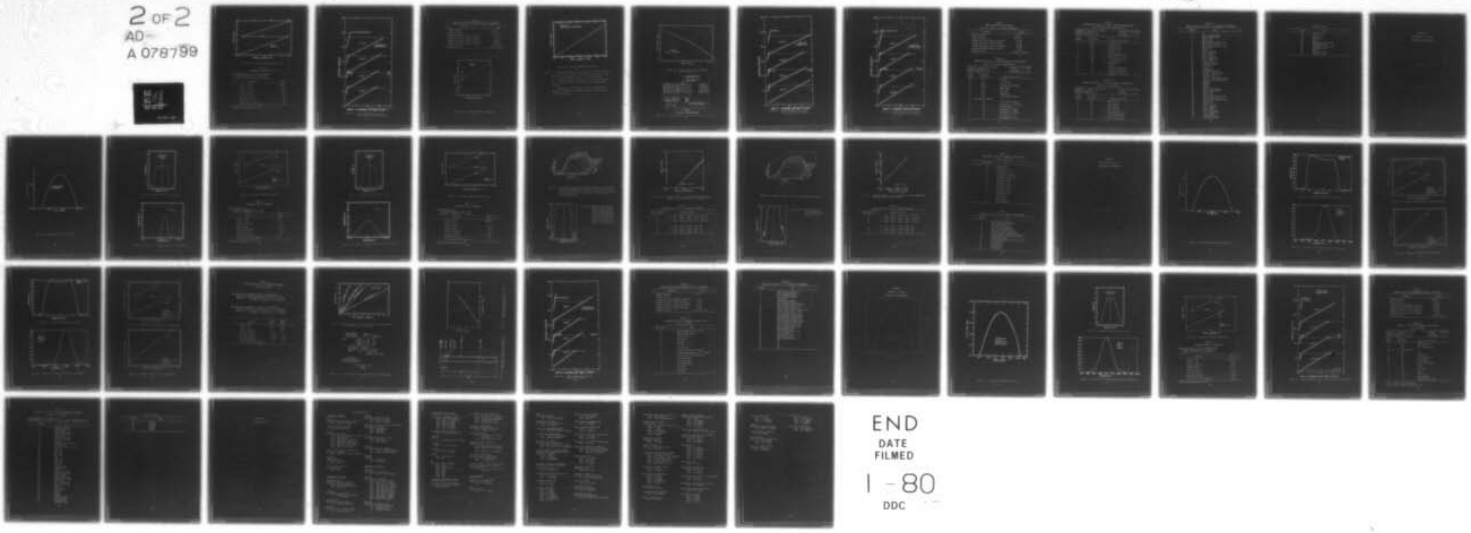


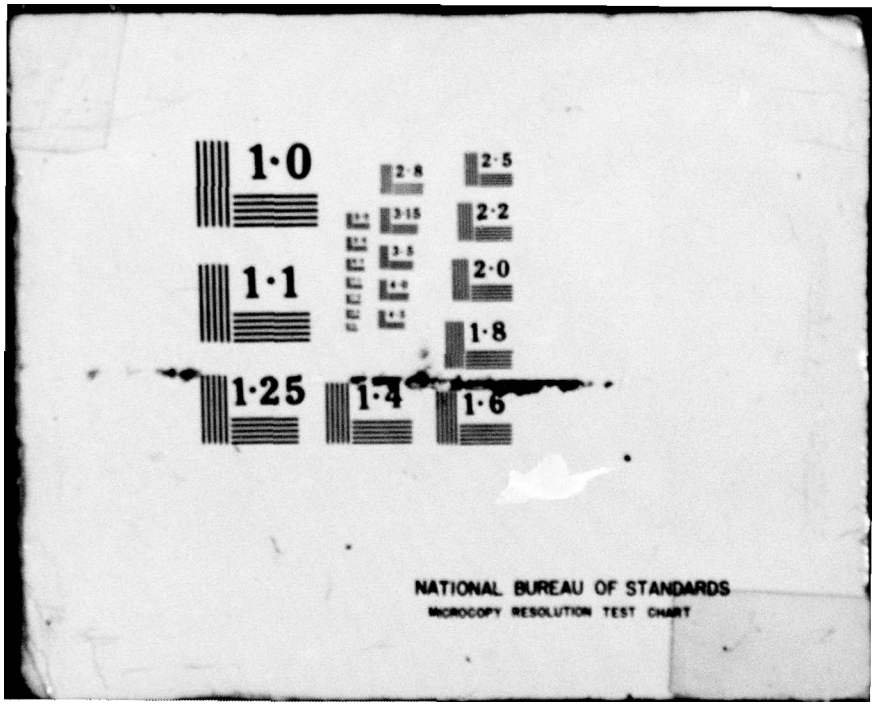
Figure D-7. Photometer (PM2-51) Bandpass Filter Transmission.

AD-A078 799 UTAH STATE UNIV LOGAN SPACE MEASUREMENTS LAB F/G 4/1
ROCKETBORNE IONOSPHERIC STUDIES: 1976-1979.(U)
AUG 79 D A BURT , G D ALLRED F19628-76-C-0261
UNCLASSIFIED AFGL-TR-79-0179 NL

2 OF 2
AD-
A 078799



END
DATE
FILMED
1-80
DDC


1·0
1·1
1·25
1·4
1·6
2·8
3·15
3·5
2·5
2·2
2·0
1·8
NATIONAL BUREAU OF STANDARDS
MICROCOPY RESOLUTION TEST CHART

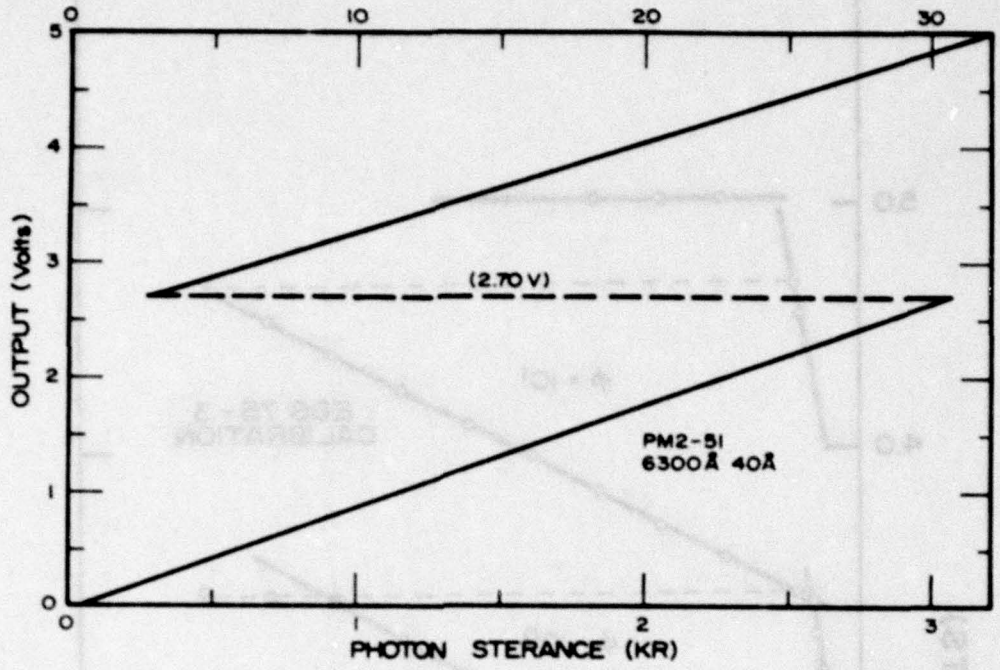


Figure D-8. Photometer (PM2-51) Responsivity.

TABLE D-2

PHOTOMETER PARAMETERS (PM2-51)

Conversion Equations (volts to Kilorayleighs)
1.119V + 0.040 for $V_0 \leq 2.700$ volts
12.583 V - 30.914 for $V_0 \geq 2.700$ volts

Parameter	Value
Filter λ_0 (Å)	6305.0
Filter $\Delta\lambda$ (Å)	37.0
Filter T_r Peak (%)	59.6
Offset (volts)	+0.03
H.V. Mon. (volts)	2.68
Temp. Mon. (volts)*	1.48
Check Pulse (volts)	0.50
Field of View (^{o}Full Angle)	5.0

* Ambient room temperature of 24^{o}C

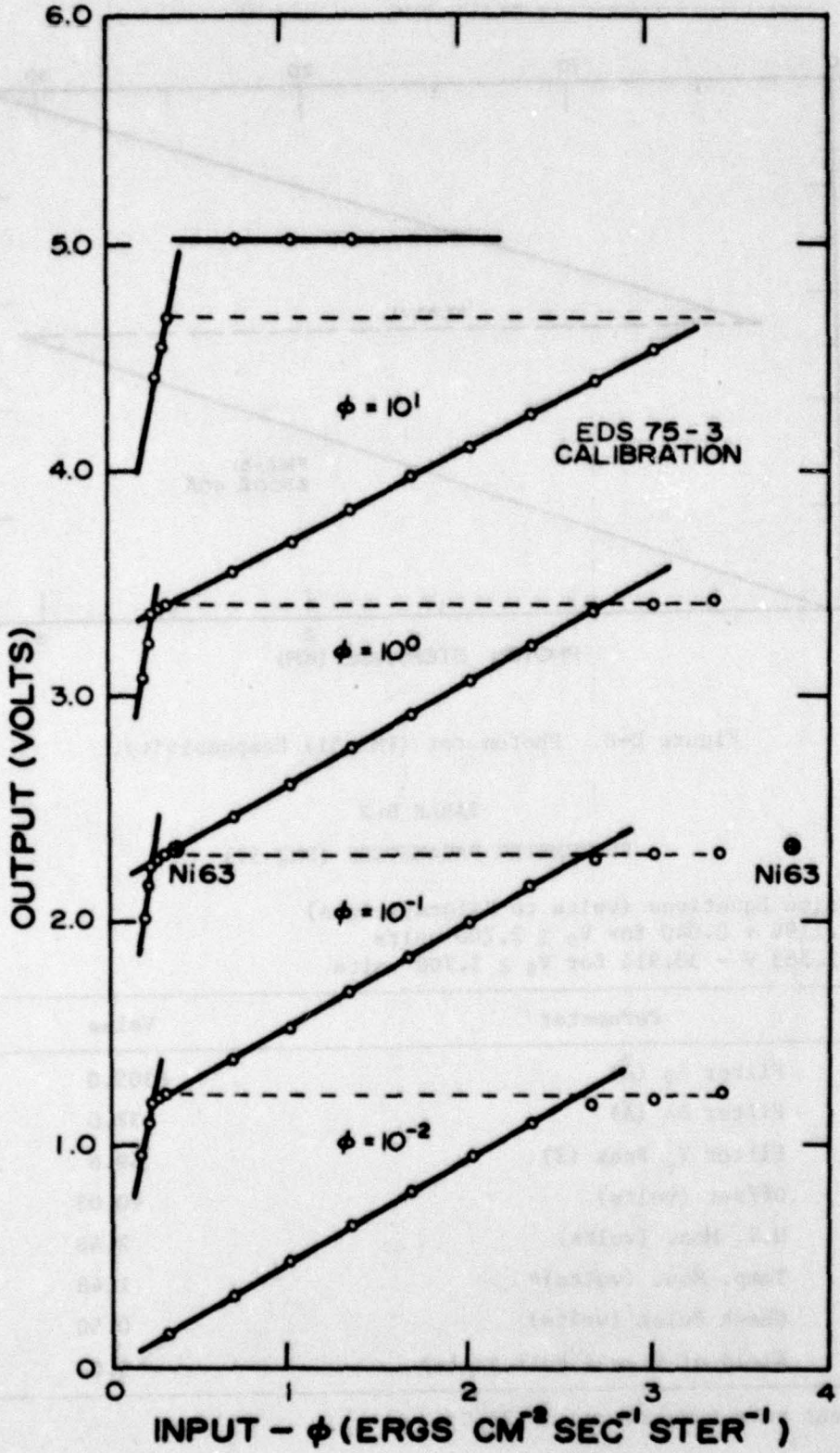


Figure D-9. Energy deposition scintillator (EDS 75-3 main payload) calibration.

TABLE D-3

ENERGY DEPOSITION SCINTILLATOR (EDS 75-3) PARAMETERS

Parameter	Value
Window thickness	1510 Å
Aperture radius	0.736 cm
Minimum detectable energy (electrons)	3.6 KeV
Minimum detectable energy (protons)	31 KeV
Maximum detectable energy (electrons)	200 KeV
Maximum detectable energy (protons)	26 MeV
Geometric Factor	0.109 cm^2 ster.

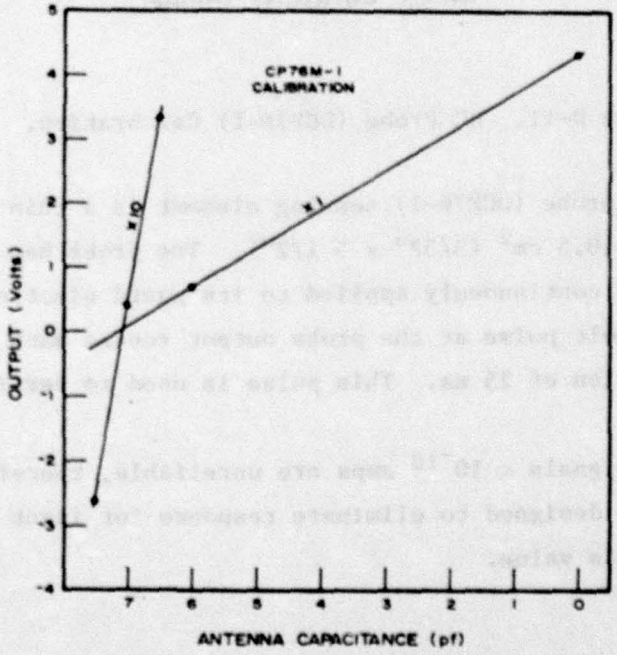


Figure D-10. C-Probe (CP76M-1) calibration.

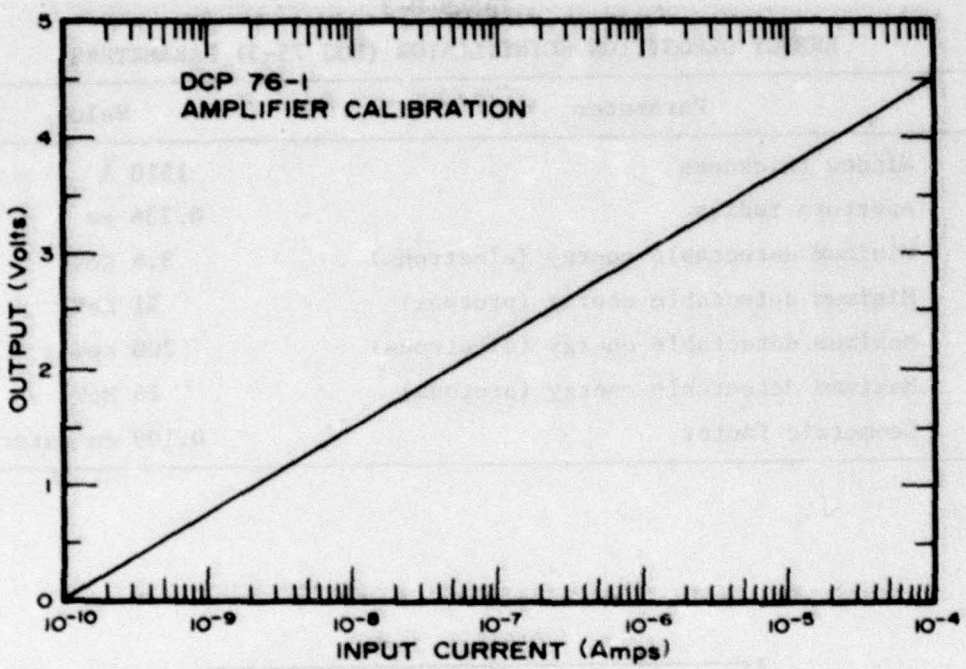


Figure D-11. DC Probe (DCP76-1) Calibration.

Note: The DC probe (DCP76-1) sensing element is a thin cylinder of active area 10.5 cm^2 (3/32" x 5 1/2"). The probe has a dc level of +4.74 VDC continuously applied to its guard electrode.

A 4.0 volt pulse at the probe output recurs each 25 seconds with a duration of 25 ms. This pulse is used to verify probe operation.

Input signals $\leq 10^{-10}$ amps are unreliable, therefore the amplifier is designed to eliminate response for input signals less than this value.

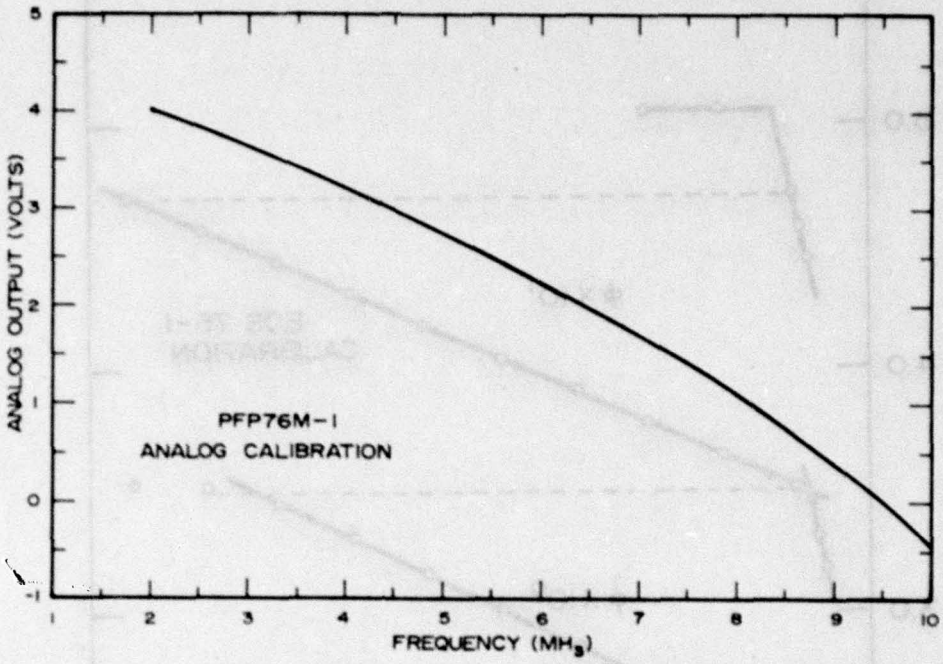


Figure D-12. Plasma Frequency Probe PFP76M-1 Analog Calibration.

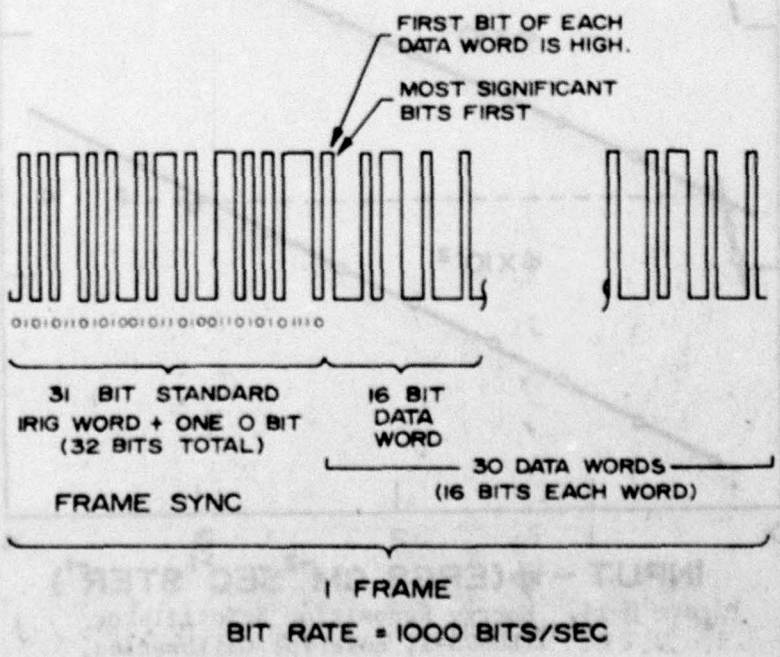


Figure D-13. Plasma Frequency Probe (PFP 76M-1) digital PCM format.

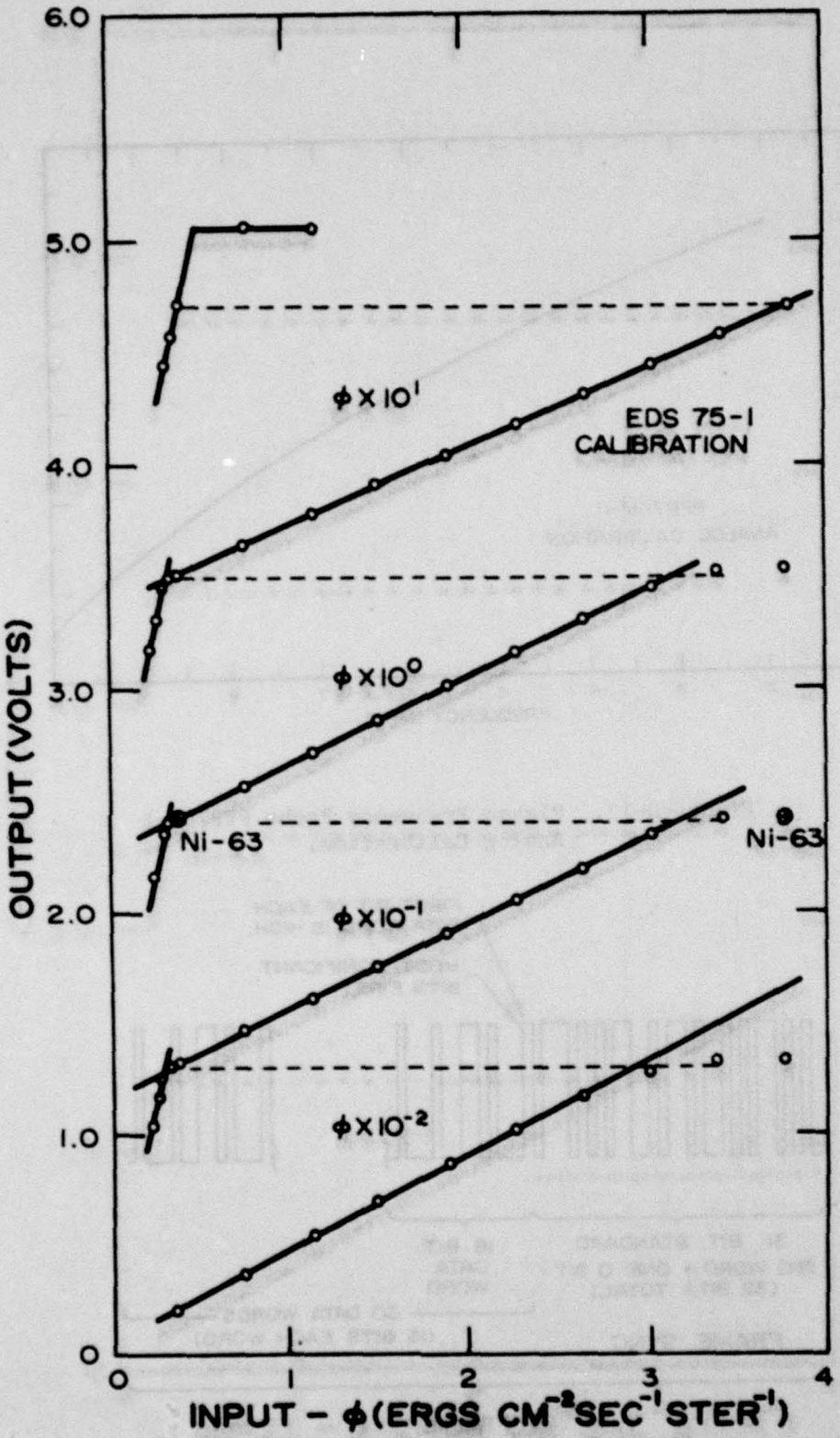


Figure D-14. Energy Deposition Scintillator (EDS75-1, nosetip) Calibration.

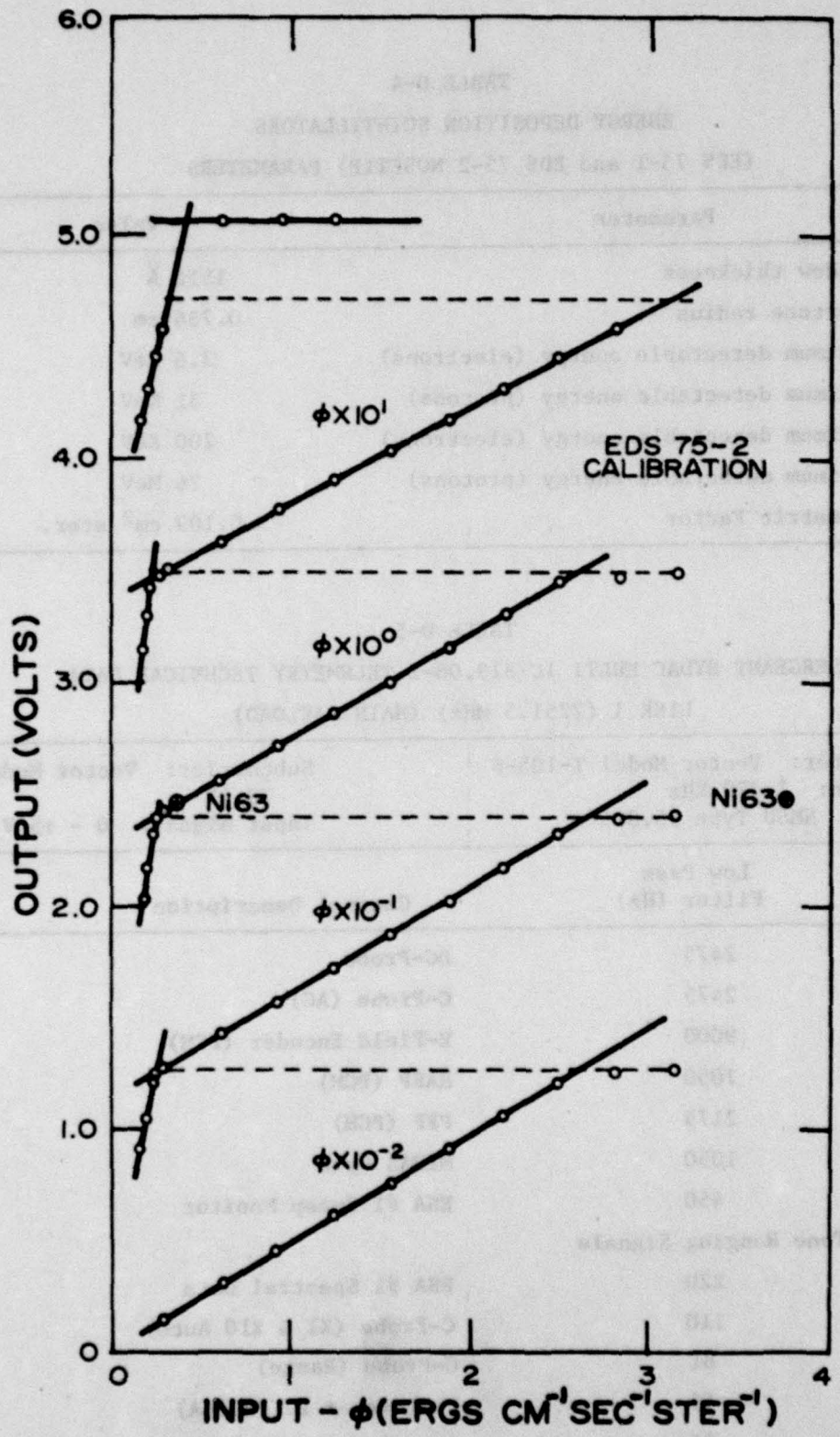


Figure D-15. Energy Deposition Scintillator (EDS75-2, nosetip) Calibration.

TABLE D-4

ENERGY DEPOSITION SCINTILLATORS

(EDS 75-1 and EDS 75-2 NOSETIP) PARAMETERS

Parameter	Value
Window thickness	1510 Å
Aperture radius	0.736 cm
Minimum detectable energy (electrons)	3.6 KeV
Minimum detectable energy (protons)	31 KeV
Maximum detectable energy (electrons)	200 KeV
Maximum detectable energy (protons)	26 MeV
Geometric Factor	0.109 cm^2 ster.

TABLE D-5

SERGEANT HYDAC MULTI IC 819.08-1 TELEMETRY TECHNICAL DATA

LINK 1 (2251.5 MHz) (MAIN PAYLOAD)

Transmitter: Vector Model T-105-S
Deviation: ± 370 KHz
Antenna: NMSU Type 55.805

Subcarrier: Vector Model TS-41
Input Signal: 0 - +5 V

IRIG Channel	Low Pass Filter (Hz)	Channel Description
21	2475	DC-Probe
20	2475	C-Probe (AC)
19	9000	E-Field Encoder (PCM)
18	1050	HARP (PCM)
17	2175	PFP (PCM)
16	1050	MIDAS Gyro
15	450	ESA #1 Sweep Monitor
14	Tone Ranging Signals	
13	220	ESA #1 Spectral Data
11	110	C-Probe (X1 & X10 Auto)
10	81	C-Probe (Range)
8	45	Photometer #2 (3914A)
7	35	Photometer #1 (6300A)
6	25	Gyro Analog Roll
5	20	Magnetometer (ESA #1)

TABLE D-6

SERGEANT HYDAC MULTI IC 819.08-1 TELEMETRY TECHNICAL DATA

LINK II (2279.5 MHz) (MAIN PAYLOAD)

Transmitter: Vector Model T-105-S
Deviation: ± 245 KHz
Antenna: NMSU Type 55.805

Subcarrier: Vector Model TS-41
Input Signal: 0 - +5 V

IRIG Channel	Low Pass Filter (Hz)	Channel Description
H	12500	E-Field (HF 12)
F	2790	E-Field (HF Z)
D	2475	E-Field (HF 34)
B	2475	E-Field (AGC)
14	450	ESA #2 Sweep Monitor
13	220	ESA #2 Spectral Data
12	2200	1 x 60 Commutator
11	110	Accelerometer
10	81	EDS #3
9	59	E-Field FWD BOOM Mon.
8	45	E-Field Aft BOOM Mon.
7	35	Magnetometer (ESA #2)

TABLE D-7

SERGEANT HYDAC MULTI IC 819.08-1 TELEMETRY TECHNICAL DATA

LINK III (2241.5) (NOSETIP)

Transmitter: Vector Model T-105-S
Deviation: ± 40 KHz
Antenna: NMSU Type 6.064

Subcarrier: Vector Model TS-41
Input Signal: 0 - +5 V

IRIG Channel	Low Pass Filter (Hz)	Channel Description
14	330	EDS #1 Output
13	220	EDS #2 Output
8	45	EDS #1 HV Mon.
7	35	EDS #1 HV Mon.
6	25	Z-Axis Magnetometer
5	20	Y-Axis Magnetometer
4	14	X-Axis Magnetometer

TABLE D-8

SERGEANT HYDAC IC 819.08-1 1 x 60 COMMUTATOR ASSIGNMENTS

Segment	Data
1	OV
2	ESA #1 +28V switched
3	ESA #1 +28V standby
4	ESA #1 +15V
5	ESA #1 -15V
6	ESA #1 Photomultiplier HV
7	ESA #1 Post Acc HV
8	ESA #1 Plate enclosure door
9	ESA #1 Temp
10	Ground
11	Door 1 (ESA #1)
12	Door 2 (ESA #2)
13	Door 3 (EDS)
14	Door 4 (C-Probe)
15	Door 5 (DC-Probe)
16	Door 6 (PFP)
17	C Probe Position
18	DC Probe Position
19	PFP Position
20	Ground
21	Tip Position
22	Baroswitch (75 kft)
23	Battery 1 (Experiments)
24	Battery 2 (HV)
25	Battery 3 (TM Link 1)
26	Battery 4 (TM Link 2, Beacon)
27	Battery 5 (Instrumentation)
28	Regulator
29	EDS HV
30	Ground
31	Ground
32	ESA #2 +28V switched
33	ESA #2 +28V standby
34	ESA #2 +15V
35	ESA #2 -15V
36	ESA #2 Photomultiplier HV
37	ESA #2 Post Accel HV
38	ESA #2 Plate enclosure door
39	ESA #2 Temp
40	Ground
41	Door 1 (ESA #1)
42	Door 2 (ESA #2)
43	Door 3 (EDS)
44	Door 4 (C-Probe)
45	Door 5 (DC-Probe)
46	Door 6 (PFP)
47	C-Probe Position
48	DC-Probe Position

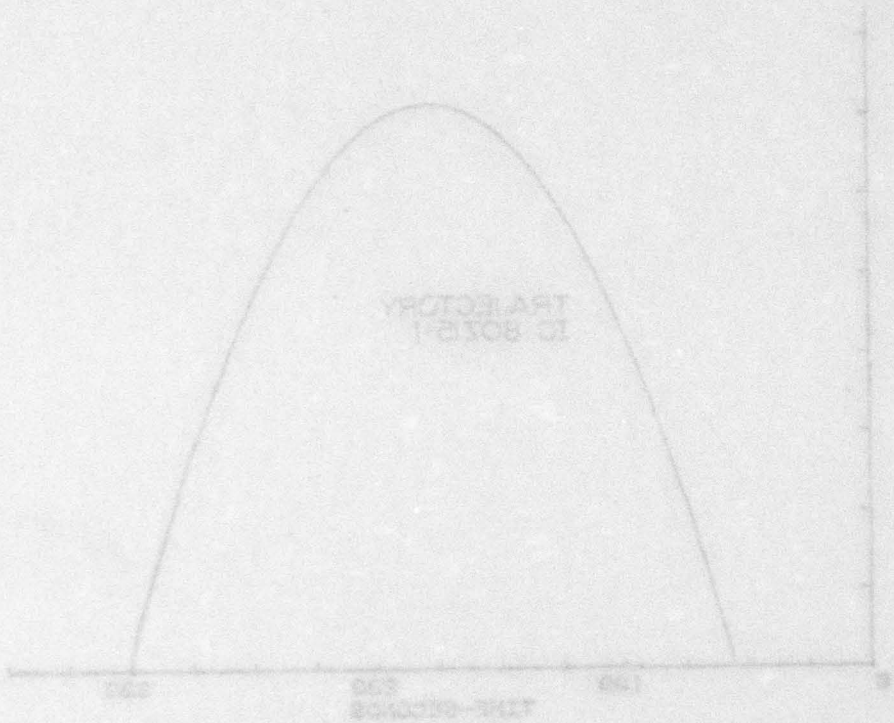
TABLE D-8 (cont.)

Segment	Data
49	PFP Position
50	Ground
51	Tip Position
52	Timer 1
53	Timer 2
54	Photometer 2 filter temp
55	Photometer 2 HV
56	Photometer 1 filter temp
57	Photometer 1 HV
58	EDS HV
59	Frame Sync (+5V)
60	Frame Sync (+5V)

APPENDIX E

NIKE HYDAC IC 807.15-1

INSTRUMENTS AND PARAMETERS



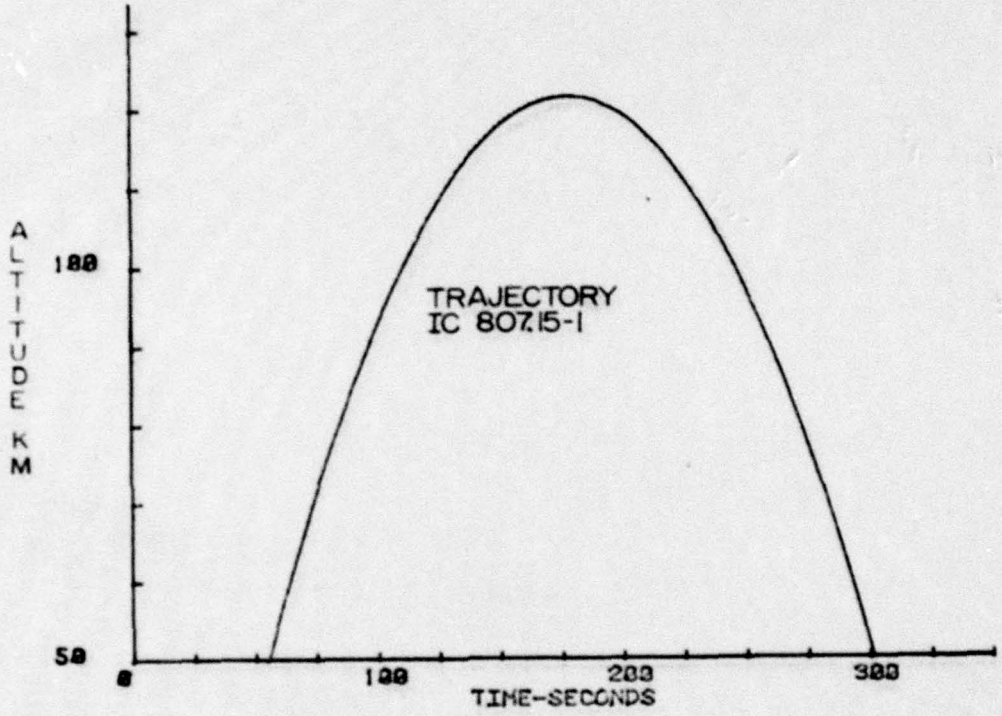


Figure E-1. Nike Hydac IC 807.15-1 Trajectory.

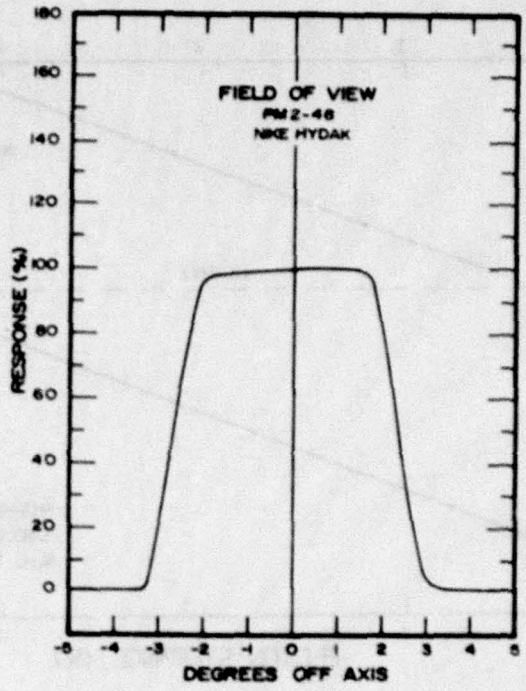


Figure E-2. Photometer (PM2-48) Field-of-View.

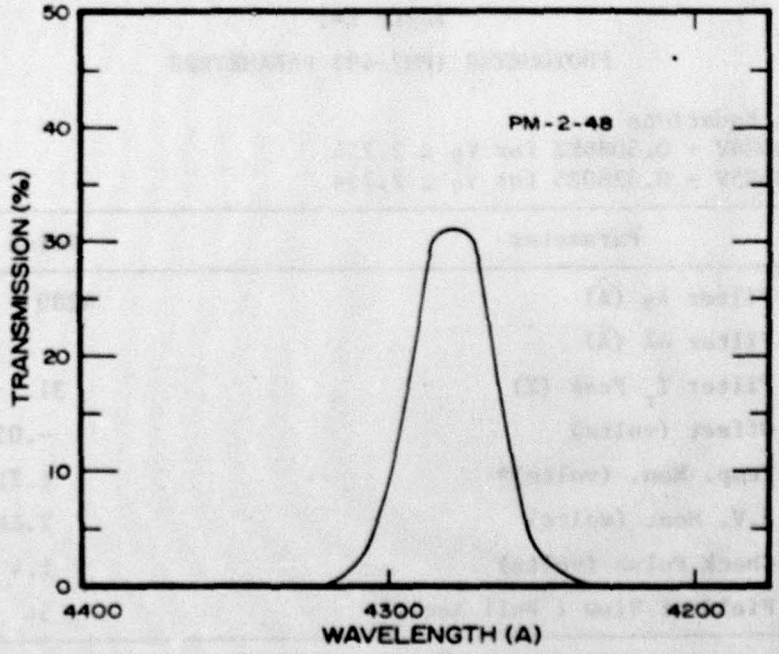


Figure E-3. Photometer (PM2-48) Bandpass Filter Transmission.

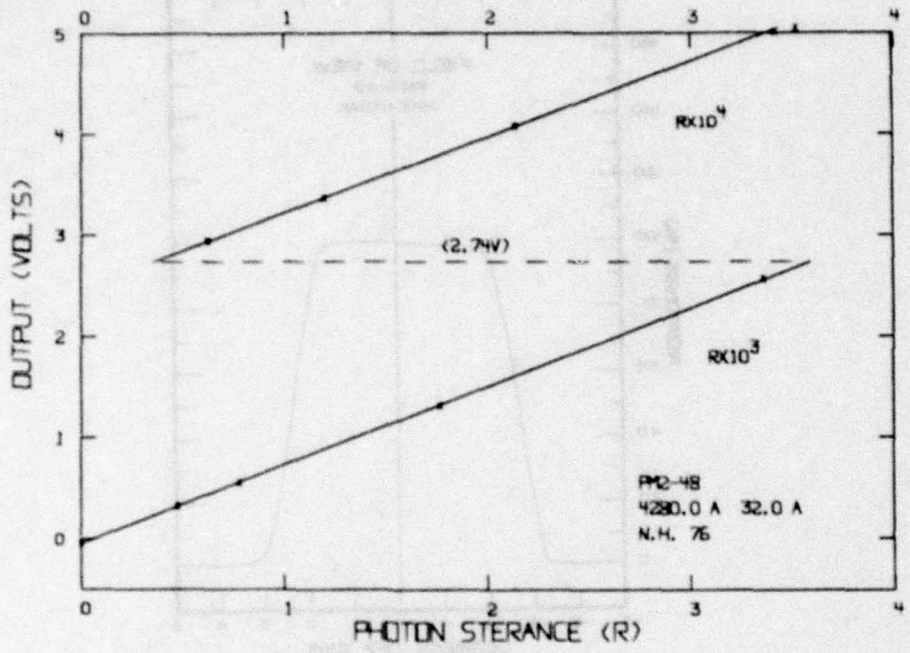


Figure E-4. Photometer (PM2-48) Responsivity.

TABLE E-1

PHOTOMETER (PM2-48) PARAMETERS

Conversion Equations

$0.1330E4V + 0.5086E2$ for $V_0 \leq 2.754$

$0.1326E5V - 0.3280E5$ for $V_0 \geq 2.754$

Parameter	Value
Filter λ_0 (Å)	4280
Filter $\Delta\lambda$ (Å)	
Filter T_r Peak (%)	31.5
Offset (volts)	-.03
Temp. Mon. (volts)*	1.71
H.V. Mon. (volts)	2.46
Check Pulse (volts)	1.4
Field of View (^{O}Full Angle)	5

* Ambient room temperature of 21^{O}C

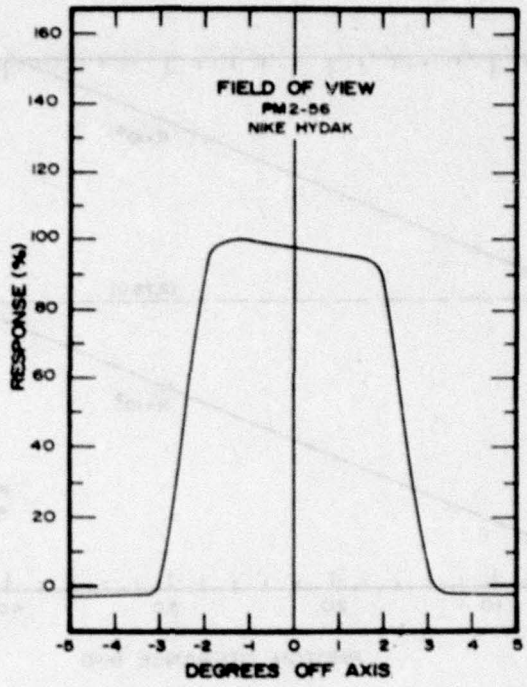


Figure E-5. Photometer (PM2-56) Field of View.

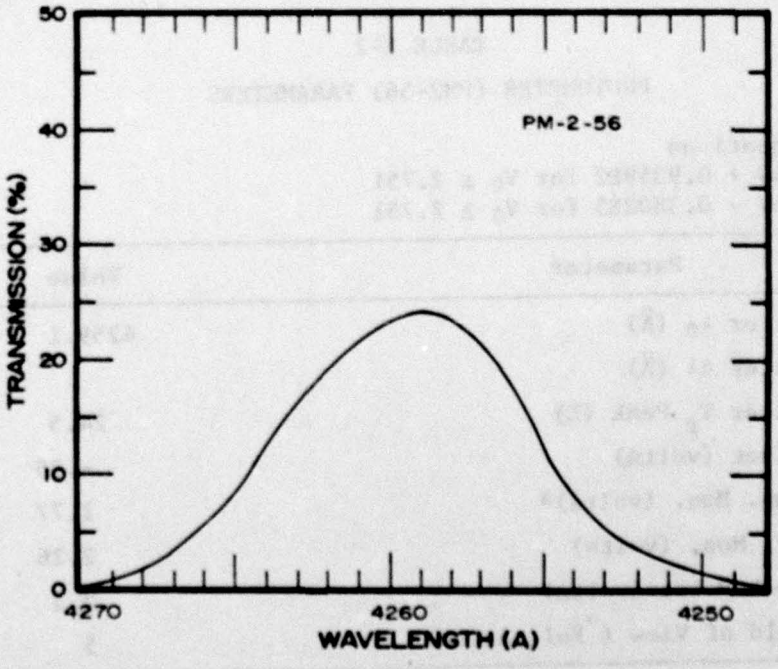


Figure E-6. Photometer (PM2-56) Bandpass Filter Transmission.

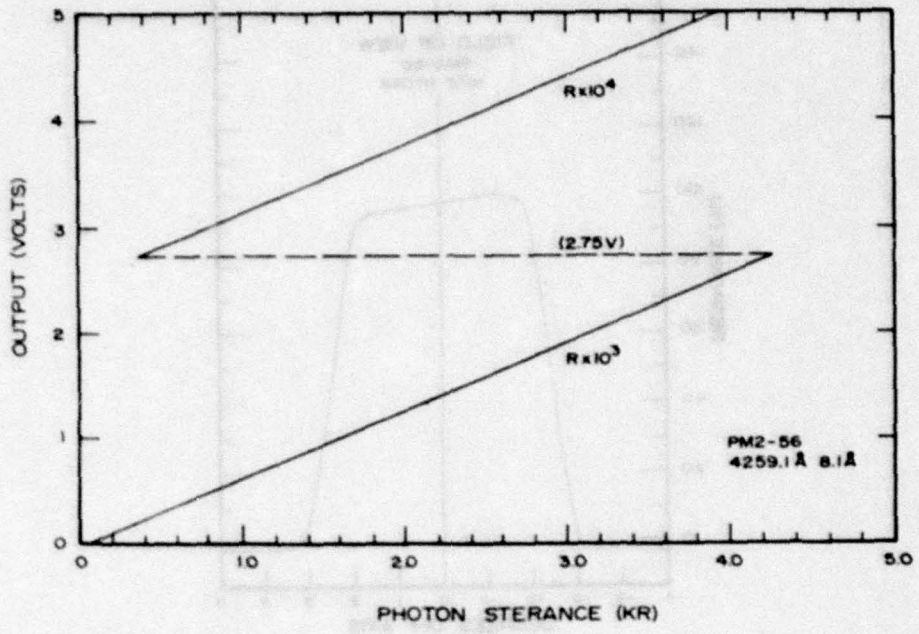


Figure E-7. Photometer (PM2-56) Responsivity.

TABLE E-2

PHOTOMETER (PM2-56) PARAMETERS

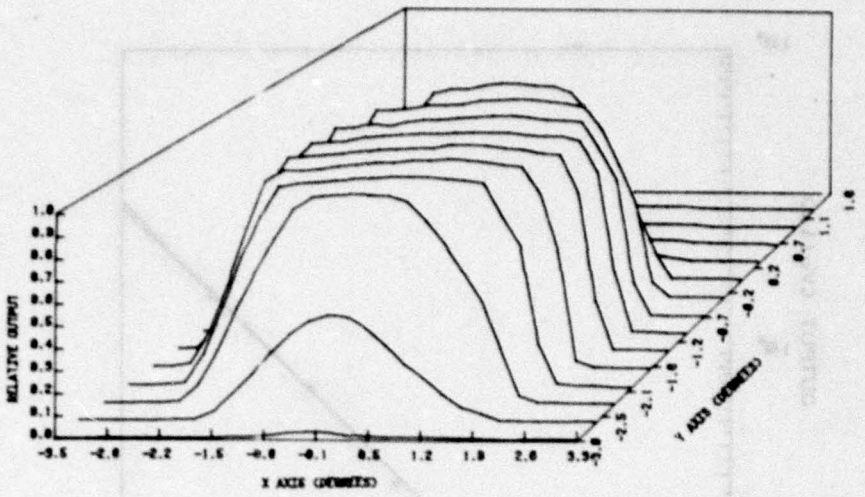
Conversion equations

0.1479E4V + 0.9359E2 for $V_0 \leq 2.751$

0.1532E5V - 0.3802E5 for $V_0 \geq 2.751$

Parameter	Value
Filter λ_0 (Å)	4259.1
Filter $\Delta\lambda$ (Å)	
Filter T_r Peak (%)	24.5
Offset (volts)	-.05
Temp. Mon. (volts)*	1.77
H.V. Mon. (volts)	2.26
Check Pulse (volts)	2.3
Field of View ($^{\circ}$Full Angle)	5

* Ambient room temperature of 21°C



NR4-C-1 (4.3)

Figure E-8. A graphical display of the radiometer NR4-C-1 (4.3 μm channel) near-field-of-view plot. The near field is defined as the linearized and normalized response to a point source at angles near the optical axis, as evaluated in detail to about 1% of the on-axis response.

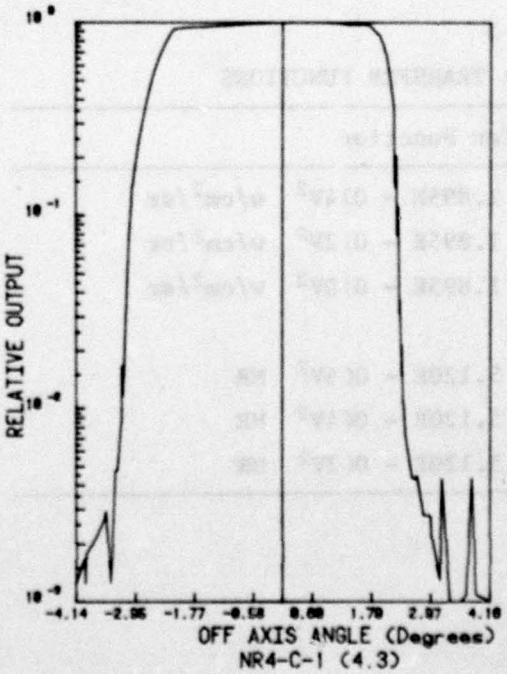


Figure E-9. The far-field-of-view (NR4-C-1, 4.3 μm channel) cross section. The far field is defined as the linearized and normalized sensor response to a point source at angles far from the optical axis as evaluated to many orders below the on-axis response.

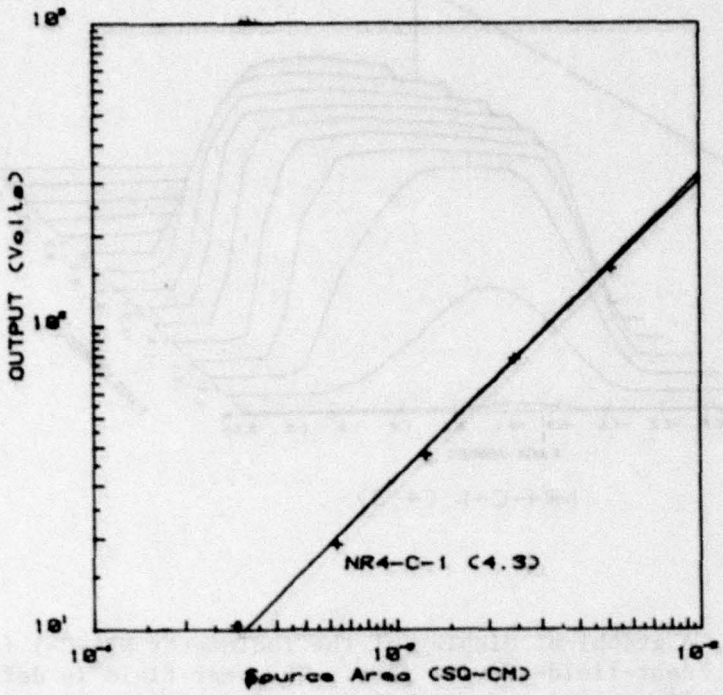
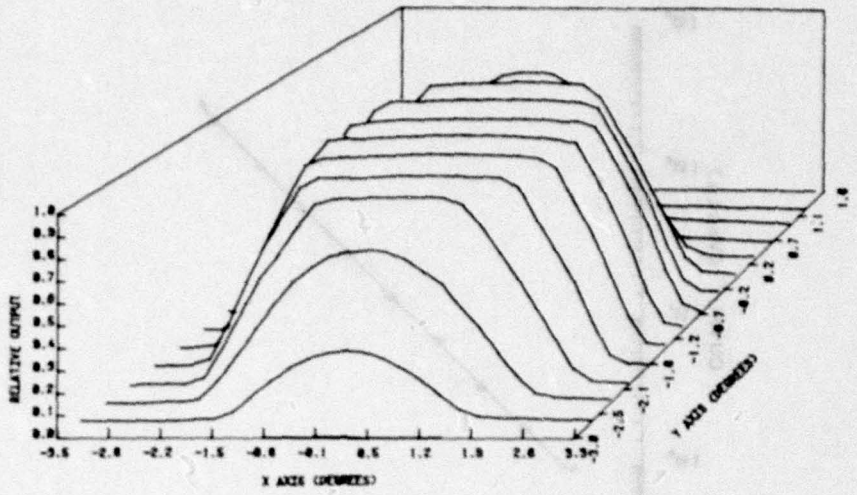


Figure E-10. Radiometer NR4-C-1 (4.3 μm) linearity data superimposed on the instrument transfer function.

TABLE E-3

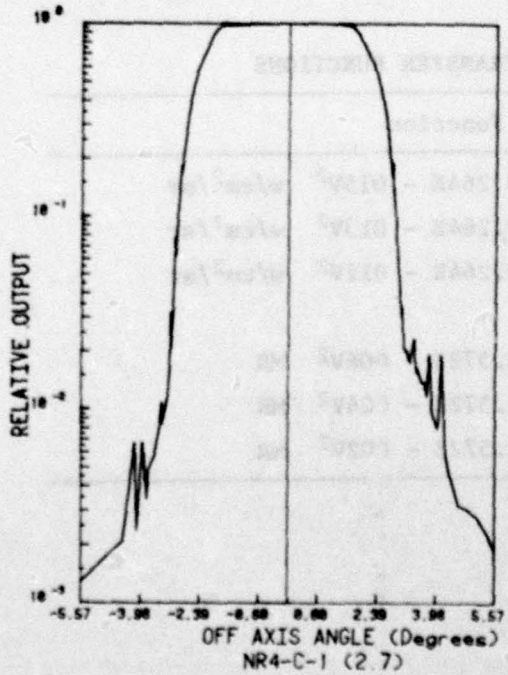
RADIOMETER NR4-C-1 (4.3 μm) TRANSFER FUNCTIONS

Output Channel	Transfer Function	
G2	L = 1.162E - 010V + 1.895E - 01 4V^2	w/cm^2/sr
G1	L = 1.162E - 009V + 1.895E - 01 2V^2	w/cm^2/sr
G0	L = 1.162E - 008V + 1.895E - 01 0V^2	w/cm^2/sr
G2	L = 3.140E - 002V + 5.120E - 00 5V^2	MR
G1	L = 3.140E - 001V + 5.120E - 00 4V^2	MR
G0	L = 3.140E + 000V + 5.120E - 00 2V^2	MR



NR4-C-1 (2.7)

Figure E-11. Radiometer NR4-C-1 (2.7 μm channel) near-field-of-view.



NR4-C-1 (2.7)

Figure E-12. Radiometer NR4-C-1 (2.7 μm channel) far-field-of-view cross section.

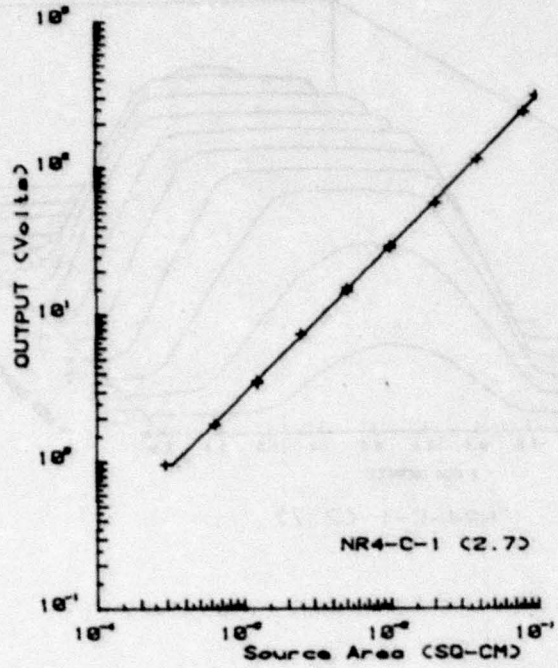


Figure E-13. Radiometer NR4-C-1 (2.7 μm) linearity data superimposed on the instrument transfer function.

TABLE E-4

RADIOMETER NR4-C-1 (2.7 μm) TRANSFER FUNCTIONS

Output Channel	Transfer Function	
G2	$L = 1.506E - 010V - 9.264E - 015V^2$	$w/cm^2/sr$
G1	$L = 1.506E - 009V - 9.264E - 013V^2$	$w/cm^2/sr$
G0	$L = 1.506E - 008V - 9.264E - 011V^2$	$w/cm^2/sr$
G2	$L = 2.555E - 002V - 1.572E - 006V^2$	MR
G1	$L = 2.555E - 001V - 1.572E - 004V^2$	MR
G0	$L = 2.555E + 000V - 1.572E - 002V^2$	MR

TABLE E-5

NIKE HYDAC IC 807.15-1 TELEMETRY TECHNICAL DATA

LINK I 2251.5 MHz

IRIG Channel	Data
18	Midas Gyro
14	Ranging Tones
13	Commutator, 1 x 16
12	Photometer 4259A (#1)
11	Photometer 4278A (#2)
10	Radiometer #2 G2
9	Radiometer #2 G1
8	Radiometer #2 G0
7	Radiometer #1 G2
6	Radiometer #1 G1
5	Radiometer #1 G0
4	Accelerometer
3	Magnetometer
2	Gyro Analog Roll

TABLE E-6

NIKE HYDAC IC 807.15-1 1 x 16 COMMUTATOR ASSIGNMENTS

Channel	Data
1	CFC Temperature Monitor
2	Baffle Temperature Monitor
3	+28V Battery Monitor
4	CFW Temperature Monitor
5	Nosetip Separation Monitor
6	Primary Pyro Battery Monitor
7	Secondary Pyro Battery Monitor
8	4278A Photometer Temperature Monitor
9	4278A Photometer High Voltage Monitor
10	Magnetometer Bias
11	4259A Photometer High Voltage Monitor
12	0 volts Reference
13	+5V Reference
14	+5V Reference
15	+5V Reference
16	OV Reference

APPENDIX F

NIKE HYDAC IR 807.57-1

INSTRUMENTS AND PARAMETERS

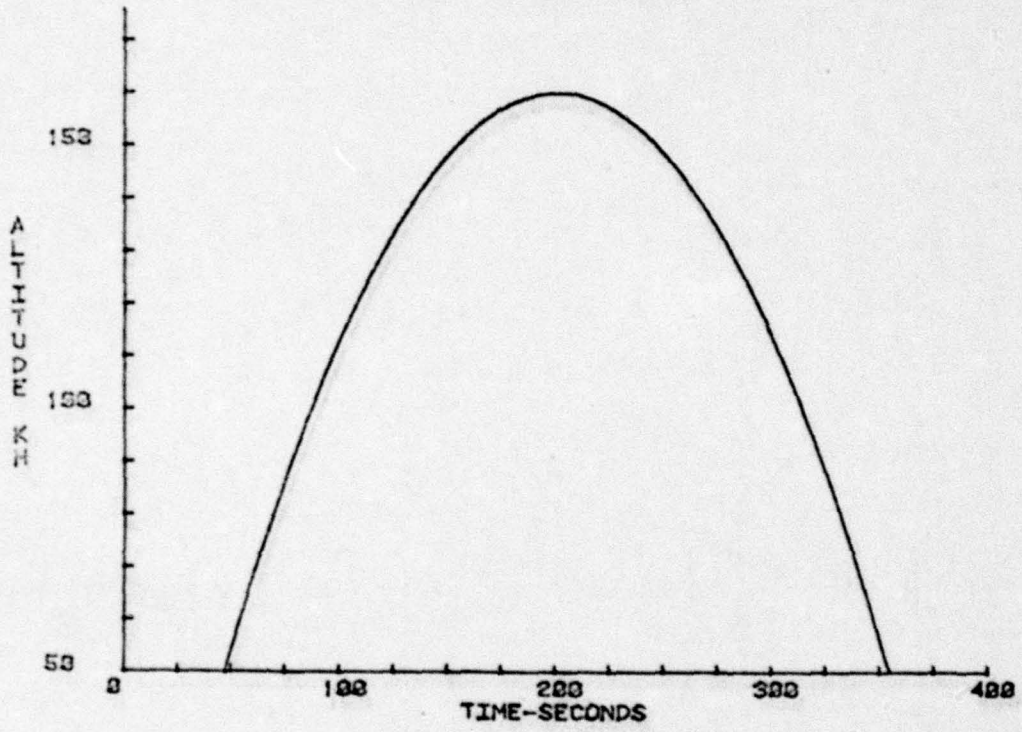


Figure F-1. Nike Hydac IR 807.57-1 Trajectory.

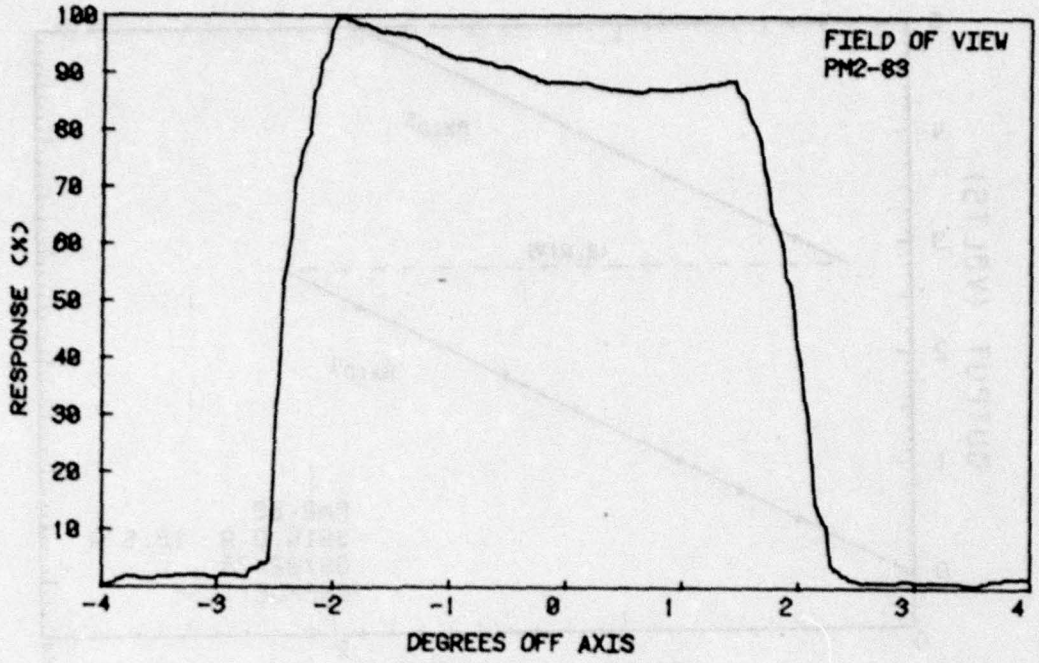


Figure F-2. Photometer (PM2-83) Field-of-View.

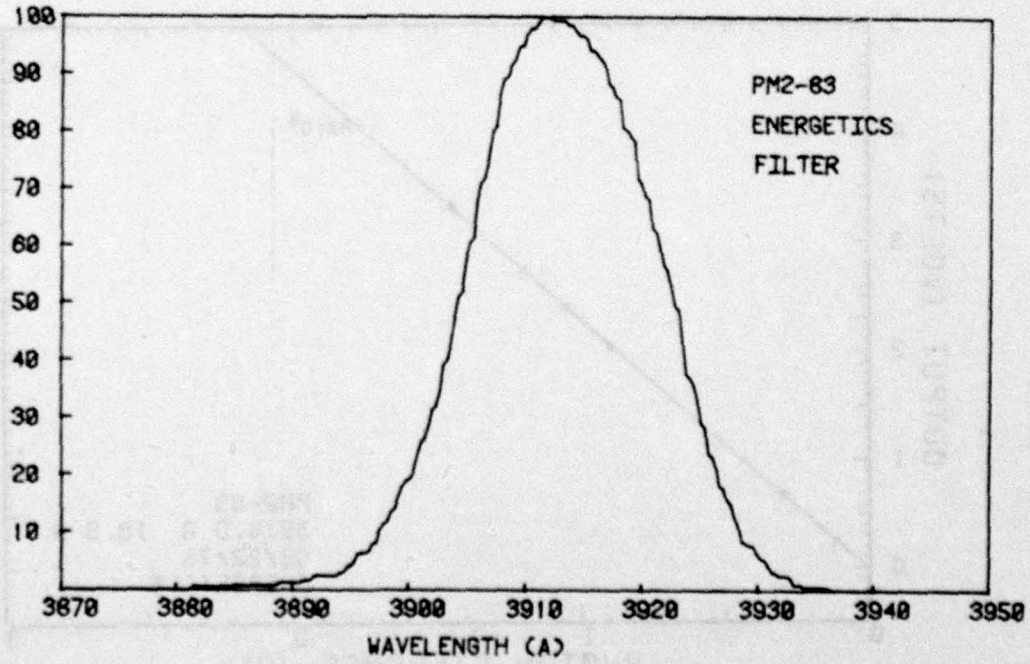


Figure F-3. Photometer (PM2-83) Bandpass Filter Transmission.

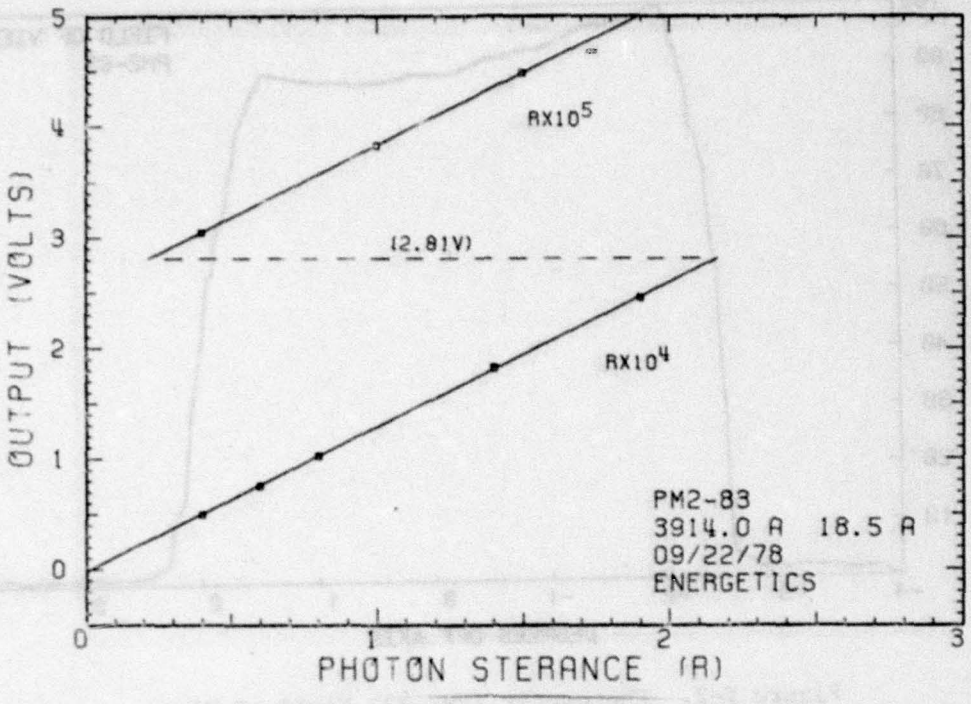


Figure F-4. Photometer (PM2-83) Variable Gain Responsivity.

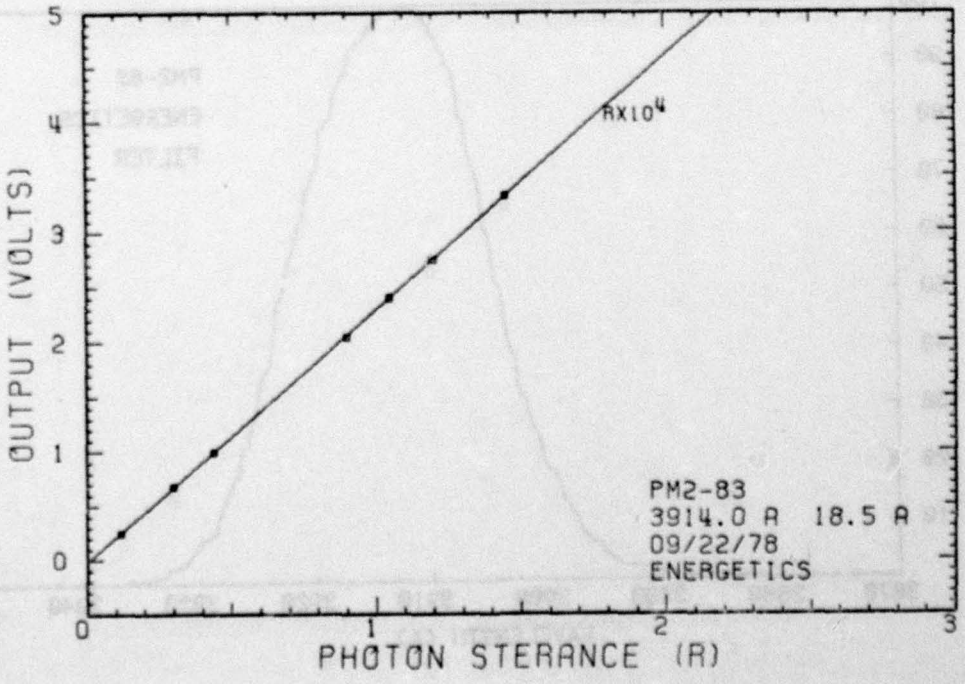


Figure F-5. Photometer (PM2-83) x10 Gain Responsivity

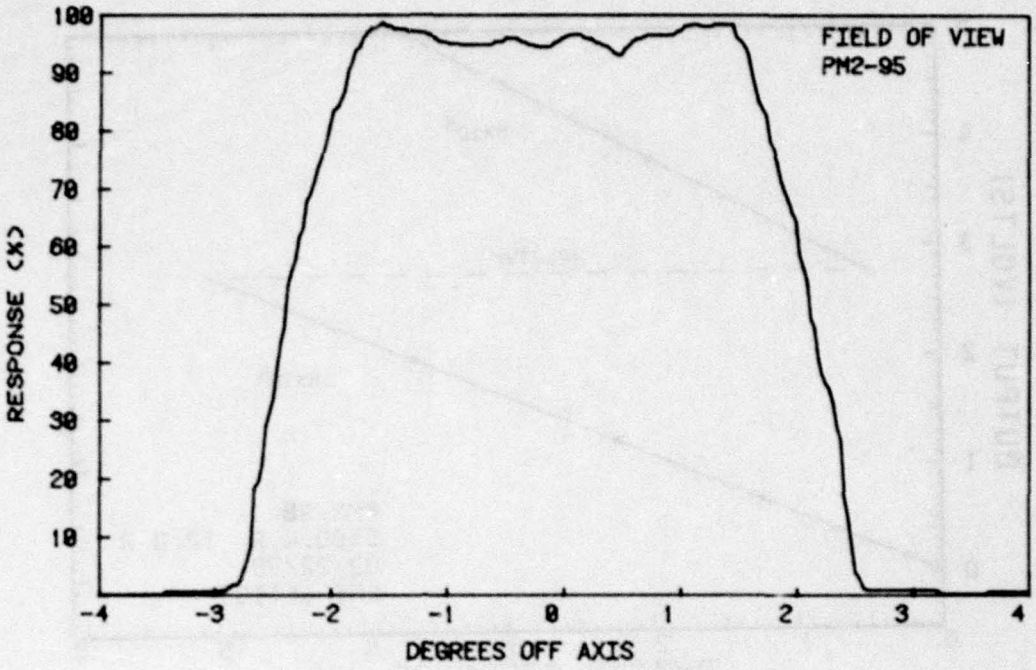


Figure F-6. Photometer (PM2-95) Field-of-View.

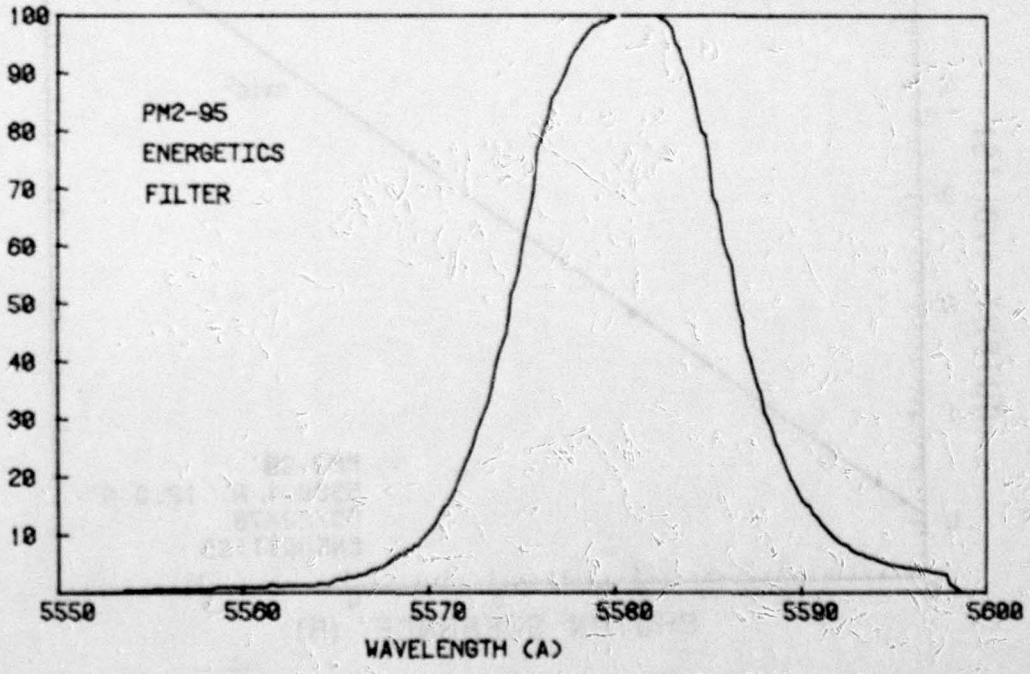


Figure F-7. Photometer (PM2-95) Bandpass Filter Transmission.

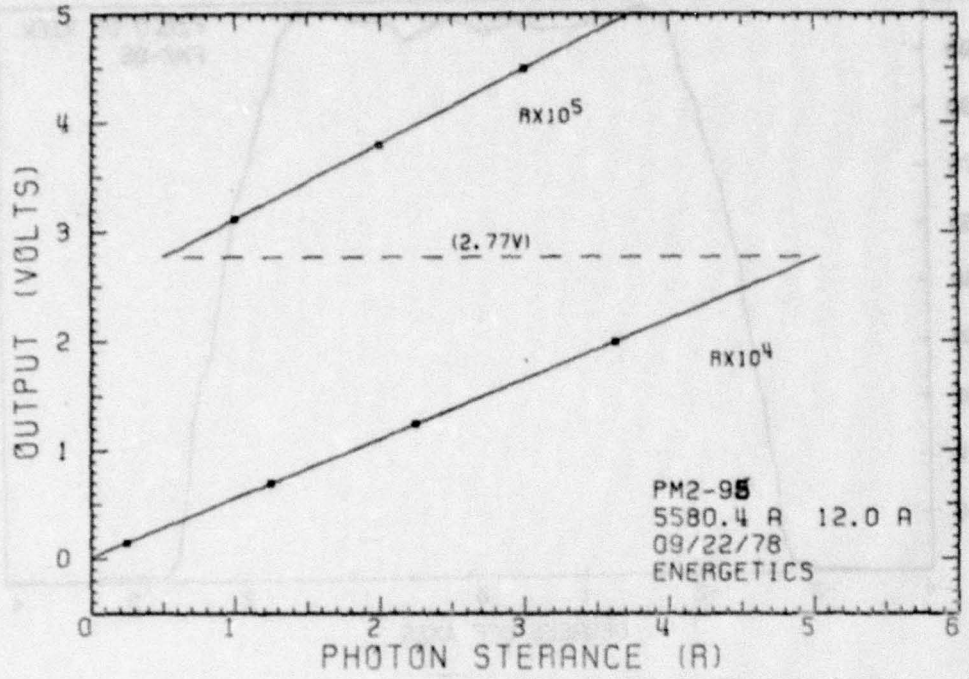


Figure F-8. Photometer (PM2-95) Variable Gain Responsivity.

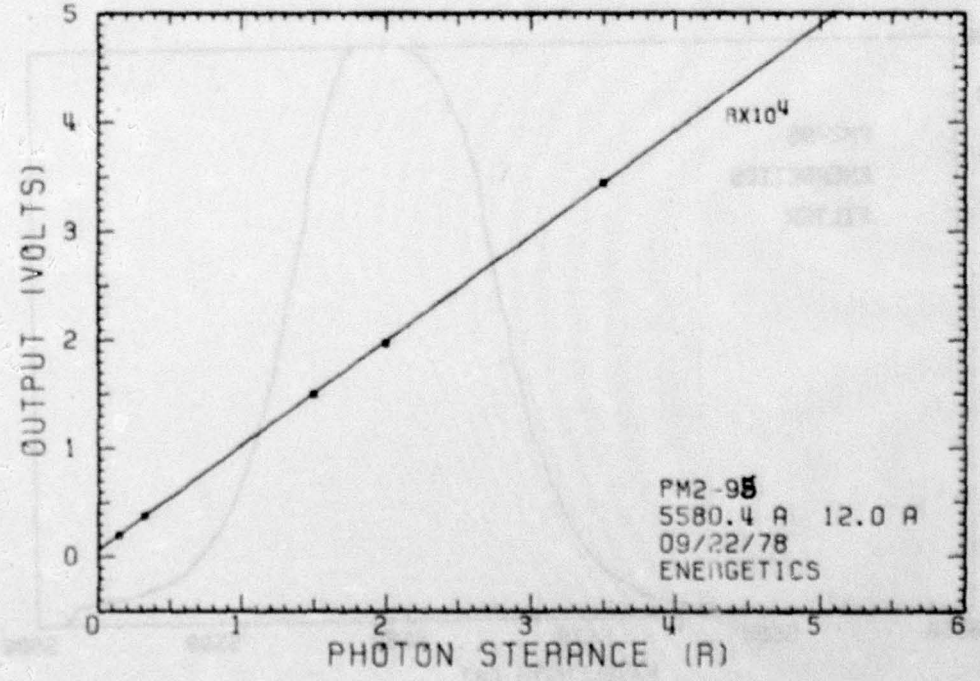


Figure F-9. Photometer (PM2-95) x10 Gain Responsivity.

TABLE F-1

NIKE HYDAC IR 807.57-1 PHOTOMETER PARAMETERS

(PM2-83 AND PM2-95)

PM2-83 Conversion equations (volts to Kilorayleighs)

x10 gain 0.4333E4V + 0.8789E2 for V_0 = 0 to 5 volts

Variable gain 0.7638E4V + 0.1641E3 for $V_0 \leq 2.81$ volts

0.7692E5V - 0.1946E6 for $V_0 \geq 2.81$ volts

PM2-95 Conversion equations (volts to Kilorayleighs)

x10 gain 0.1034E5V - 0.5798E3 for V_0 = 0 to 5 volts

Variable gain 0.1827E5V - 0.2739E3 for $V_0 \leq 2.77$ volts

0.1449E6V - 0.3517E6 for $V_0 \geq 2.77$ volts

Parameter	Value PM2-83	Value PM2-95
Filter λ_0 (Å)	3914	5580.4
Filter $\Delta\lambda$ (Å)	18.5	12.0
Filter T_r Peak (%)	99	100
Temp. Mon. (volts)	1.69	1.73
H.V. Mon. (volts)	2.90	2.93
Check Pulse (volts)	2.00	0.40
Field of View ($^\circ$Full Angle)	5	5

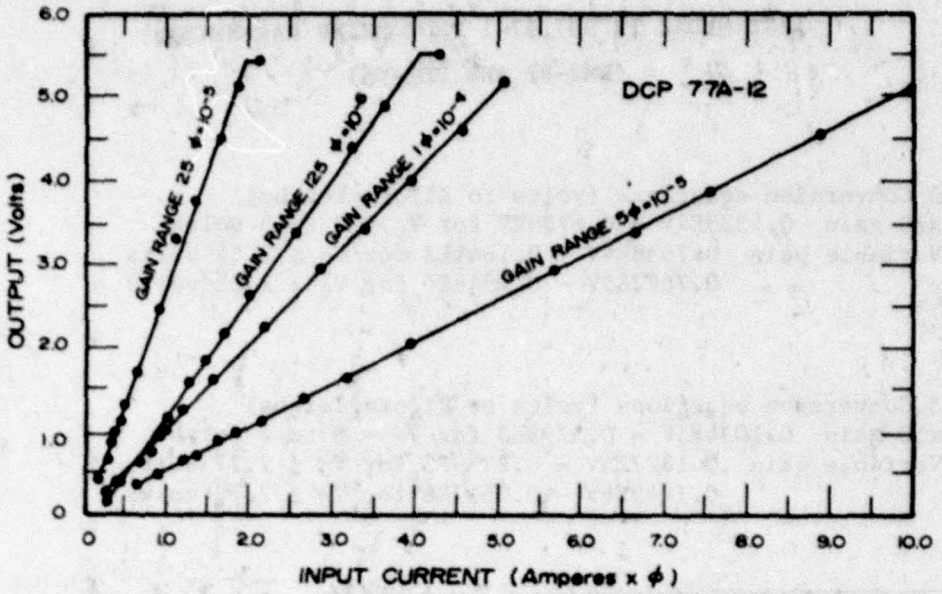


Figure F-10. DC Probe (DCP 77A-12) output voltage vs. input current calibration for four gain ranges.

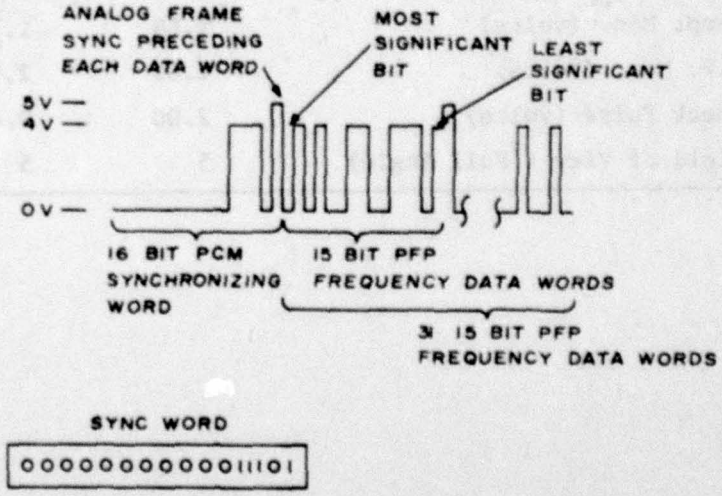


Figure F-11. Plasma Frequency Probe (PFP 77A-12) digital PCM format.

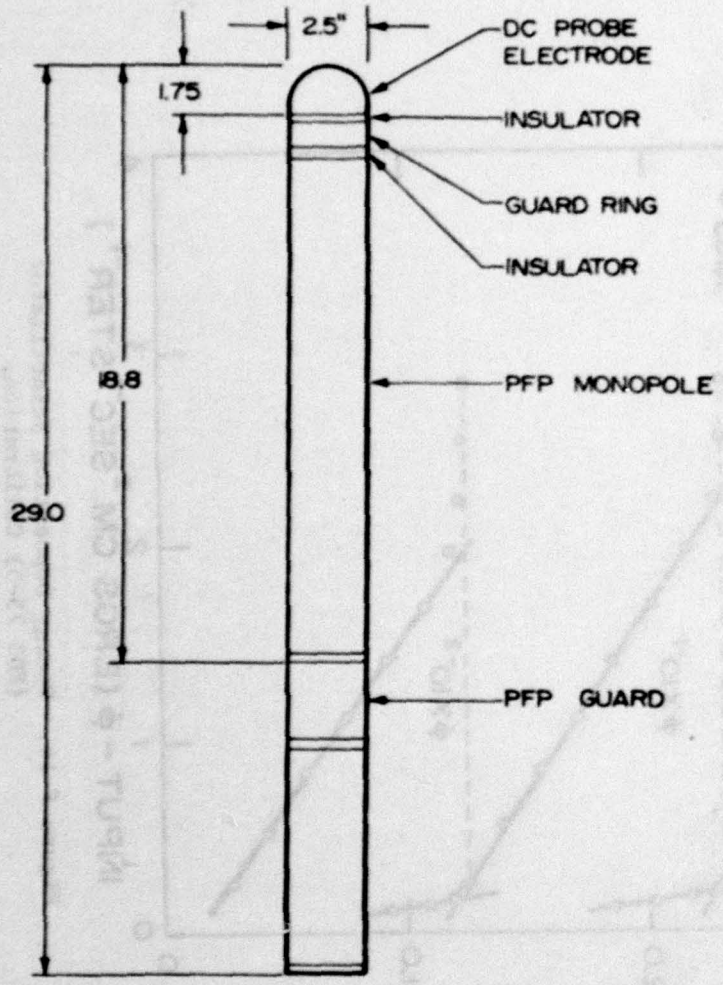


Figure F-12. Mike Hydac IR 807.57-1 Nosespike Electrode Configuration (PFP and DCP).

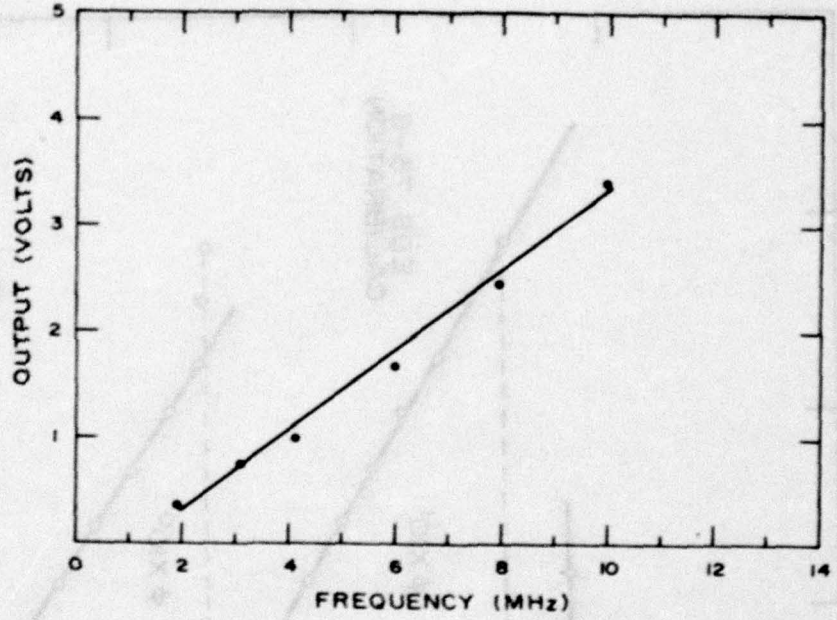


Figure F-13. Plasma Frequency Probe (PFP 77A-12) Analog Output Calibration.

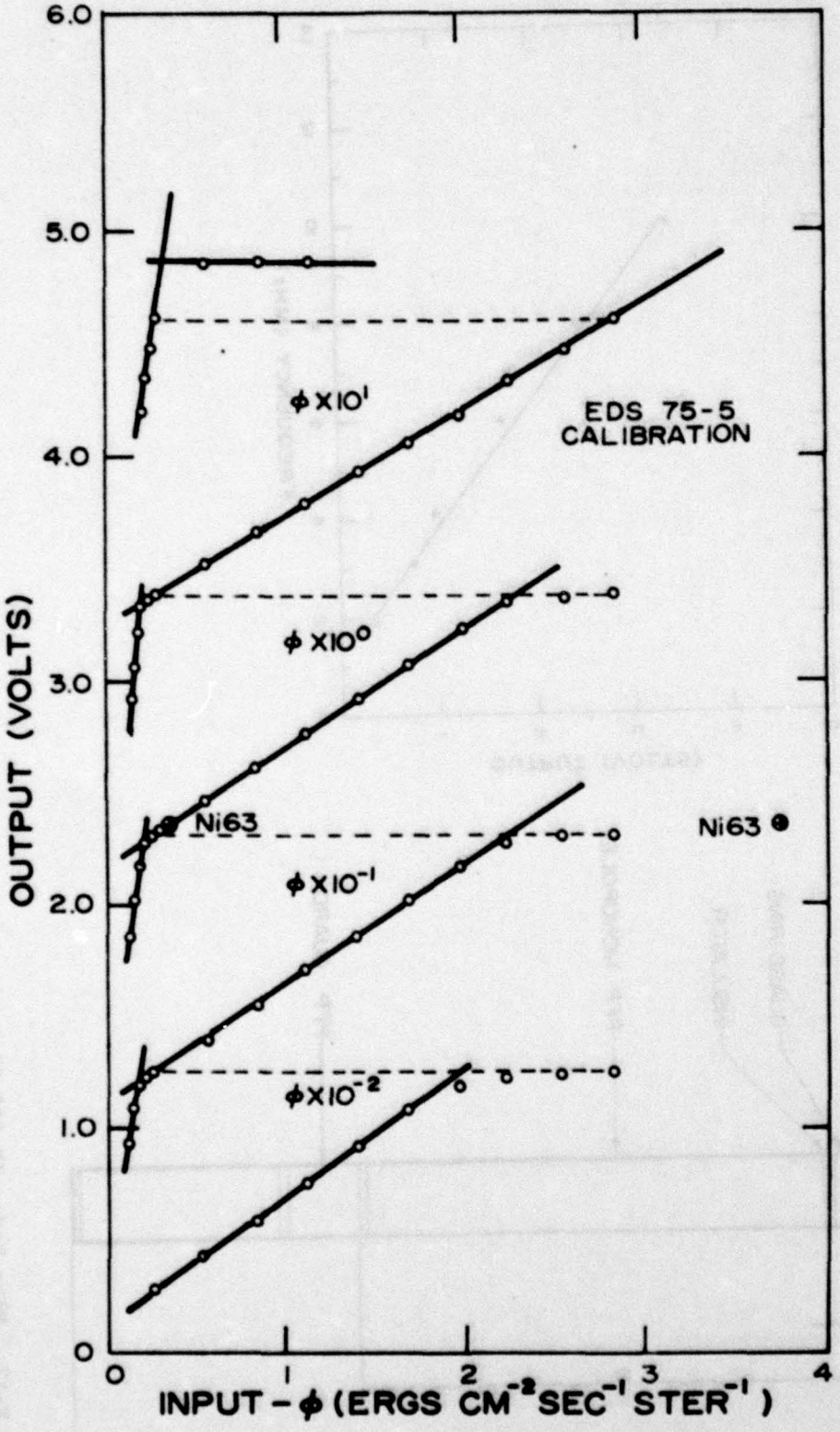


Figure F-14. Energy Deposition Scintillator (EDS 75-5) Calibration.

TABLE F-2

ENERGY DEPOSITION SCINTILLATOR (EDS 75-5) PARAMETERS

Parameter	Value
Window thickness	1510 Å
Aperture radius	
Minimum detectable energy (electrons)	3.6 KeV
Minimum detectable energy (protons)	31 KeV
Maximum detectable energy (electrons)	200 KeV
Maximum detectable energy (protons)	26 MeV
Geometric Factor	0.109 cm^2 ster.

TABLE F-3

NIKE HYDAC IR 807.57-1 TELEMETRY TECHNICAL DATA

LINK I 2215.5 MHz

IRIG Channel	Data
18	Plasma Frequency Probe Digital
17	Atomic Oxygen Digital
16	DC Probe x1
15	DC Probe x5
14	Ranging
13	DC Probe x25
12	DC Probe x125
11	Plasma Frequency Probe Analog
10	Housekeeping Commutator (1 x 32 NRZ)
9	Energy Deposition Scintillator
8	3914A Photometer
7	5577A Photometer
6	Roll Magnetometer
5	Roll Gyro
4	Pitch Gyro
3	Yaw Gyro

TABLE F-4

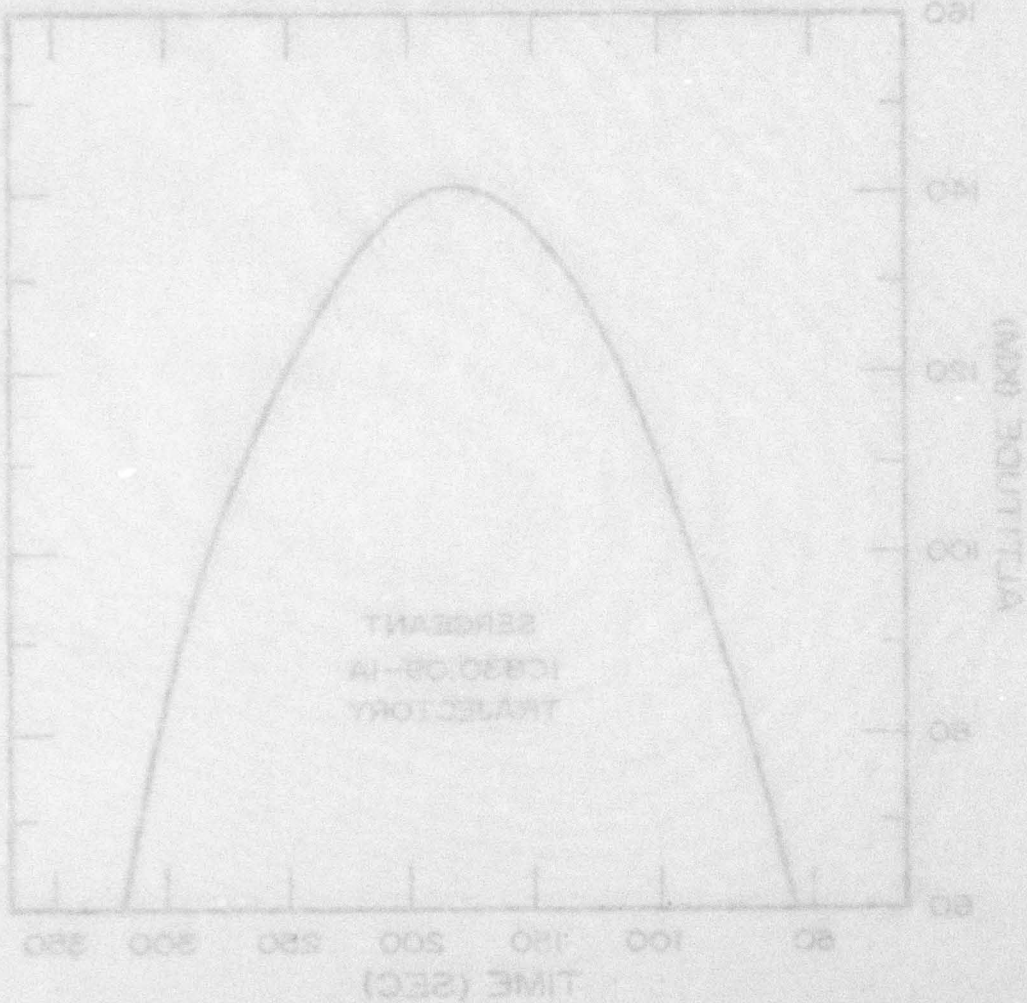
NIKE HYDAC IR 807.57-1 1 x 32 COMMUTATOR ASSIGNMENTS

Channel	Data
1	Lamp Intensity Monitor xl
2	EDS High Voltage Monitor
3	Pyro A Battery Monitor
4	Pyro B Battery Monitor
5	28V Monitor
6	Temperature (payload)
7	Lamp Intensity Monitor xl
8	Lamp Pressure (regulated Input)
9	Lamp Intensity Monitor x10
10	Lamp Intensity Monitor xl
11	Atomic Oxygen Detector High Voltage
12	Atomic Oxygen Detector Valve
13	Lamp Intensity Monitor x10
14	3914A Photometer High Voltage
15	3914A Photometer Temperature
16	Lamp Intensity Monitor x10
17	5577A Photometer High Voltage
18	5577A Photometer Temperature
19	Lamp Intensity Monitor x10
20	Atomic Oxygen Detector Door
21	Lamp Intensity Monitor xl
22	Photometer/EDS Door
23	Lamp Intensity Monitor x10
24	Mirror Position
25	Lamp Intensity Monitor xl
26	Magnetometer Bias
27	Lamp Intensity Monitor xl
28	0V
29	5V
30	5V
31	5V
32	2.5V

APPENDIX G

SERGEANT IC 830.09-1A

INSTRUMENTS AND PARAMETERS



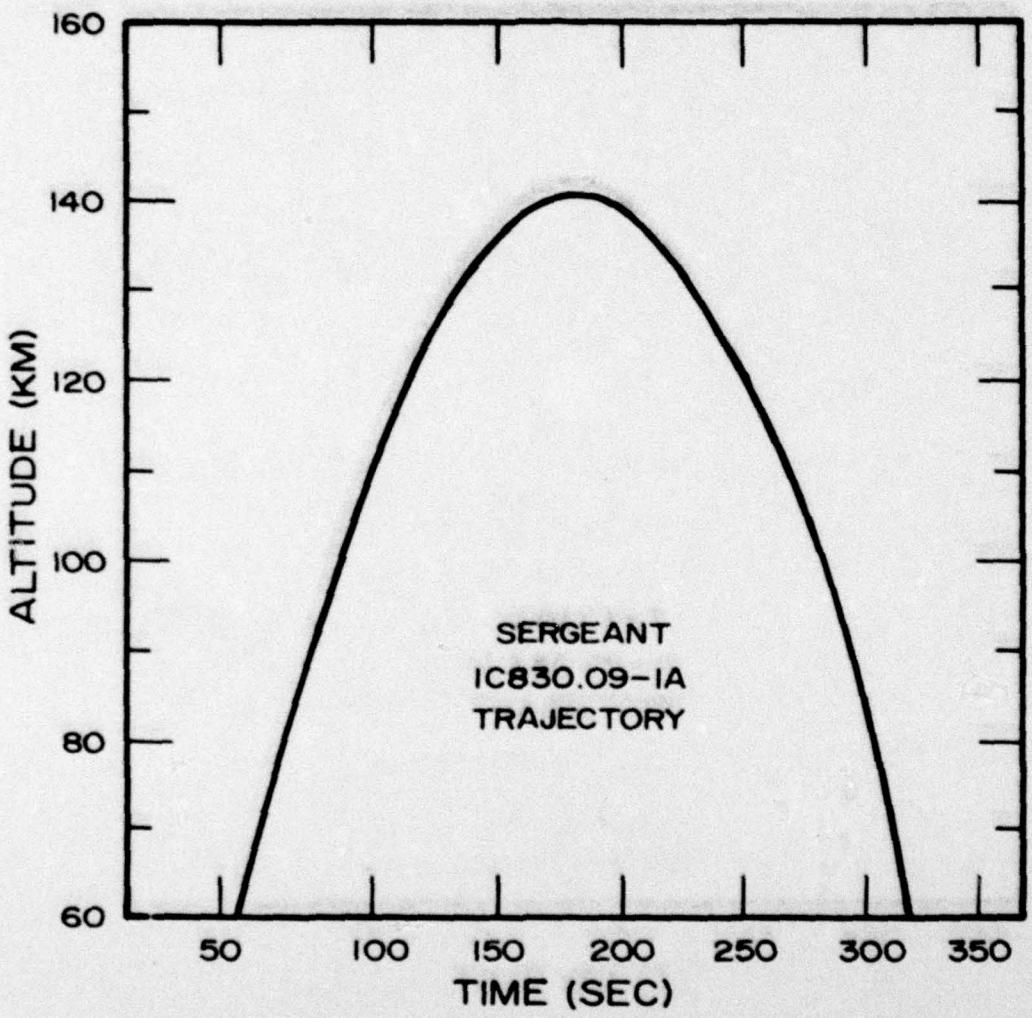


Figure G-1. Sergeant IC 830.09-1A Trajectory.

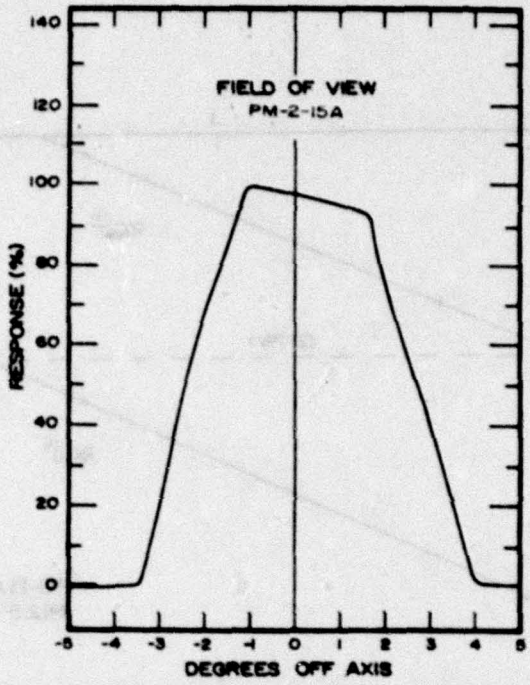


Figure G-2. Photometer (PM2-15A) Field-of-View.

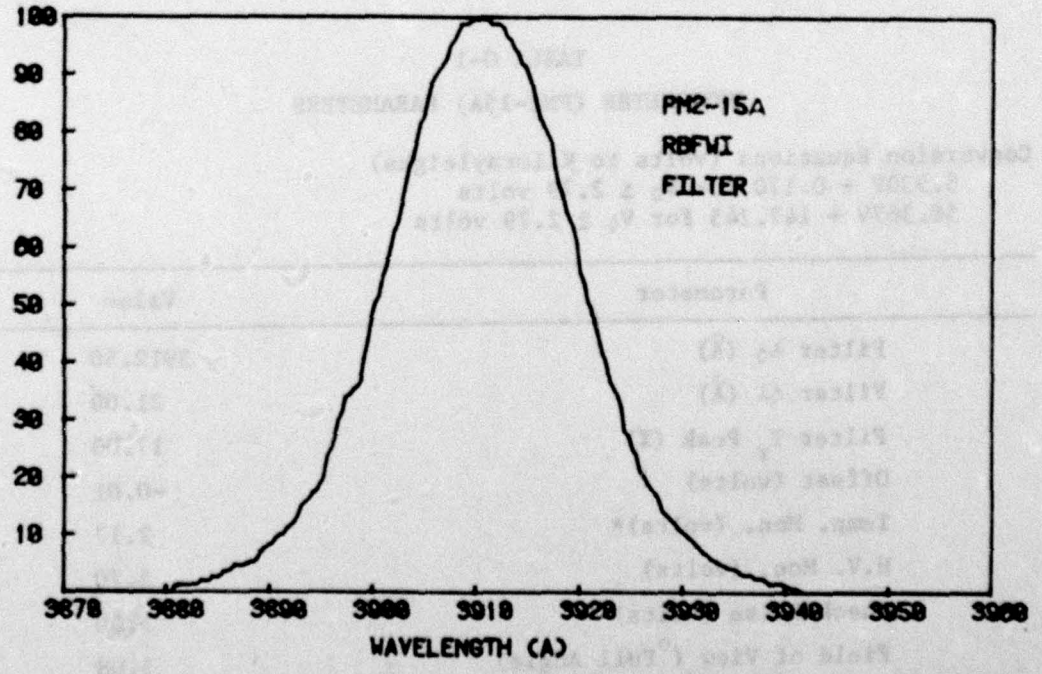


Figure G-3. Photometer (PM2-15A) Bandpass Filter Transmission.

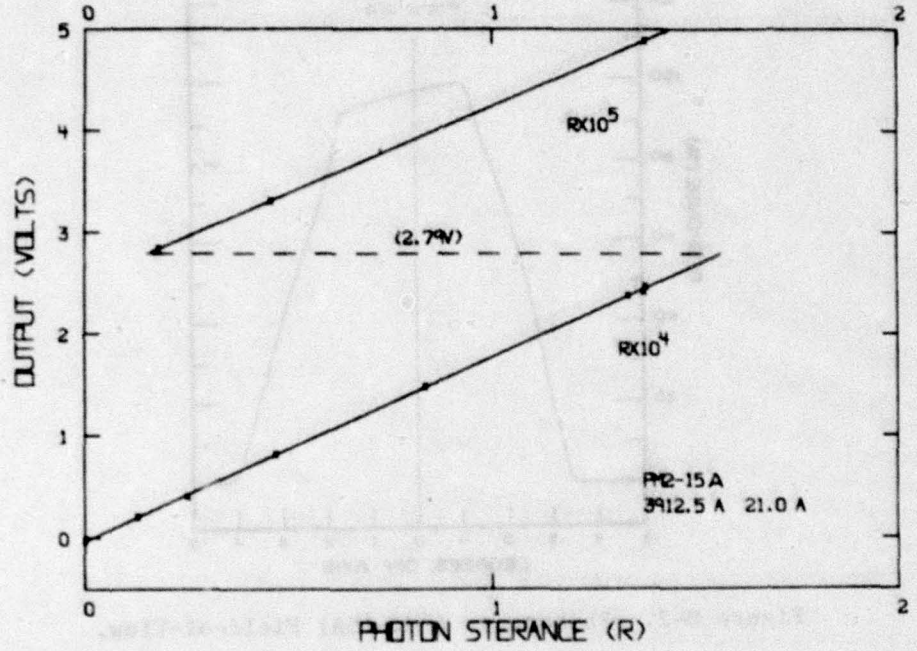


Figure G-4. Photometer (PM2-15A) Responsivity.

TABLE G-1

PHOTOMETER (PM2-15A) PARAMETERS

Conversion Equations (volts to Kilorayleighs)
5.530V + 0.170 for $V_0 \leq 2.79$ volts
58.367V + 147.245 for $V_0 \geq 2.79$ volts

Parameter	Value
Filter λ_0 (Å)	3912.50
Filter $\Delta\lambda$ (Å)	21.00
Filter T_r Peak (%)	17.00
Offset (volts)	-0.01
Temp. Mon. (volts)*	2.17
H.V. Mon. (volts)	3.70
Check Pulse (volts)	1.00
Field of View ($^\circ$Full Angle)	5.08

* Ambient room temperature of 23°C

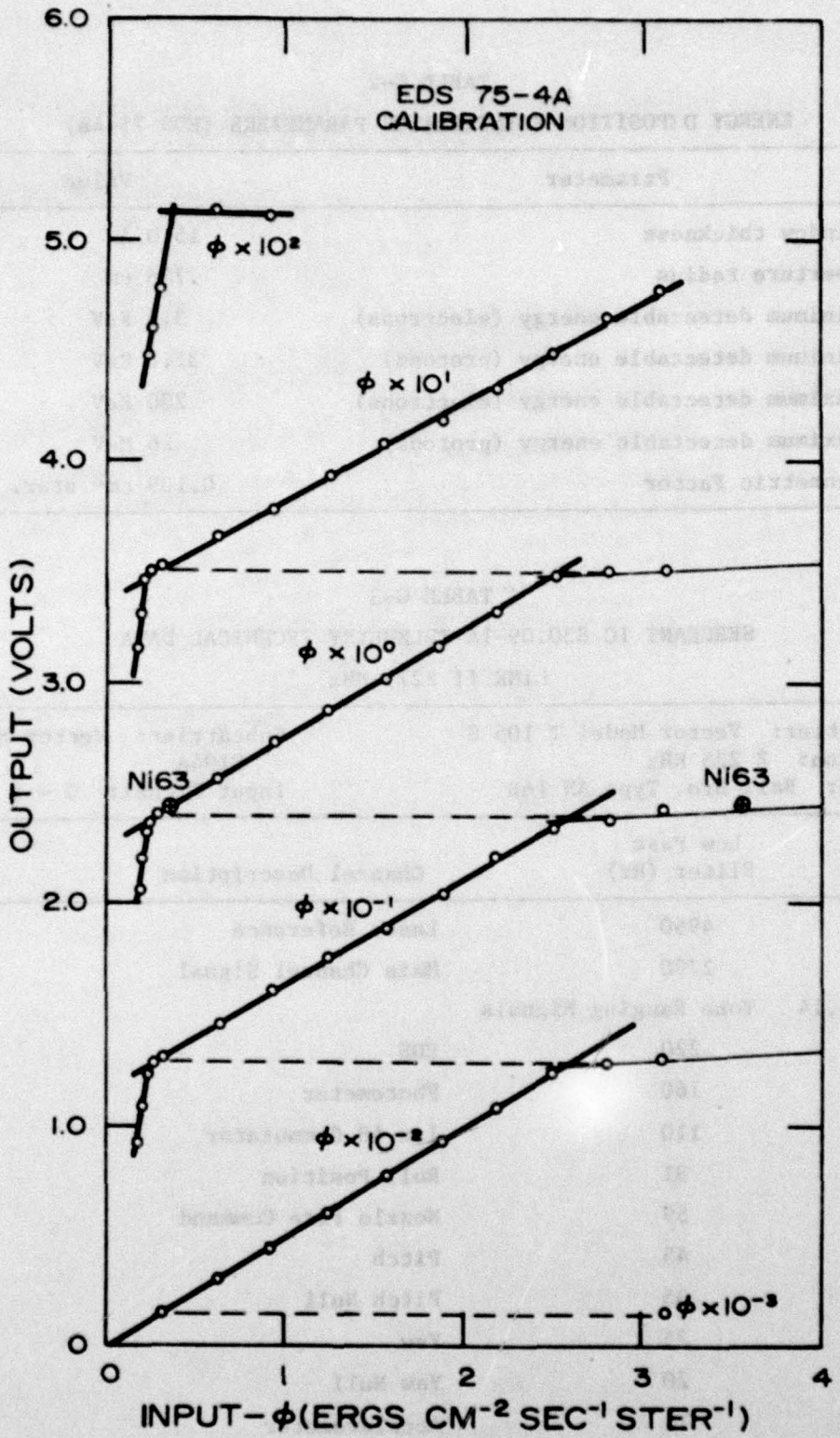


Figure G-5. Energy Deposition Scintillator (EDS 75-4A) Calibration.

TABLE G-2

ENERGY DEPOSITION SCINTILLATOR PARAMETERS (EDS 75-4A)

Parameter	Value
Window thickness	1510 Å
Aperture radius	.736 cm
Minimum detectable energy (electrons)	3.6 KeV
Minimum detectable energy (protons)	31.0 KeV
Maximum detectable energy (electrons)	200 KeV
Maximum detectable energy (protons)	26 MeV
Geometric Factor	0.109 cm^2 ster.

TABLE G-3

SERGEANT IC 830.09-1A TELEMETRY TECHNICAL DATA

LINK II 2279 MHz

Transmitter: Vector Model T 105 S
Deviation: ± 225 KHz
Antenna: Ball Bro. Type AN 16B

Subcarrier: Vector Model N194A
Input Signal: 0 - 5 V

IRIG Channel	Low Pass Filter (Hz)	Channel Description
H	4950	Laser Reference
F	2790	Main Channel Signal
16,15,14	Tone Ranging Signals	
13	220	EDS
12	160	Photometer
11	110	1 x 48 Commutator
10	81	Roll Position
9	59	Nozzle Fire Command
8	45	Pitch
7	35	Pitch Null
6	25	Yaw
5	20	Yaw Null
4	14	Accelerometer
3	11	Voltage Monitor (USU)

Link I is used for the PCM signal
and the format is NRZ with 420K bit rate.

TABLE G-4

SERGEANT IC 830.09-1A 1 x 48 NRZ COMMUTATOR ASSIGNMENTS

LINK II IRIG CHANNEL 11

Data Channels: 0.0 - +5.0 volts
Frame SYNC Pulse: +5.0 volts Switch Action: Make Before Break

Channel	Data
1	Main Pre Amp Temp
2	Main Detector Temp
3	CUTM Up Right
4	Slide Casting Temp
5	Beam Splitter Temp
6	Window Temp
7	Ref. Pre Amp Temp
8	Ref. Detector Temp
9	EDS H.V.
10	Photometer EDS Door Mon
11	Pressure Tank
12	Cal Diode & Pop Cover Mon
13	OV Ref.
14	Main +15V
15	Main -15V
16	Ref. +15V
17	Ref. -15V
18	+28V
19	Drive +15V
20	Drive -15V
21	PCM +18V
22	PCM -18V
23	Primary PYRO
24	Secondary PYRO
25	OV Ref.
26	Main Pre Amp Temp
27	Main Detector Temp
28	CUTM Up Right
29	Slide Casting Temp
30	Beam Splitter Temp
31	Window Temp
32	Ref. Pre Amp Temp
33	Ref. Detector Temp
34	OV Ref.
35	Nose Tip Mon
36	Lid Eject
37	IV Ref.
38	OV Ref.
39	OV Ref.
40	ACS Press (ACS)
41	AV Press (ACS)
42	Photometer H.V.
43	Photometer Temp

TABLE G-4 (cont.)

Channel	Data
44	OV Ref.
45	+5V Ref.
46	+5V Ref.
47	+5V Ref.
48	OV Ref.

APPENDIX H

DISTRIBUTION LIST

DISTRIBUTION LIST

DEPARTMENT OF DEFENSE

Director
Defense Advanced Rsch. Proj. Agency
Attn: LTC W.A. Whitaker

Defense Documentation Center
Attn: TC (2 Copies)

Director
Defense Nuclear Agency
Attn: TITL Tech. Library (3 copies)
Attn: TISI Archives
Attn: RAEV Harold C. Fitz, Jr.
Attn: RAAE Lt/Col. McKechney
Attn: RAAE Capt. Peter Lund
Attn: RAAE Dr. Patrick Crowley
Attn: RAAE Maj. R. Bigoni

Dir. of Defense Rsch. & Engineering
Department of Defense
Attn: DD/S&SS (OS) Daniel Brockway

Commander
Field Command
Defense Nuclear Agency
Attn: FCPR

Chief Livermore Division
FLD Command DNA
Attn: FCPRL

DEPARTMENT OF THE ARMY

Commander/Director
Atmospheric Sciences Laboratory
U.S. Army Electronics Command
Attn: DRSEL-BL-SY-A.F. Niles
Attn: H. Ballard

Commander
Harry Diamond Laboratories
Attn: DRXDO-NP, F.H. Wiminetz
(2 Copies)

Superintendent
Naval Post Graduate School
Attn: Rsch Rpts Librarian

Commander
Naval Intelligence Support Center
Attn: Document Control

Director
BMD Advanced Technical Center
Attn: ATC-T, M. Capps
Attn: ATC-O, M. Davies

Dep. Chief of Staff for Rsch. Dev & Accout.
Department of the Army
Attn: MCB Division
Attn: DAMA-CSZ-C
Attn: DAMA-WSZC

Director
U.S. Army Ballistic Rsch. Labs.
Attn: John Mester
Attn: Tech. Library

Commander
U.S. Army Electronics Command
Attn: Inst. for Expl. Research
Attn: Weapons Effects Section

Commander
CORADCOM
Attn: PP-Library
Attn: DRDCO-COM-D

DEPARTMENT OF THE NAVY

Commander
Naval Oceans Systems Center
Attn: Code 2200 William Moler

Director
Naval Research Laboratory
Attn: Code 7712 D.P. McNut
Attn: Code 6701 J.D. Brown
Attn: Code 2600 Tech. Library
Attn: Code 7175J C.Y. Johnson
Attn: Code 6700 T.P. Coffey
Attn: Code 7709 Wahab Ali
Attn: Code 6780 D.F. Strobel
Attn: Code 6780 P. Juluenne
Attn: Code 67800 J. Fedder
Attn: Code 6780 S. Ossakow
Attn: Code 6707 J. Davis

Commander
Naval Surface Weapons Center
Attn: Code WA 501 Navy NUC
Programs Office
Attn: Technical Library

DEPARTMENT OF THE AIR FORCE

AF Geophysics Laboratory, AFSC
Attn: LKB, K.S.W. Champion
Attn: OPR, A.T. Stair, Jr.
Attn: OPR, P.G. Doyle
Attn: OPR, R. Murphy
Attn: LKO, R. Huffman
Attn: OPR, J. Kennealy

AF Weapons Laboratory, AFSC
Attn: Maj. Gary Ganong, DES

Commander
ASD
Attn: ASD-YH-EX-LTC R. Leverette

SAMSO/AW
Attn: SZJ Lt. Col. Doan

SAMSO/YN
Attn: Maj. P. Sivgals

AFTAC
Attn: Tech Library
Attn: TD

HQ
Air Force Systems Command
Attn: DLS
Attn: Tech Library
Attn: DLCAE
Attn: DLTW
Attn: DLXP
Attn: SDR
Attn: RDQ

US ENERGY RSCH. AND DEV. ADMIN

Division of Military Application
U.S. Energy Rsch. & Dev. Admin.
Attn: DOC CON

Los Alamos Scientific Laboratory
Attn: DOC CON for H.V. Argo
Attn: DOC CON for M.B. Pongratz
Attn: DOC CON for R. Brownlee
Attn: Group AP-4, MS 567
Attn: DOC CON for J. Zinn

University of California
Los Alamos Scientific Laboratory
Attn: Librarian MS 362

Sandia Laboratories
Attn: DOC CON for W.B. Brown, Org. 1353
Attn: Tech Library Org. 3141

Argonne National Laboratory
Records Control
Attn: DOC CON for D.W. Green
Attn: DOC CON for LIR SVCS Rpts Sec.
Attn: DON CON for G.T. Reedy

University of California
Lawrence Livermore Laboratory
Attn: W.H. Duewer, L-262
Attn: J. Chang, L-71

U.S. Energy Rsch. & Dev. Administration
Division of Headquarters Services,
Library Branch
Attn: DOC CON for Class. Tech. Library

OTHER GOVERNMENT

Department of Transportation
Office of the Secretary
Attn: S.C. Coroniti

NASA
Langley Station
Attn: Tech. Library

NASA
Ames Research Center
Attn: N-245-3 R. Whitten

Department of the Army
Bal. Missl. Def. Adv. Tech. Ctr.
Attn: W.O. Davies

Federal Aviation Administration
Attn: HAPP/AEQ-10/James W. Rogers

Central Intelligence Agency
Attn: ED/SI RM 5G48 HQ Bldg.
Attn: NED/OS I-2G4R HQS

Department of Commerce
National Bureau of Standards
Attn: Sec. Officer for M. Krauss
Attn: Sec. Off. for L.H. Gevantman

National Oceanic & Atmospheric Admin.
Environmental Research Laboratories
Department of Commerce
Attn: G. Reid
Attn: E. Ferguson
Attn: F. Fehsenfeld

DEPARTMENT OF DEFENSE CONTRACTORS

Science Applications, Inc.
Attn: D.G. Hopper

Aero-Chem Research Laboratories, Inc.
Attn: A. Fontign
Attn: H. Pergament

Aerodyne Research, Inc.
Attn: F. Bien
Attn: M. Camac

Aerospace Corporation
Attn: N. Cohen
Attn: H. Mayer
Attn: R.J. McNeal
Attn: T.D. Taylor
Attn: J. Reinheimer
Attn: R.D. Rawcliffe
Attn: R. Horm

Battelle Memorial Institute
Attn: H.L. LaMuth
Attn: STOIAC

Brown Engineering Company, Inc.
Attn: N. Passino

General Research Corporation
Attn: D. Jones
Attn: J. Ise, Jr.

California At Riverside, University of
Attn: J.N. Pitts, Jr.
Attn: A.M. Winer

California At San Diego, University of
Attn: S.C. Lin

California University of Berkley
Attn: Sec. Off. for H. Johnston
Attn: Sec. Officer for Dept of Chem., H.L. Strauss

Calspan Corporation
Attn: C.E. Treanor
Attn: J.M. Grace
Attn: M.G. Dunn
Attn: W. Wruster

University of Colorado
Astro-Geophysics
Attn: J.B. Pearce

Colorado, University of
Office of Contracts and Grants
Attn: G.M. Lawrence, LASP

Concord Sciences
Attn: E.A. Sutton

University of Denver
Space Science Laboratory
Attn: B. Van Zyl

University of Denver
Denver Research Laboratory
Attn: Sec Officer for D. Murcray

AVCO-Everett Research Laboratory Inc.
Attn: Tech. Library
Attn: C.W. Von Rosenberg, Jr.

General Electric Company
Space Division
Attn: M.H. Bortner, Space Sci. Lab
Attn: J. Burns
Attn: F. Alyea
Attn: P. Zavitsands
Attn: R.H. Edsall
Attn: T. Baurer

Geophysical Institute
University of Alaska
Attn: J.S. Wagner

Lowell University of
Center for Atmospheric Research
Attn: G.T. Best

Lockheed Missiles and Space Company
Attn: J. Kumer, Dept 52-54
Attn: J.B. Cladis, Dept 52-12, B202
Attn: B.M. McCormac, Dept 52-54
Attn: T. James, Dept 52-54
Attn: M. Walt, Dept 52-10
Attn: R.D. Sears, Dept 52-54

Institute for Defense Analysis
Attn: E. Bauer
Attn: H. Wolfhard

Mission Research Corporation
Attn: D. Archer
Attn: D. Fischer
Attn: M. Scheibe
Attn: D. Sappenfield
Attn: D. Sowle

Photometrics, Inc.
Attn: I.L. Kofsky

Berkeley Research Associates
Attn: J.B. Workman

Physical Dynamics, Inc.
Attn: A. Thomas

General Electric Company
Tempo-Center for Advanced Studies
Attn: DASAIC
Attn: W.S. Knapp
Attn: T. Stephens
Attn: D. Chandler
Attn: V.R. Strull

Physics International Company
Attn: DOC CON for Tech Library

Pittsburg, University of the Comwlth
System of Higher Education
Attn: W.L. Fite
Attn: M.A. Biondi
Attn: F. Kaufman

R&D Associates
Attn: R. Latter
Attn: R.G. Lindgren
Attn: B. Gabbard
Attn: R. Lelevier
Attn: A.L. Latter
Attn: F. Gilmore
Attn: H.J. Mitchell

Rand Corporation
Attn: C. Crain

Science Applications, Inc.
Attn: D.A. Hamlin
Attn: D. Sachs
Attn: D.G. Hopper

Stanford Research Institute International
Attn: M. Baron
Attn: W.G. Chesnut

Technology International Corporation
Attn: W.P. Boquist

United Technologies Corporation
Attn: R.H. Bullis

Utah State University
Attn: D. Baker
Attn: K. Baker
Attn: C. Wyatt
Attn: A. Steed

Physical Science, Inc.
Attn: K. Wray
Attn: R.L. Taylor
Attn: G. Caledonia

Commander
Rome Air Development Center
Attn: OSCA, J.J. Simons

Steward Radiance Laboratory
Attn: R. Huppi

Boston College
Space Data Analysis Laboratory
Attn: E.R. Hegblom
Attn: W.F. Grieder

Forrestial Campus Library
Princeton University
Attn: Librarian

Visidyne, Inc.
Attn: H. Smith
Attn: J.W. Carpenter
Attn: T.C. Degges
Attn: C. Humphrey

Wayne State University
Attn: R.H. Kummler
Attn: W.E. Kaupplia